Hyperbolic Conservation Laws: An Illustrated Tutorial

Alberto Bressan

Abstract These notes provide an introduction to the theory of hyperbolic systems of conservation laws in one space dimension. The various chapters cover the following topics: (1) Meaning of a conservation equation and definition of weak solutions. (2) Hyperbolic systems. Explicit solutions in the linear, constant coefficients case. Nonlinear effects: loss of regularity and wave interactions. (3) Shock waves: Rankine–Hugoniot equations and admissibility conditions. (4) Genuinely nonlinear and linearly degenerate characteristic fields. Centered rarefaction waves. The general solution of the Riemann problem. Wave interaction estimates. (5) Weak solutions to the Cauchy problem, with initial data having small total variation. Approximations generated by the front-tracking method and by the Glimm scheme. (6) Continuous dependence of solutions w.r.t. the initial data, in the $\mathbf{L}^1$ distance. (7) Characterization of solutions which are limits of front tracking approximations. Uniqueness of entropy-admissible weak solutions. (8) Vanishing viscosity approximations. (9) Extensions and open problems. The survey is concluded with an Appendix, reviewing some basic analytical tools used in the previous sections.
Throughout the exposition, technical details are mostly left out. The main goal of these notes is to convey basic ideas, also with the aid of a large number of figures.

A. Bressan
Department of Mathematics, Penn State University,
University Park, PA 16802, USA
e-mail: bressan@math.psu.edu

L. Ambrosio et al., *Modelling and Optimisation of Flows on Networks*, Lecture Notes in Mathematics 2062, DOI 10.1007/978-3-642-32160-3_2,

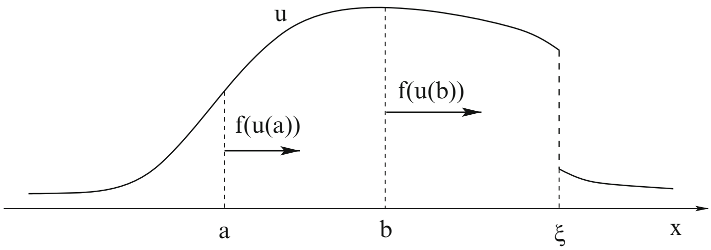

Fig. 1 Flow across two points

1 Conservation Laws

1.1 The Scalar Conservation Law

A *scalar conservation law* in one space dimension is a first order partial differential equation of the form

$$u_t + f(u)_x = 0. \tag{1}$$

Here $u = u(t, x)$ is called the *conserved quantity*, while f is the *flux*. The variable t denotes time, while x is the one-dimensional space variable. Integrating (1) over a given interval $[a, b]$ one obtains

$$\begin{aligned} \frac{d}{dt}\int_a^b u(t,x)\,dx = \int_a^b u_t(t,x)\,dx \; &= \; -\int_a^b f\big(u(t,x)\big)_x\,dx \\ &= \; f\big(u(t,a)\big) - f\big(u(t,b)\big) \; = \; [\text{inflow at } a] - [\text{outflow at } b]. \end{aligned} \tag{2}$$

According to (2), the quantity u is neither created nor destroyed: the total amount of u contained inside any given interval $[a, b]$ can change only due to the flow of u across the two boundary points (Fig. 1).

Using the chain rule, (1) can be written in the quasilinear form

$$u_t + a(u)u_x = 0, \tag{3}$$

where $a = f'$ is the derivative of f. For smooth solutions, the two (1) and (3) are entirely equivalent. However, if u has a jump at a point ξ, the left hand side of (3) will contain the product of a discontinuous function $a(u)$ with the distributional derivative u_x, which in this case contains a Dirac mass at the point ξ. In general, such a product is not well defined. Hence (3) is meaningful only within a class of continuous functions. On the other hand, working with the equation in divergence form (1) allows us to consider discontinuous solutions as well, interpreted in distributional sense.

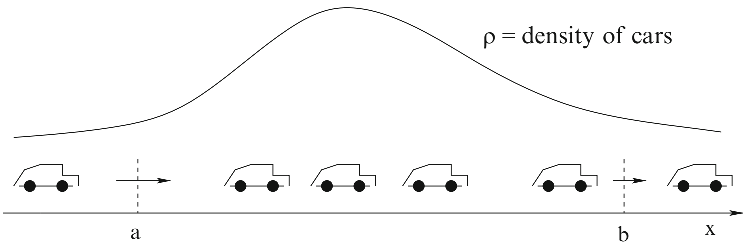

Fig. 2 The density of cars can be described by a conservation law

A function $u = u(t,x)$ will be called a *weak solution* of (1) provided that

$$\iint \{u\phi_t + f(u)\phi_x\}\, dxdt \;=\; 0 \tag{4}$$

for every continuously differentiable function with compact support $\phi \in \mathscr{C}_c^1$. Notice that (4) is meaningful as soon as both u and $f(u)$ are *locally integrable* in the t-x plane.

Example 1 (traffic flow). Let $\rho(t,x)$ be the density of cars on a highway, at the point x at time t. For example, u may be the number of cars per kilometer (Fig. 2). In the classic Lighthill–Witham model [33,43], one assumes that the velocity v of the cars depends only on their density, say

$$v = v(\rho), \qquad\qquad \text{with} \qquad \frac{dv}{d\rho} < 0.$$

Given any two points a, b on the highway, the number of cars between a and b therefore varies according to the law

$$\int_a^b \rho_t(t,x)\,dx = \frac{d}{dt}\int_a^b \rho(t,x)\,dx \;=\; [\text{inflow at} a] - \;[\text{outflow at} b]$$

$$= \; v\big(\rho(t,a)\big)\cdot\rho(t,a) - v\big(\rho(t,b)\big)\cdot\rho(t,b) = -\int_a^b \big[v(\rho)\,\rho\big]_x\,dx. \tag{5}$$

Since (5) holds for all a, b, this leads to the conservation law

$$\rho_t + \big[v(\rho)\,\rho\big]_x = 0,$$

where ρ is the conserved quantity and $f(\rho) = v(\rho)\rho$ is the flux function.

1.2 Strictly Hyperbolic Systems

The main object of our study will be the $n \times n$ *system of conservation laws*

$$\begin{cases} \dfrac{\partial}{\partial t} u_1 + \dfrac{\partial}{\partial x} f_1(u_1, \ldots, u_n) = 0, \\ \qquad \cdot \quad \cdot \quad \cdot \\ \dfrac{\partial}{\partial t} u_n + \dfrac{\partial}{\partial x} f_n(u_1, \ldots, u_n) = 0. \end{cases} \tag{6}$$

To shorten notation, it is convenient to write this system also in the form (1). However, one should keep in mind that now $u = (u_1, \ldots, u_n)$ is a vector in $I\!R^n$ while $f = (f_1, \ldots, f_n)$ is a map from $I\!R^n$ into $I\!R^n$. Calling

$$A(u) \doteq Df(u) = \begin{pmatrix} \frac{\partial f_1}{\partial u_1} & \cdots & \frac{\partial f_1}{\partial x_n} \\ & \cdots & \\ \frac{\partial f_n}{\partial u_1} & \cdots & \frac{\partial f_n}{\partial x_n} \end{pmatrix},$$

the $n \times n$ Jacobian matrix of the map f at the point u, the system (6) can be written in the quasilinear form

$$u_t + A(u) u_x = 0. \tag{7}$$

A $\mathscr{C}^1$ function $u = u(t, x)$ provides a classical solution to (6) if and only if it solves (7). In addition, for the conservative system (6) one can also consider weak solutions $u \in \mathbf{L}^1_{loc}$ in distributional sense, according (4).

In order to achieve the well-posedness of the initial value problem, a basic algebraic property will now be introduced.

Definition 1 (strictly hyperbolic system). The system of conservation laws (6) is *strictly hyperbolic* if, for every u, the Jacobian matrix $A(u) = Df(u)$ has n real, distinct eigenvalues: $\lambda_1(u) < \cdots < \lambda_n(u)$.

If the matrix $A(u)$ has real distinct eigenvalues, one can find bases of left and right eigenvectors, denoted by $l_1(u), \ldots, l_n(u)$ and $r_1(u), \ldots, r_n(u)$. The left eigenvectors are regarded as row vectors, while right eigenvectors are column vectors. For every $u \in I\!R^n$ and $i = 1, \ldots, n$, we thus have

$$A(u) r_i(u) = \lambda_i(u) r_i(u), \qquad l_i(u) A(u) = \lambda_i(u) l_i(u).$$

It is convenient to choose dual bases of left and right eigenvectors, so that

$$|r_i| = 1, \qquad l_i \cdot r_j = \begin{cases} 1 & \text{if} \quad i = j, \\ 0 & \text{if} \quad i \neq j. \end{cases} \tag{8}$$

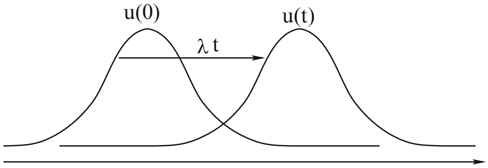

Fig. 3 A traveling wave solution to the linear, scalar Cauchy problem (10)–(11)

Example 2 (gas dynamics). The Euler equations describing the evolution of a non viscous gas take the form

$$\begin{cases} \rho_t + (\rho v)_x = 0 & \text{(conservation of mass)} \\ (\rho v)_t + (\rho v^2 + p)_x = 0 & \text{(conservation of momentum)} \\ (\rho E)_t + (\rho E v + p v)_x = 0 & \text{(conservation of energy)} \end{cases}$$

Here ρ is the mass density, v is the velocity while $E = e + v^2/2$ is the energy density per unit mass. The system is closed by a *constitutive relation* of the form $p = p(\rho, e)$, giving the pressure as a function of the density and the internal energy. The particular form of p depends on the gas under consideration. Denoting by $u = (u_1, u_2, u_3) = (\rho, \rho v, \rho E)$ the vector of conserved quantities, one checks that for physically meaningful functions $p = p(\rho, e)$ the above system is strictly hyperbolic [26, 57].

1.3 Linear Systems

We describe here two elementary cases where the solution of the initial value problem can be written explicitly.

Consider the initial value problem for a scalar conservation law

$$u_t + f(u)_x = 0, \tag{9}$$

$$u(0, x) = \bar{u}(x). \tag{10}$$

In the special case where the flux f is an affine function, say $f(u) = \lambda u + c$, the (9) reduces to

$$u_t + \lambda u_x = 0. \tag{11}$$

The Cauchy problem (10)–(11) admits an explicit solution, namely

$$u(t, x) = \bar{u}(x - \lambda t). \tag{12}$$

As shown in Fig. 3, this has the form of a traveling wave, with speed $\lambda = f'(u)$. If $\bar{u} \in \mathscr{C}^1$, the function $u = u(t, x)$ defined by (12) is a classical solution. On the other

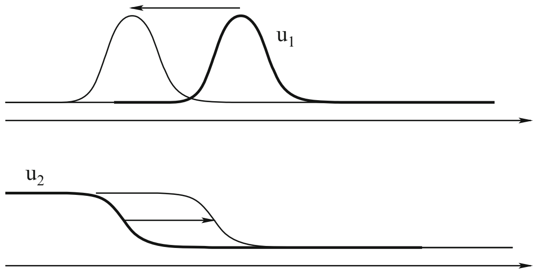

Fig. 4 The solution to the linear hyperbolic system (13) is obtained as the superposition of n traveling waves

hand, if the initial condition $\bar{u}$ is not differentiable and we only have $\bar{u} \in \mathbf{L}^1_{loc}$, the above function u can still be interpreted as a weak solution in distributional sense.

Next, consider the linear homogeneous system with constant coefficients

$$u_t + Au_x = 0, \qquad\qquad u(0,x) = \bar{u}(x), \tag{13}$$

where A is a $n \times n$ hyperbolic matrix, with real eigenvalues $\lambda_1 < \cdots < \lambda_n$ and right and left eigenvectors r_i, l_i, chosen as in (8).

Call $u_i \doteq l_i \cdot u$ the coordinates of a vector $u \in I\!R^n$ w.r.t. the basis of right eigenvectors $\{r_1, \cdots, r_n\}$. Multiplying (13) on the left by $l_1, \dots, l_n$ we obtain

$$\begin{aligned} (u_i)_t + \lambda_i (u_i)_x = \ (l_i u)_t + \lambda_i (l_i u)_x \ &= \ l_i u_t + l_i A u_x \ = \ 0, \\ u_i(0,x) = \ l_i \bar{u}(x) \ &\doteq \ \bar{u}_i(x). \end{aligned}$$

Therefore, (13) decouples into n scalar Cauchy problems, which can be solved separately in the same way as (10)–(11). The function

$$u(t,x) \ = \ \sum_{i=1}^{n} \bar{u}_i(x - \lambda_i t)\, r_i \tag{14}$$

now provides the explicit solution to (13), because

$$u_t(t,x) \ = \ \sum_{i=1}^{n} -\lambda_i \big(l_i \cdot \bar{u}_x(x - \lambda_i t)\big) r_i \ = \ -Au_x(t,x).$$

Observe that in the scalar case (11) the initial profile is shifted with constant speed $\lambda = f'(u)$. For the system (13), the initial profile is decomposed as a sum of n waves (Fig. 4), each traveling with one of the characteristic speeds $\lambda_1, \dots, \lambda_n$.

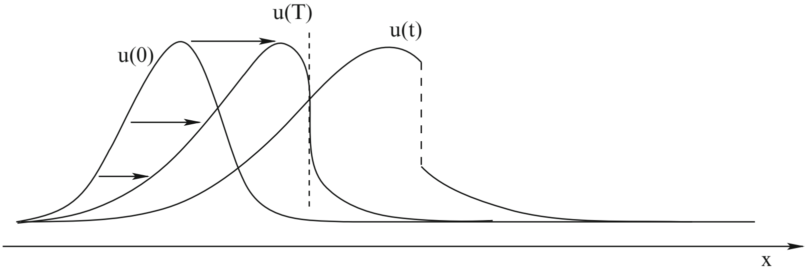

Fig. 5 If the wave propagation speed depends on u, the profile of the solution changes in time, eventually leading to shock formation at a finite time T

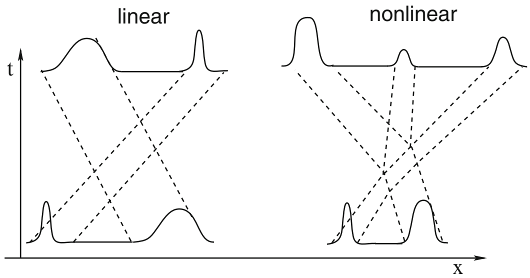

Fig. 6 *Left*: for the linear hyperbolic system (13), the solution is a simple superposition of traveling waves. *Right*: For the general non-linear system (6), waves of different families have nontrivial interactions

1.4 Nonlinear Effects

In the general case where the matrix A depends on the state u, new features will appear in the solutions.

(a) Since the eigenvalues λ_i now depend on u, the shape of the various components in the solution will vary in time (Fig. 5). Rarefaction waves will decay, and compression waves will become steeper, possibly leading to shock formation in finite time.
(b) Since the eigenvectors r_i also depend on u, nontrivial interactions between different waves will occur (Fig. 6). The strength of the interacting waves may change, and new waves of different families can be created, as a result of the interaction.

The strong nonlinearity of the equations and the lack of regularity of solutions, also due to the absence of second order terms that could provide a smoothing effect, account for most of the difficulties encountered in a rigorous mathematical analysis of the system (1). It is well known that the main techniques of abstract functional analysis do not apply in this context. Solutions cannot be represented as fixed points of continuous transformations, or in variational form, as critical points of suitable functionals. Dealing with vector valued functions, comparison principles based on upper or lower solutions cannot be used. Moreover, the theory of accretive operators and contractive nonlinear semigroups works well in the scalar case [25], but does not apply to systems. For the above reasons, the theory of hyperbolic conservation laws has largely developed by *ad hoc* methods, along two main lines.

1. The BV setting, considered by J. Glimm [34]. Solutions are here constructed within a space of functions with bounded variation, controlling the BV norm by a wave interaction functional.
2. The $\mathbf{L}^\infty$ setting, considered by L. Tartar and R. DiPerna [29], based on weak convergence and a compensated compactness argument.

Both approaches yield results on the global existence of weak solutions. However, the method of compensated compactness appears to be suitable only for 2×2 systems. Moreover, it is only in the BV setting that the well-posedness of the Cauchy problem could recently be proved, as well as the stability and convergence of vanishing viscosity approximations. In these lecture we thus restrict ourselves to the analysis of BV solutions, referring to [29] or [50,56] for the alternative approach based on compensated compactness.

1.5 Loss of Regularity

A basic feature of nonlinear systems of the form (1) is that, even for smooth initial data, the solution of the Cauchy problem may develop discontinuities in finite time. To achieve a global existence result, it is thus essential to work within a class of discontinuous functions, interpreting the (1) in their distributional sense (4).

The loss of regularity can be seen already in the solution to a scalar equation with nonlinear flux. Consider the scalar Cauchy problem

$$u_t + f(u)_x = 0 \qquad\qquad u(0,x) = \phi(x). \tag{15}$$

In the case of smooth solutions, the equation can be written in quasilinear form

$$u_t + f'(u)u_x = 0. \tag{16}$$

Geometrically, this means that the directional derivative of $u(t,x)$ in the direction of the vector $(1\,,\ f'(u))$ vanishes. Hence u is constant on each line of the form $\Big\{(t,x)\,;\ \ x = x_0 + tf'(u(x_0))\Big\}$. For each $x_0 \in I\!R$ we thus have

$$u\Big(t,\ x_0 + t\ f'(\phi(x_0))\Big) \ =\ \phi(x_0). \tag{17}$$

This is indeed the solution to the first order PDE (16) provided by the classical method of characteristics, see for example [31]. In general, beyond a finite time T, the map

$$x_0 \mapsto x_0 + t\ f'(\phi(x_0))$$

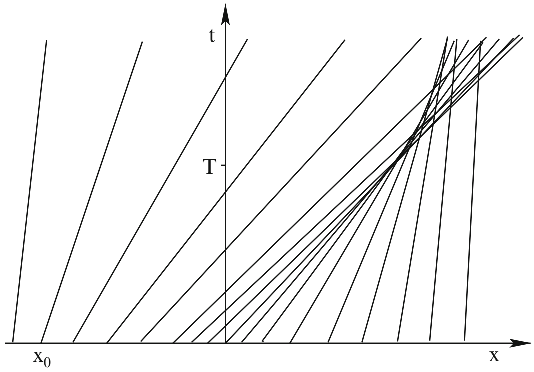

Fig. 7 At time T when characteristics start to intersect, a shock is produced

is no longer one-to-one, and the implicit (17) does not define a single valued function $u = u(t, x)$. At time T a shock is formed, and the solution can be extended for $t > T$ in the weak sense, as in (4).

Example 3 (shock formation in Burgers' equation). Consider the scalar conservation law (inviscid Burgers' equation)

$$u_t + \left(\frac{u^2}{2}\right)_x \;=\; 0 \tag{18}$$

with initial condition

$$u(0, x) \;=\; \bar{u}(x) \;=\; \frac{1}{1 + x^2}.$$

For $t > 0$ small the solution can be found by the method of characteristics. Indeed, if u is smooth, (18) is equivalent to

$$u_t + uu_x = 0. \tag{19}$$

By (19) the directional derivative of the function $u = u(t, x)$ along the vector $(1, u)$ vanishes. Therefore, u must be constant along the characteristic lines in the t-x plane:

$$t \;\mapsto\; \big(t,\; x + t\bar{u}(x)\big) \;=\; \left(t,\; x + \frac{t}{1 + x^2}\right).$$

For $t < T \doteq 8/\sqrt{27}$, these lines do not intersect (Fig. 7). The solution to our Cauchy problem is thus given implicitly by

$$u\left(t,\; x + \frac{t}{1 + x^2}\right) \;=\; \frac{1}{1 + x^2}. \tag{20}$$

On the other hand, when $t > T$, the characteristic lines start to intersect. As a result, the map

$$x \mapsto x + \frac{t}{1+x^2}$$

is not one-to-one and (20) no longer defines a single valued solution of our Cauchy problem.

An alternative point of view is the following (Fig. 5). As time increases, points on the graph of $u(t,\cdot)$ move horizontally with speed u, equal to their distance from the x-axis. This determines a change in the profile of the solution. As t approaches the critical time $T \doteq 8/\sqrt{27}$, one has

$$\lim_{t\to T-} \left\{ \inf_{x\in I\!R} u_x(t,x) \right\} = -\infty,$$

and no classical solution exists beyond time T. The solution can be prolonged for all times $t \geq 0$ only within a class discontinuous functions.

1.6 Wave Interactions

Consider the quasilinear, strictly hyperbolic system

$$u_t = -A(u)u_x. \tag{21}$$

If the matrix A is independent of u, then the solution can be obtained as a superposition of traveling waves. On the other hand, if A depends on u, these waves can interact with each other, producing additional waves. To understand this nonlinear effect, define the i-th component of the gradient u_x as

$$u_x^i \doteq l_i \cdot u_x. \tag{22}$$

We regard u_x^i as the i-th component of the gradient u_x w.r.t. the basis of eigenvectors $\{r_1(u),\ldots,r_n(u)\}$. Equivalently, one can also think of u_x^i as the density of i-waves in the solution u. From (22) and (8), (21) it follows

$$u_x = \sum_{i=1}^n u_x^i r_i(u) \qquad\qquad u_t = -\sum_{i=1}^n \lambda_i(u) u_x^i r_i(u)$$

Differentiating the first equation w.r.t. t and the second one w.r.t. x, then equating the results, one obtains a system of evolution equations for the scalar components u_x^i, namely

$$(u_x^i)_t + (\lambda_i u_x^i)_x = \sum_{j>k} (\lambda_j - \lambda_k)\Big(l_i \cdot [r_j, r_k]\Big) u_x^j u_x^k. \tag{23}$$

See [8] or [42] for details. Notice that the left hand side of (23) is in conservation form. However, here the total amount of waves can increase in time, due to the source terms on the right hand side. The source term

$$S_{ijk} \doteq (\lambda_j - \lambda_k)\Big(l_i \cdot [r_j, r_k]\Big) u_x^j u_x^k$$

describes the amount of i-waves produced by the interaction of j-waves with k-waves. Here

$$\begin{aligned}
\lambda_j - \lambda_k &= [\text{difference in speed}] \\
&= [\text{rate at which} j - \text{waves and} k - \text{waves cross each other}] \\
u_x^j u_x^k &= [\text{density of} j - \text{waves}] \times [\text{density of} k - \text{waves}] \\
[r_j, r_k] &= (Dr_k)r_j - (Dr_j)r_k \quad (\text{Lie bracket}) \\
&= [\text{directional derivative of } r_k \text{ in the direction of } r_j] \\
&\quad - [\text{directional derivative of } r_j \text{ in the direction of } r_k].
\end{aligned}$$

Finally, the product $l_i \cdot [r_j, r_k]$ gives the i-th component of the Lie bracket $[r_j, r_k]$ along the basis of eigenvectors $\{r_1, \dots, r_n\}$.

2 Weak Solutions

A basic feature of nonlinear hyperbolic systems is the possible loss of regularity: solutions which are initially smooth may become discontinuous within finite time. In order to construct solutions globally in time, we are thus forced to work in a space of discontinuous functions, and interpret the conservation equations in a distributional sense.

Definition 2 (weak solution). Let $f : I\!R^n \mapsto I\!R^n$ be a smooth vector field. A measurable function $u = u(t,x)$, defined on an open set $\Omega \subseteq I\!R \times I\!R$ and with values in $I\!R^n$, is a *weak solution* of the system of conservation laws

$$u_t + f(u)_x = 0 \tag{24}$$

if, for every $\mathscr{C}^1$ function $\phi : \Omega \mapsto I\!R$ with compact support, one has

$$\iint_\Omega \{u\,\phi_t + f(u)\,\phi_x\}\, dxdt = 0. \tag{25}$$

Observe that no continuity assumption is made on u. To make sense of the integral in (25) we only need that u and $f(u)$ be locally integrable in Ω. Notice also that weak solutions are defined up to $\mathbf{L}^1$ equivalence. A solution is not affected by changing its values on a set of measure zero in the t-x plane. An easy consequence of the above definition is the closure of the set of solutions w.r.t. convergence in $\mathbf{L}^1_{\mathrm{loc}}$.

Lemma 1. *Let $(u_m)_{m\geq 1}$ be a uniformly bounded sequence of distributional solutions of (24). If $u_m \to u$ and $f(u_m) \to f(u)$ in $\mathbf{L}^1_{\mathrm{loc}}$ then the limit function u is also a weak solution.*

Indeed, for every $\phi \in \mathscr{C}^1_c$ one has

$$\iint_\Omega \left\{u\,\phi_t + f(u)\,\phi_x\right\} dxdt \;=\; \lim_{m\to\infty} \iint_\Omega \left\{u_m\,\phi_t + f(u_m)\,\phi_x\right\} dxdt \;=\; 0.$$

□

We observe that, in particular, the assumptions of the lemma are satisfied if $u_m \to u$ in $\mathbf{L}^1_{loc}$ and the flux function f is bounded.

In the following, we shall be mainly interested in solutions defined on a strip $[0,T] \times I\!R$, with an assigned initial condition

$$u(0,x) = \bar{u}(x). \tag{26}$$

Here $\bar{u} \in \mathbf{L}^1_{\mathrm{loc}}(I\!R)$. To treat the initial value problem, it is convenient to require some additional regularity w.r.t. time.

Definition 3 (weak solution to the Cauchy problem). A function $u : [0,T] \times I\!R \mapsto I\!R^n$ is a *weak solution* of the Cauchy problem (24), (26) if u is continuous as a function from $[0,T]$ into $\mathbf{L}^1_{\mathrm{loc}}$, the initial condition (26) holds and the restriction of u to the open strip $]0,T[\,\times I\!R$ is a distributional solution of (24).

Remark 1 (classical solutions). Let u be a weak solution of (24). If u is continuously differentiable restricted to an open domain $\widetilde{\Omega} \subseteq \Omega$, then at every point $(t,x) \in \widetilde{\Omega}$, the function u must satisfy the quasilinear system

$$u_t + A(u)u_x = 0, \tag{27}$$

with $A(u) \doteq Df(u)$. Indeed, from (25) an integration by parts yields

$$\iint \left[u_t + A(u)u_x\right]\phi\, dxdt = 0.$$

Since this holds for every $\phi \in \mathscr{C}^1_c(\widetilde{\Omega})$, the identity (27) follows.

2.1 Rankine–Hugoniot Conditions

Next, we look at a discontinuous solution and derive some conditions which must be satisfied at points of jump. Consider first the simple case of a piecewise constant function, say

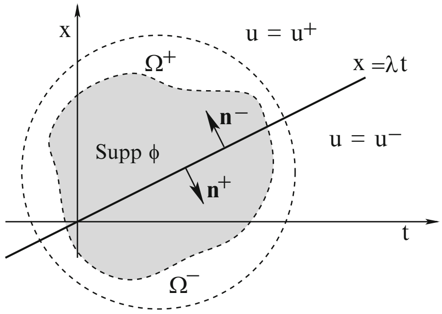

Fig. 8 Deriving the Rankine–Hugoniot equations. Here the *shaded area* describes the support of the test function ϕ

$$U(t,x) = \begin{cases} u^+ & \text{if} \quad x > \lambda t, \\ u^- & \text{if} \quad x < \lambda t, \end{cases} \tag{28}$$

for some $u^-, u^+ \in I\!R^n$, $\lambda \in I\!R$.

Lemma 2. *If the function U in (2.5) is a weak solution of the system of conservation laws (2.1), then*

$$\lambda\,(u^+ - u^-) = f(u^+) - f(u^-). \tag{29}$$

Proof. Let $\phi = \phi(t,x)$ be any continuously differentiable function with compact support. Let Ω be an open disc containing the support of ϕ and consider the two domains

$$\Omega^+ \doteq \Omega \cap \{x > \lambda t\}, \qquad \Omega^- \doteq \Omega \cap \{x < \lambda t\},$$

as in Fig. 8. Introducing the vector field $\mathbf{v} \doteq \big(U\phi,\ f(U)\phi\big)$, and recalling that U is constant separately on Ω_- and on Ω_+, we write the identity (25) as

$$\iint_{\Omega^+\cup\Omega^-} \Big\{U\phi_t + f(U)\phi_x\Big\}\,dxdt \;=\; \left(\iint_{\Omega^+} + \iint_{\Omega^-}\right) \operatorname{div}\mathbf{v}\,dxdt \;=\; 0. \tag{30}$$

We now apply the divergence theorem separately on the two domains Ω^+, Ω^-. Call $\mathbf{n}^+, \mathbf{n}^-$ the outer unit normals to Ω^+, Ω^-, respectively. Observe that $\phi = 0$ on the boundary $\partial\Omega$. Therefore, the only portion of the boundaries $\partial\Omega_-, \partial\Omega_+$ where $\mathbf{v} \neq 0$ is the line where $x = \lambda t$. Denoting by ds the differential of the arc-length, along the line $\{x = \lambda t\}$ we have

$$\mathbf{n}^+\,ds = (\lambda,\ -1)\,dt \qquad\qquad \mathbf{n}^-\,ds = (-\lambda,\ 1)\,dt\,,$$

$$\begin{aligned} 0 = \iint_{\Omega^+\cup\Omega^-} \operatorname{div}\mathbf{v}\,dxdt \;&=\; \int_{\partial\Omega^+} \mathbf{n}^+\cdot\mathbf{v}\,ds + \int_{\partial\Omega^-} \mathbf{n}^-\cdot\mathbf{v}\,ds \\ &= \int \big[\lambda u^+ - f(u^+)\big]\,\phi(t,\lambda t)\,dt + \int \big[-\lambda u^- + f(u^-)\big]\,\phi(t,\lambda t)\,dt. \end{aligned}$$

Therefore, the identity

$$\int \big[\lambda(u^+ - u^-) - f(u^+) + f(u^-)\big]\,\phi(t, \lambda t)\,dt \;=\; 0$$

must hold for every function $\phi \in \mathscr{C}^1_c$. This implies (29). □

The vector equations (29) are the famous *Rankine–Hugoniot conditions*. They form a set of n scalar equations relating the right and left states $u^+, u^- \in I\!R^n$ and the speed λ of the discontinuity, namely:

$$\text{[speed of the shock]} \times \text{[jump in the state]} \;=\; \text{[jump in the flux]}.$$

An alternative way of writing these conditions is as follows. Denote by $A(u) = Df(u)$ the $n \times n$ Jacobian matrix of f at u. For any $u, v \in I\!R^n$, define the averaged matrix

$$A(u,v) \doteq \int_0^1 A\big(\theta v + (1-\theta)u\big)\,d\theta \tag{31}$$

and call $\lambda_i(u,v)$, $i = 1,\ldots,n$, its eigenvalues. We observe that $A(u,v) = A(v,u)$ and $A(u,u) = A(u)$. Equation (29) can now be written in the equivalent form

$$\begin{aligned} \lambda\,(u^+ - u^-) \;&=\; f(u^+) - f(u^-) = \int_0^1 Df\big(\theta u^+ + (1-\theta)u^-\big)\cdot(u^+ - u^-)\,d\theta \\ &= A(u^-, u^+)\cdot(u^+ - u^-). \end{aligned} \tag{32}$$

In other words, the Rankine–Hugoniot conditions hold if and only if the jump $u^+ - u^-$ is an eigenvector of the averaged matrix $A(u^-, u^+)$ and the speed λ coincides with the corresponding eigenvalue.

Remark 2. In the scalar case, one arbitrarily assign the left and right states $u^-, u^+ \in I\!R$ and determine the shock speed as

$$\lambda \;=\; \frac{f(u^+) - f(u^-)}{u^+ - u^-} \;=\; \frac{1}{u^+ - u^-}\int_{u^-}^{u^+} f'(s)\,ds. \tag{33}$$

A geometric interpretation of these identities (see Fig. 9) is that

$$\begin{aligned} \text{[speed of the shock]} \;&=\; \text{[slope of secant line through } u^-, u^+ \text{ on the graph of } f] \\ &=\; \text{[average of the characteristic speeds between } u^- \text{ and } u^+]. \end{aligned}$$

We now consider a more general solution $u = u(t,x)$ of (24) and show that the Rankine–Hugoniot equations are still satisfied at every point (τ, ξ) where u has an approximate jump, in the following sense [32].

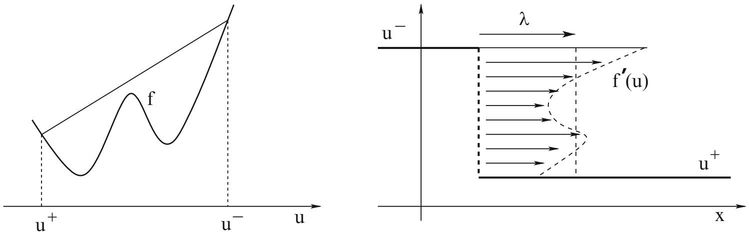

Fig. 9 The Rankine–Hugoniot equation in the scalar case

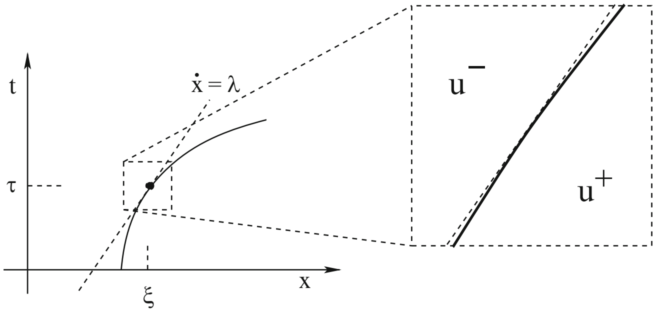

Fig. 10 A point of approximate jump. Looking through a microscope, i.e. rescaling the variables t, x in a neighborhood of the point (τ, ξ), the function u becomes arbitrarily close (in an integral sense) to the piecewise constant function U in (28)

Definition 4 (approximate jump). We say that a function $u = u(t, x)$ has an *approximate jump discontinuity* at the point (τ, ξ) if there exists vectors $u^+ \neq u^-$ and a speed λ such that, defining U as in (28), there holds

$$\lim_{r \to 0+} \frac{1}{r^2} \int_{-r}^{r} \int_{-r}^{r} \Big| u(\tau + t,\ \xi + x) - U(t, x) \Big|\, dxdt \;=\; 0. \tag{34}$$

Moreover, we say that u is *approximately continuous* at the point (τ, ξ) if the above relations hold with $u^+ = u^-$ (and λ arbitrary).

Observe that the above definitions depend only on the $\mathbf{L}^1$ equivalence class of u. Indeed, the limit in (34) is unaffected if the values of u are changed on a set $\mathcal{N} \subset I\!R^2$ of Lebesgue measure zero.

Example 4 (a piecewise smooth function). Let $g^-, g^+ : I\!R^2 \mapsto I\!R^n$ be any two continuous functions and let $x = \gamma(t)$ be a smooth curve, with derivative $\dot\gamma(t) \doteq \frac{d}{dt}\gamma(t)$. Define the function (see Fig. 10)

$$u(t, x) \doteq \begin{cases} g^-(t, x) & \text{if} \quad x < \gamma(t), \\ g^+(t, x) & \text{if} \quad x > \gamma(t). \end{cases}$$

At a point (τ,ξ), with $\xi = \gamma(\tau)$, call $u^- \doteq g^-(\tau,\xi)$, $u^+ \doteq g^+(\tau,\xi)$. If $u^+ = u^-$, then u is continuous at (τ,ξ), hence also approximately continuous. On the other hand, if $u^+ \neq u^-$, then u has an approximate jump at (τ,ξ). Indeed, writing $\dot\gamma(t) = \frac{d\gamma}{dt}$, the limit (34) holds with $\lambda = \dot\gamma(\tau)$ and U as in (28).

We now prove the Rankine–Hugoniot conditions in the more general case of a point of approximate jump.

Theorem 1 (Rankine–Hugoniot equations). *Let u be a bounded distributional solution of (24) having an approximate jump at a point (τ,ξ). In other words, assume that (34) holds, for some states u^-, u^+ and a speed λ, with U as in (28). Then the Rankine–Hugoniot equations (29) hold.*

Proof. For any given $\theta > 0$, the rescaled function

$$u^\theta(t,x) \doteq u(\tau + \theta t,\ \xi + \theta x)$$

is also a solution to the system of conservation laws. We claim that, as $\theta \to 0$, the convergence $u^\theta \to U$ holds in $\mathbf{L}^1_{\mathrm{loc}}(I\!R^2;\ I\!R^n)$. Indeed, for any $R > 0$ one has

$$\begin{aligned}
&\lim_{\theta\to 0} \int_{-R}^{R}\int_{-R}^{R} \left|u^\theta(t,x) - U(t,x)\right| dxdt \\
&\quad = \lim_{\theta\to 0} \frac{1}{\theta^2} \int_{-\theta R}^{\theta R}\int_{-\theta R}^{\theta R} \left|u(\tau + t,\ \xi + x) - U(t,x)\right| dxdt = 0
\end{aligned}$$

because of (34). Lemma 1 now implies that U itself is a distributional solution of (24), hence by Lemma 2 the Rankine–Hugoniot equations (29) hold. □

2.2 *Construction of Shock Curves*

In this section we consider the following problem. Given $u_0 \in I\!R^n$, find the states $u \in I\!R^n$ which, for some speed λ, satisfy the Rankine–Hugoniot equations

$$\lambda(u - u_0) = f(u) - f(u_0) = A(u_0, u)(u - u_0). \tag{35}$$

Trivially, the (35) are satisfied by setting $u = u_0$, with $\lambda \in I\!R$ arbitrary. Our aim is to construct non-trivial solutions with u close to u_0, relying on the implicit function theorem. Since this goal cannot be achieved by looking directly at the system (35), we adopt an alternative formulation.

Fix $i \in \{1,\dots,n\}$. By a classical result in linear algebra, the jump $u - u_0$ is a right i-eigenvector of the averaged matrix $A(u_0,u)$ if and only if it is orthogonal to all left eigenvectors $l_j(u_0,u)$ of $A(u_0,u)$, for every $j \neq i$. This means

$$\psi_j(u) \doteq l_j(u_0,u)\cdot(u - u_0) = 0 \qquad \text{for all } j \neq i. \tag{36}$$

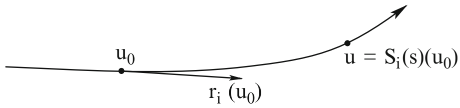

Fig. 11 Parameterization of the i-th shock curve through a point u_0

Instead of the system (35) of n equations in the $n + 1$ variables $(u, \lambda) = (u_1, \ldots, u_n, \lambda)$, we thus look at the system (36), consisting of $n - 1$ equations for the n variables $(u_1, \ldots, u_n)$.

The point $u = u_0$ is of course a solution. Moreover, the definition (31) trivially implies $A(u_0, u_0) = A(u_0)$, hence $l_j(u_0, u_0) = l_j(u_0)$ for all j. Linearizing the system (36) at $u = u_0$ we obtain the linear system of $n - 1$ equations

$$l_j(u_0) \cdot (u - u_0) = 0 \qquad\qquad j \neq i. \tag{37}$$

Since the left eigenvectors $l_j(u_0)$ are linearly independent, this has maximum rank.

We can thus apply the implicit function theorem to the nonlinear system (36) and conclude that, for each $i \in \{1, \ldots, n\}$, there exists a curve $s \mapsto S_i(s)(u_0)$ of points that satisfy (36). At the point u_0, this curve has to be perpendicular to all vectors $l_j(u_0)$, for $j \neq i$. Therefore, it must be tangent to the i-th eigenvector $r_i(u_0)$ (Fig. 11).

2.3 *Admissibility Conditions*

To motivate the following discussion, we first observe that the concept of weak solution is usually not stringent enough to achieve uniqueness for a Cauchy problem. In some cases, infinitely many weak solutions can be found, all with the same initial condition.

Example 5 (multiple weak solutions). For Burgers' equation

$$u_t + (u^2/2)_x = 0\,, \tag{38}$$

consider the Cauchy problem with initial data

$$u(0, x) = \begin{cases} 1 & \text{if} \quad x \geq 0, \\ 0 & \text{if} \quad x < 0. \end{cases}$$

As shown in Fig. 12, for every $0 < \alpha < 1$, a weak solution is

$$u_\alpha(t, x) = \begin{cases} 0 & \text{if} \quad x < \alpha t/2, \\ \alpha & \text{if} \quad \alpha t/2 \leq x < (1 + \alpha)t/2, \\ 1 & \text{if} \quad x \geq (1 + \alpha)t/2. \end{cases} \tag{39}$$

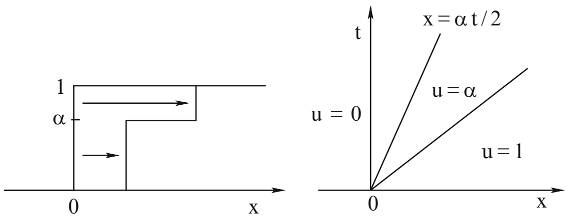

Fig. 12 For every $\alpha \in [0, 1]$ one obtains a different weak solution of Burgers' equation, always with the same initial data

Indeed, the piecewise constant function u_α trivially satisfies the equation outside the jumps. Moreover, the Rankine–Hugoniot conditions hold along the two lines of discontinuity $\{x = \alpha t/2\}$ and $\{x = (1+\alpha)t/2\}$, for all $t > 0$.

From the previous example it is clear that, in order to achieve the uniqueness of solutions and their continuous dependence on the initial data, the notion of weak solution must be supplemented with further "admissibility conditions". Three main approaches can be followed.

I: Singular limits.

Assume that, by physical considerations, the system of conservation laws (24) can be regarded as an approximation to a more general system, say

$$u_t + f(u)_x = \varepsilon \Lambda(u), \tag{40}$$

for some $\varepsilon > 0$ small. Here $\Lambda(u)$ is typically a higher order differential operator.

We then say that a weak solution $u = u(t, x)$ of the system of conservation laws (24) is "admissible" if there exists a sequence of solutions u^ε to the perturbed (40) which converges to u in $\mathbf{L}^1_{loc}$, as $\varepsilon \to 0+$.

A natural choice is to take the diffusion operator $\Lambda(u) \doteq u_{xx}$. This leads to

Admissibility Condition 1 (vanishing viscosity). A weak solution u of (24) is *admissible in the vanishing viscosity sense* if there exists a sequence of smooth solutions u^ε to

$$u^\varepsilon_t + f(u^\varepsilon)_x \;=\; \varepsilon u^\varepsilon_{xx} \tag{41}$$

which converge to u in $\mathbf{L}^1_{\text{loc}}$ as $\varepsilon \to 0+$.

The main drawback of this approach is that it is very difficult to provide a priori estimates on general solutions to the higher order system (40), and characterize the corresponding limits as $\varepsilon \to 0+$. For the vanishing viscosity approximations (41), this goal has been reached only recently in [7], within the class of solutions with small total variation. From the above condition, however, one can deduce other conditions which can be more easily verified in practice.

II: Entropy conditions.

An alternative approach relies on the concept of entropy.

Definition 5 (entropy and entropy flux). A continuously differentiable function $\eta : I\!R^n \mapsto I\!R$ is called an *entropy* for the system of conservation laws (24), with *entropy flux* $q : I\!R^n \mapsto I\!R$, if for all $u \in I\!R^n$ there holds

$$D\eta(u)\cdot Df(u) = Dq(u). \tag{42}$$

An immediate consequence of (42) is that, if $u = u(t,x)$ is a $\mathscr{C}^1$ solution of (24), then

$$\eta(u)_t + q(u)_x = 0. \tag{43}$$

Indeed,

$$\eta(u)_t + q(u)_x \;=\; D\eta(u)u_t + Dq(u)u_x \;=\; D\eta(u)\big(-Df(u)u_x\big) + Dq(u)u_x \;=\; 0.$$

In other words, for a smooth solution u, not only the quantities $u_1, \ldots, u_n$ are conserved but the additional conservation law (43) holds as well. However one should be aware that, when u is discontinuous, the quantity $\eta(u)$ may not be conserved.

Example 6. Consider Burgers' equation (38). Here the flux is $f(u) = u^2/2$. Taking $\eta(u) = u^3$ and $q(u) = (3/4)u^4$, one checks that the (42) is satisfied. Hence η is an entropy and q is the corresponding entropy flux. We observe that the function

$$u(0,x) \;=\; \begin{cases} 1 & \text{if} \quad x < t/2, \\ 0 & \text{if} \quad x \geq t/2, \end{cases}$$

is a (discontinuous) weak solution of (38). However, it does not satisfy (43) in distribution sense. Indeed, calling $u^- = 1$, $u^+ = 0$ the left and right states, and $\lambda = 1/2$ the speed of the shock, one has

$$\frac{3}{4} \;=\; q(u^+) - q(u^-) \;\neq\; \lambda\Big[\eta(u^+) - \eta(u^-)\Big] \;=\; \frac{1}{2}.$$

We now study how a convex entropy behaves in the presence of a small diffusion term. Assume $\eta, q \in \mathscr{C}^2$, with η convex. Multiplying both sides of (41) on the left by $D\eta(u^\varepsilon)$ and using (42) one finds

$$\big[\eta(u^\varepsilon)\big]_t + \big[q(u^\varepsilon)\big]_x \;=\; \varepsilon D\eta(u^\varepsilon)u^\varepsilon_{xx} \;=\; \varepsilon\Big\{\big[\eta(u^\varepsilon)\big]_{xx} - D^2\eta(u^\varepsilon)\cdot\big(u^\varepsilon_x \otimes u^\varepsilon_x\big)\Big\}. \tag{44}$$

Observe that the last term in (44) satisfies

$$D^2\eta(u^\varepsilon)\big(u^\varepsilon_x \otimes u^\varepsilon_x\big) \;=\; \sum_{i,j=1}^{n} \frac{\partial^2\eta(u^\varepsilon)}{\partial u_i \partial u_j} \cdot \frac{\partial u^\varepsilon_i}{\partial x}\frac{\partial u^\varepsilon_j}{\partial x} \geq 0,$$

because η is convex, hence its second derivative at any point u^ε is a positive semidefinite quadratic form. Multiplying (44) by a nonnegative smooth function φ with compact support and integrating by parts, we thus have

$$\iint \big\{\eta(u^\varepsilon)\varphi_t + q(u^\varepsilon)\varphi_x\big\}\, dxdt \;\geq\; -\varepsilon \iint \eta(u^\varepsilon)\varphi_{xx}\, dxdt.$$

If $u^\varepsilon \to u$ in $\mathbf{L}^1$ as $\varepsilon \to 0$, the previous inequality yields

$$\iint \left\{ \eta(u)\varphi_t + q(u)\varphi_x \right\} dxdt \ \geq \ 0 \tag{45}$$

whenever $\varphi \in \mathscr{C}_c^1$, $\varphi \geq 0$. The above can be restated by saying that $\eta(u)_t + q(u)_x \leq 0$ in distribution sense. The previous analysis leads to:

Admissibility Condition 2 (entropy inequality). A weak solution u of (24) is *entropy-admissible* if

$$\eta(u)_t + q(u)_x \ \leq \ 0 \tag{46}$$

in the sense of distributions, for every pair (η, q), where η is a convex entropy for (24) and q is the corresponding entropy flux.

For the piecewise constant function U in (28), an application of the divergence theorem shows that $\eta(U)_t + q(U)_x \leq 0$ in distribution if and only if

$$\lambda \left[\eta(u^+) - \eta(u^-) \right] \ \geq \ q(u^+) - q(u^-). \tag{47}$$

More generally, let $u = u(t, x)$ be a bounded function which satisfies the conservation law (24). Assume that u has an approximate jump at (τ, ξ), so that (34) holds with U as in (28). Then, by the rescaling argument used in the proof of Theorem 1, one can show that the inequality (47) must again hold.

We remark that the above admissibility condition can be useful only if some nontrivial convex entropy for the system (24) is known. For $n \times n$ systems of conservation laws, the (42) can be regarded as a first order system of n equations for the two scalar variables η, q, namely

$$\left(\frac{\partial \eta}{\partial u_1} \cdots \frac{\partial \eta}{\partial u_n} \right) \begin{pmatrix} \frac{\partial f_1}{\partial u_1} & \cdots & \frac{\partial f_1}{\partial u_n} \\ & \cdots & \\ \frac{\partial f_n}{\partial u_1} & \cdots & \frac{\partial f_n}{\partial u_n} \end{pmatrix} = \left(\frac{\partial q}{\partial u_1} \cdots \frac{\partial q}{\partial u_n} \right).$$

When $n \geq 3$, this system is overdetermined. In general, one should thus expect to find solutions only in the case $n \leq 2$. However, there are important physical examples of larger systems which admit a nontrivial entropy function.

III: Stability conditions.

Admissibility conditions on shocks can also be derived purely from stability consideration, without any reference to physical models.

We consider first the scalar case. Let $U = U(t, x)$ be the piecewise constant solution introduced in (28), with left and right states u^-, u^+. Let us slightly perturb the initial data by inserting an intermediate state $u^* \in [u^-, u^+]$, as in Fig. 13. The original shock is thus split in two smaller shocks, whose speeds are determined by the Rankine–Hugoniot equations.

To ensure that the $\mathbf{L}^1$ distance between the original solution and the perturbed one does not increase in time, we need:

$$[\text{speed of jump behind}] \ \geq \ [\text{speed of jump ahead}].$$

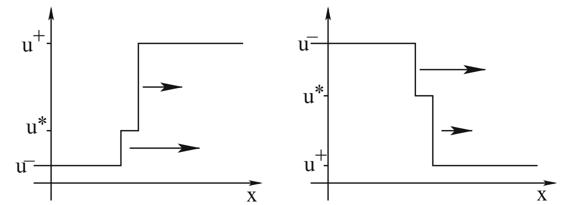

Fig. 13 In both cases $u^- < u^+$ or $u^- > u^+$, the solution is stable if the speed of the shock behind is greater or equal than the speed of the one ahead

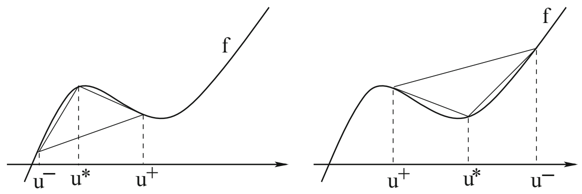

Fig. 14 Geometric interpretation of the stability conditions (48). In both cases, the jump with left state u^- and right state u^+ is admissible

By (33), this is the case if and only if

$$\frac{f(u^*) - f(u^-)}{u^* - u^-} \geq \frac{f(u^+) - f(u^*)}{u^+ - u^*} \qquad \text{for all} \quad u^* \in [u^-, u^+]. \tag{48}$$

From (48) we thus obtain the following stability conditions (see Fig. 14).

1. If $u^- < u^+$, on the interval $[u^-, u^+]$ the graph of f should remain above the secant line.
2. If $u^+ < u^-$, on the interval $[u^+, u^-]$ the graph of f should remain below the secant line.

Next, we seek a generalization of this stability conditions, valid also for $n \times n$ hyperbolic systems. Observe that, still in the scalar case, the condition (48) is equivalent to

$$\frac{f(u^*) - f(u^-)}{u^* - u^-} \geq \frac{f(u^+) - f(u^-)}{u^+ - u^-} \qquad \text{for all} \quad u^* \in [u^-, u^+]. \tag{49}$$

In other words, the speed of the original shock (u^-, u^+) should be not greater than the speed of any intermediate shock (u^-, u^*), where $u^* \in [u^-, u^+]$ is any intermediate state (Fig. 15).

Next, we consider $n \times n$ hyperbolic systems. As in Sect. 2.2, we let $s \mapsto S_i(s)(u^-)$ describe the i-shock curve through u^-. This is the curve of all states u that can be connected to u^- by a shock of the i-th family (Fig. 16).

Observe that, if $u^+ = S_i(\sigma)(u^-)$ and $u^* = S_i(s)(u^-)$ are two points on the i-shock curve through u^-, in general it is not true that the two states u^+ and u^* can be connected by a shock. For this reason, a straightforward generalization of the condition (48) to systems is not possible. However, the equivalent condition (49) has a natural extension to the vector valued case, namely:

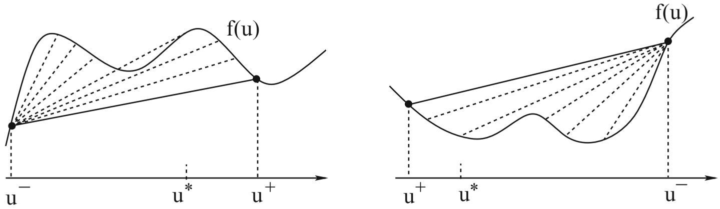

Fig. 15 Geometric interpretation of the stability conditions (49)

Fig. 16 The i-shock (u^-, u^+) satisfies the Liu admissibility conditions if its speed satisfies $\lambda_i(u^-, u^+) \le \lambda_i(u^-, u^*)$ for every intermediate state u^* along the i-shock curve through u^-

Admissibility Condition 3 (Liu condition). Let $u^+ = S_i(\sigma)(u^-)$ for some $\sigma \in I\!R$. We say that the shock with left and right states u^-, u^+ *satisfies the Liu admissibility condition* provided that its speed is less or equal to the speed of every smaller shock, joining u^- with an intermediate state $u^* = S_i(s)(u^-)$, $s \in [0, \sigma]$.

This condition was introduced by T.P. Liu in [45]. Much later, the paper [7] showed that, among solutions with small total variation, the Liu condition completely characterizes the ones which can be obtained as vanishing viscosity limits.

We conclude this section by mentioning another admissibility condition, introduced by Lax in [40] and widely used in the literature.

Admissibility Condition 4 (Lax condition). A shock of the i-th family, connecting the states u^-, u^+ and traveling with speed $\lambda = \lambda_i(u^-, u^+)$, *satisfies the Lax admissibility condition* if

$$\lambda_i(u^-) \ge \lambda_i(u^-, u^+) \ge \lambda_i(u^+). \tag{50}$$

To appreciate the geometric meaning of this condition, consider a piecewise smooth solution, having a discontinuity along the line $x = \gamma(t)$, where the solution jumps from a left state u^- to a right state u^+ (see Fig. 17). According to (32), this discontinuity must travel with a speed $\lambda \doteq \dot{\gamma} = \lambda_i(u^-, u^+)$ equal to the i-eigenvalue of the averaged matrix $A(u^-, u^+)$, for some $i \in \{1, \dots, n\}$. If we now look at the *i-characteristics*, i.e. at the solutions of the O.D.E.

$$\dot{x} = \lambda_i\big(u(t, x)\big),$$

we see that the Lax condition requires that these lines run into the shock, from both sides.

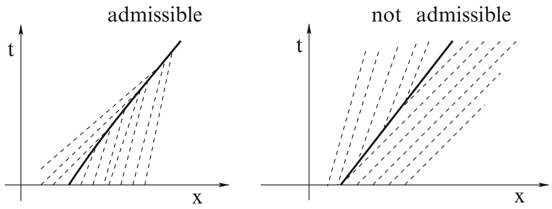

Fig. 17 *Left*: a shock satisfying the Lax condition. As time increases, characteristics run toward the shock, from both sides. *Right*: a shock violating this condition

3 The Riemann Problem

In this chapter we construct the solution to the *Riemann problem*, consisting of the system of conservation laws

$$u_t + f(u)_x = 0 \tag{51}$$

together with the simple, piecewise constant initial data

$$u(0,x) = \bar{u}(x) \doteq \begin{cases} u^- & \text{if} \qquad x < 0, \\ u^+ & \text{if} \qquad x > 0. \end{cases} \tag{52}$$

This will provide the basic building block toward the solution of the Cauchy problem with more general initial data.

This problem was first studied by B. Riemann in [52], in connection with the 2×2 system of isentropic gas dynamics. In [40], P. Lax constructed solutions to the Riemann problem for a wide class of $n \times n$ strictly hyperbolic systems. Further results were provided by T. P. Liu in [44], dealing with systems under generic assumptions. The paper [6] by S. Bianchini provides a fully general construction, valid even for systems not in conservation form. In this case, “solutions” are interpreted as limits of vanishing viscosity approximations.

The central role played by the Riemann problem, within the general theory of conservation laws, can be explained in terms of symmetries. We observe that, if $u = u(t,x)$ is a weak solution of (51), then for every $\theta > 0$ the rescaled function

$$u^\theta(t,x) \doteq u(\theta t,\ \theta x) \tag{53}$$

provides yet another solution. Among all solutions to a system of conservation laws, the Riemann problems yield precisely those weak solutions which are invariant w.r.t. the above rescaling: $u^\theta = u$ for every $\theta > 0$ (see Fig. 18).

3.1 Some Examples

We begin by describing the explicit solution of the Riemann problem (51)–(52) in a few elementary cases.

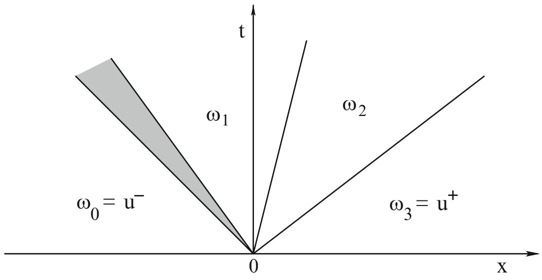

Fig. 18 The solution to a Riemann problem is constant along rays through the origin, in the t-x plane. Hence it is invariant w.r.t. the symmetry transformation (53)

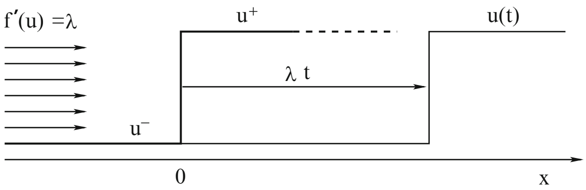

Fig. 19 A contact discontinuity. Here the characteristic speed $f'(u) \equiv \lambda$ is constant, for all values of $u \in [u^-, u^+]$

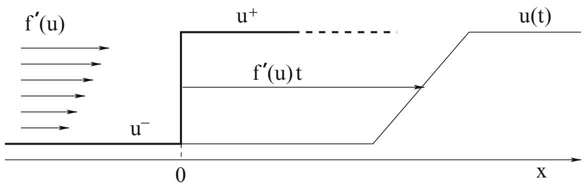

Fig. 20 The centered rarefaction wave defined at (54)

Example 7. Consider a scalar conservation law with linear flux $f(u) = \lambda u + c$.

As shown in Fig. 19, the solution of the Riemann problem is

$$u(t,x) = \begin{cases} u^- & \text{if} \quad x < \lambda t, \\ u^+ & \text{if} \quad x > \lambda t. \end{cases}$$

It consists of a single jump, called a *contact discontinuity*, traveling with speed λ.

Example 8. Consider a scalar conservation law with strictly convex flux, so that $u \mapsto f'(u)$ is strictly increasing. Moreover, assume that $u^+ > u^-$.

The solution is then a *centered rarefaction wave*, obtained by the method of characteristics (Fig. 20).

$$u(t,x) = \begin{cases} u^- & \text{if} \quad \frac{x}{t} < f'(u^-), \\ u^+ & \text{if} \quad \frac{x}{t} > f'(u^+), \\ \omega & \text{if} \quad \frac{x}{t} = f'(\omega) \text{ for some } \omega \in [u^-, u^+]. \end{cases} \tag{54}$$

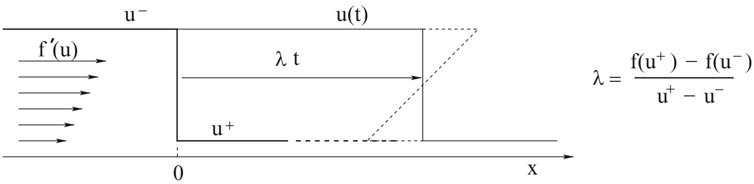

Fig. 21 A shock satisfying the admissibility conditions

Since the mapping $\omega \mapsto f'(\omega)$ is strictly increasing, for $\frac{x}{t} \in [f'(u^-)\,,\ f'(u^+)]$ there exists a unique value $\omega \in [u^-, u^+]$ such that $\frac{x}{t} = f'(\omega)$. The above function u is thus well defined.

Example 9. Consider again a scalar conservation law with strictly convex flux. However, we now assume that $u^+ < u^-$.

The solution consists of a single *shock*:

$$u(t,x) = \begin{cases} u^- & \text{if} \qquad x < \lambda t, \\ u^+ & \text{if} \qquad x > \lambda t, \end{cases} \tag{55}$$

As usual, the shock speed is determined by the Rankine–Hugoniot equations (33). We observe that this shock satisfies both the Liu and the Lax admissibility conditions.

Remark 3. The formula (55) defines a weak solution to the Riemann problem also in Example 8. However, if $u^- < u^+$, this solution does not satisfy the Liu admissibility condition. The Lax condition fails as well.

On the other hand, if $u^+ < u^-$, the formula (54) does not define a single valued function (Fig. 21). Hence it cannot provide a solution in Example 9.

Example 10. Consider the Riemann problem for a linear system:

$$u_t + Au_x = 0 \qquad\qquad u(0,x) = \begin{cases} u^- & \text{if} \qquad x < 0, \\ u^+ & \text{if} \qquad x > 0. \end{cases}$$

For linear systems, the general solution to the Cauchy problem was already constructed in (14).

For this particular initial data, the solution can be obtained as follows. Write the vector $u^+ - u^-$ as a linear combination of eigenvectors of A, i.e.

$$u^+ - u^- = \sum_{j=1}^{n} c_j r_j\,.$$

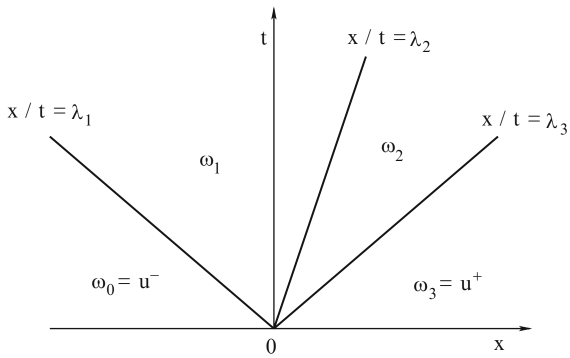

Fig. 22 Solution to the Riemann problem for a linear system

Define the intermediate states

$$\omega_i \doteq u^- + \sum_{j \le i} c_j r_j, \qquad i = 0, \dots, n.$$

The solution then takes the form

$$u(t,x) = \begin{cases} \omega_0 = u^- & for \quad x/t \ < \lambda_1, \\ & \dots \\ \omega_i & for \quad \lambda_i < x/t < \lambda_{i+1}, \\ & \dots \\ \omega_n = u^+ & for \quad x/t \ > \lambda_n. \end{cases} \tag{56}$$

Notice that, in this linear case, the general solution to the Riemann problem consists of n jumps. The i-th jump: $\omega_i - \omega_{i-1} = c_i r_i$ is parallel to the i-eigenvector of the matrix A and travels with speed λ_i, given by the corresponding eigenvalue (Fig. 22).

3.2 A Class of Hyperbolic Systems

We shall consider hyperbolic systems which satisfy the following simplifying assumption, introduced by P. Lax [40].

(H) For each $i = 1, \dots, n$, the i-th field is either *genuinely nonlinear*, so that $D\lambda_i(u) \cdot r_i(u) > 0$ for all u, or *linearly degenerate*, with $D\lambda_i(u) \cdot r_i(u) = 0$ for all u.

We recall that $D\lambda_i$ denotes the gradient of the scalar function $u \mapsto \lambda_i(u)$. Hence $D\lambda_i(u) \cdot r_i(u)$ is the directional derivative of λ_i in the direction of the vector r_i. Notice that, in the genuinely nonlinear case, the i-th eigenvalue λ_i is strictly increasing along each integral curve of the corresponding field of eigenvectors r_i.

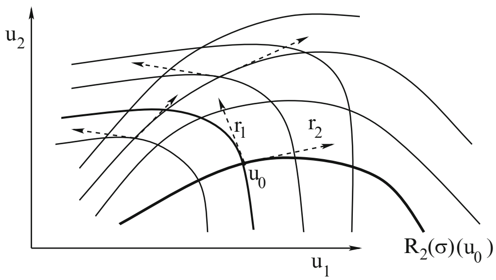

Fig. 23 Integral curves of the vector fields $r_1(u)$, $r_2(u)$

In the linearly degenerate case, on the other hand, the eigenvalue λ_i is constant along each such curve (see Fig. 23). With the above assumption (H), we are ruling out the possibility that, along some integral curve of an eigenvector r_i, the corresponding eigenvalue λ_i may partly increase and partly decrease, having several local maxima and minima.

Example 11 (isentropic gas dynamics). Denote by ρ the density of a gas, by $v = \rho^{-1}$ its specific volume and by u its velocity. A simple model for isentropic gas dynamics (in Lagrangian coordinates) is then provided by the so-called "p-system"

$$\begin{cases} v_t - u_x = 0\,, \\ u_t + p(v)_x = 0. \end{cases} \tag{57}$$

Here $p = p(v)$ is a function which determines the pressure in terms of of the specific volume. An appropriate choice is $p(v) = kv^{-\gamma}$, with $1 \le \gamma \le 3$. In the region where $v > 0$, the Jacobian matrix of the system is

$$A \doteq Df = \begin{pmatrix} 0 & -1 \\ p'(v) & 0 \end{pmatrix}.$$

The eigenvalues and eigenvectors are found to be

$$\lambda_1 = -\sqrt{-p'(v)}\,, \qquad \lambda_2 = \sqrt{-p'(v)}\,, \tag{58}$$

$$r_1 = \begin{pmatrix} 1 \\ \sqrt{-p'(v)} \end{pmatrix}, \qquad r_2 = \begin{pmatrix} -1 \\ \sqrt{-p'(v)} \end{pmatrix}. \tag{59}$$

It is now clear that the system is strictly hyperbolic provided that $p'(v) < 0$ for all $v > 0$. Moreover, observing that

$$D\lambda_1 \cdot r_1 = \frac{p''(v)}{2\sqrt{-p'(v)}} = D\lambda_2 \cdot r_2\,,$$

we conclude that both characteristic fields are genuinely nonlinear if $p''(v) > 0$ for all $v > 0$.

As we shall see in the sequel, if the assumption (H) holds, then the solution of the Riemann problem has a simple structure consisting of the superposition of n elementary waves: shocks, rarefactions or contact discontinuities. This considerably simplifies all further analysis. On the other hand, for strictly hyperbolic systems that do not satisfy the condition (H), basic existence and stability results can still be obtained, but at the price of heavier technicalities [44].

3.3 Elementary Waves

Fix a state $u_0 \in I\!R^n$ and an index $i \in \{1, \ldots, n\}$. As before, let $r_i(u)$ be an i-eigenvector of the Jacobian matrix $A(u) = Df(u)$. The integral curve of the vector field r_i through the point u_0 is called the *i-rarefaction curve* through u_0. It is obtained by solving the Cauchy problem in state space:

$$\frac{du}{d\sigma} = r_i(u), \qquad u(0) = u_0. \tag{60}$$

We shall denote this curve as

$$\sigma \mapsto R_i(\sigma)(u_0). \tag{61}$$

Clearly, the parametrization depends on the choice of the eigenvectors r_i. In particular, if we impose the normalization $\left|r_i(u)\right| \equiv 1$, then the rarefaction curve (61) will be parameterized by arc-length. In the genuinely nonlinear case, we always choose the orientation so that the eigenvalue $\lambda_i(u)$ increases as the parameter σ increases along the curve.

Next, for a fixed $u_0 \in I\!R^n$ and $i \in \{1, \ldots, n\}$, we consider the i-shock curve through u_0. This is the set of states u which can be connected to u_0 by an i-shock. As in Sect. 2.2, this curve will be parameterized as

$$\sigma \mapsto S_i(\sigma)(u_0). \tag{62}$$

Using a suitable parametrization (say, by arclength), one can show that the two curves R_i, S_i have a second order contact at the point u_0 (see Fig. 24). More precisely, the following estimates hold.

$$\begin{cases} R_i(\sigma)(u_0) = u_0 + \sigma r_i(u_0) + \mathcal{O}(1) \cdot \sigma^2, \\ S_i(\sigma)(u_0) = u_0 + \sigma r_i(u_0) + \mathcal{O}(1) \cdot \sigma^2, \end{cases} \tag{63}$$

$$\Big| R_i(\sigma)(u_0) - S_i(\sigma)(u_0) \Big| = \mathcal{O}(1) \cdot \sigma^3, \tag{64}$$

$$\lambda_i\Big(S_i(\sigma)(u_0),\ u_0\Big) = \lambda_i(u_0) + \frac{\sigma}{2} D\lambda_i(u_0) \cdot r_i(u_0) + \mathcal{O}(1) \cdot \sigma^2. \tag{65}$$

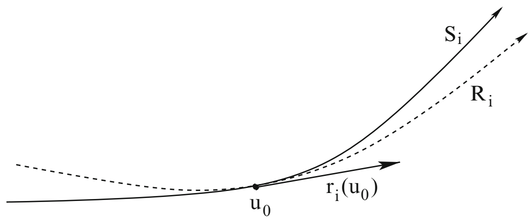

Fig. 24 The i-shock curve and the i-rarefaction curve through a point u_0

Here and throughout the following, the Landau symbol $\mathscr{O}(1)$ denotes a quantity whose absolute value satisfies a uniform bound, depending only on the system (51).

Toward the general solution of the Riemann problem (51)–(52), we first study three special cases.

1. Centered Rarefaction Waves. Let the i-th field be genuinely nonlinear, and assume that u^+ lies on the positive i-rarefaction curve through u^-, i.e. $u^+ = R_i(\sigma)(u^-)$ for some $\sigma > 0$. For each $s \in [0, \sigma]$, define the characteristic speed

$$\lambda_i(s) \;=\; \lambda_i\big(R_i(s)(u^-)\big).$$

Observe that, by genuine nonlinearity, the map $s \mapsto \lambda_i(s)$ is strictly increasing. Hence, for every $\lambda \in \big[\lambda_i(u^-),\ \lambda_i(u^+)\big]$, there is a unique value $s \in [0, \sigma]$ such that $\lambda = \lambda_i(s)$. For $t \geq 0$, we claim that the function

$$u(t,x) \;=\; \begin{cases} u^- & if \quad x/t \;<\; \lambda_i(u^-), \\ R_i(s)(u^-) & if \quad x/t \;=\; \lambda_i(s) \in \big[\lambda_i(u^-),\ \lambda_i(u^+)\big], \\ u^+ & if \quad x/t \;>\; \lambda_i(u^+), \end{cases} \tag{66}$$

is a piecewise smooth solution of the Riemann problem, continuous for $t > 0$. Indeed, from the definition it follows

$$\lim_{t \to 0+} \big\| u(t,\cdot) - \bar{u} \big\|_{\mathbf{L}^1} \;=\; 0.$$

Moreover, the (51) is trivially satisfied in the sectors where $x < t\lambda_i(u^-)$ or $x > t\lambda_i(u^+)$, because here $u_t = u_x = 0$. Next, assume $x = t\lambda_i(s)$ for some $s \in]0, \sigma[$. Since u is constant along each ray through the origin $\{x/t = c\}$, we have

$$u_t(t,x) + \frac{x}{t}\, u_x(t,x) \;=\; 0. \tag{67}$$

We now observe that the definition (66) implies $x/t = \lambda_i\big(u(t,x)\big)$. By construction, the vector u_x has the same direction as $r_i(u)$, hence it is an eigenvector of the Jacobian matrix $A(u) \doteq Df(u)$ with eigenvalue $\lambda_i(u)$. On the sector of the t-x plane where $\lambda_i(u^-) < x/t < \lambda_i(u^+)$ we thus have

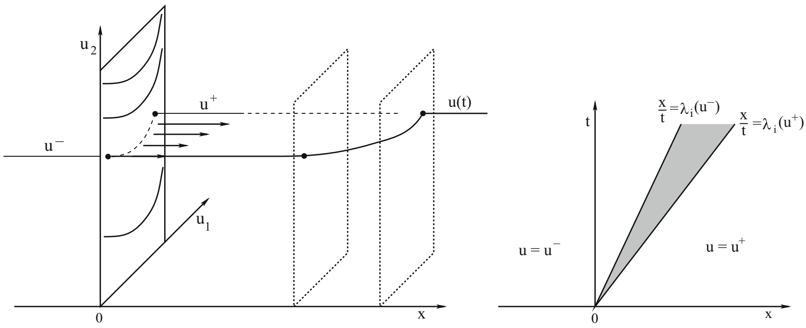

Fig. 25 A solution to the Riemann problem consisting of centered rarefaction wave. *Left*: the profile of the solution at a fixed time t, in the x-u space. *Right*: the values of u in the t-x plane

$$u_t + A(u)u_x \;=\; u_t + \lambda_i(u)u_x \;=\; 0\,,$$

proving our claim. As shown in Fig. 25, at a fixed time $t > 0$, the profile $x \mapsto u(t,x)$ is obtained as follows. Consider the rarefaction curve R_i joining u^- with u^+, on the hyperplane where $x = 0$. Move each point of this curve horizontally, in the amount $t\,\lambda_i(u)$. The new curve yields the graph of $u(t,\cdot)$. Notice that the assumption $\sigma > 0$ is essential for the validity of this construction. In the opposite case $\sigma < 0$, the definition (66) would yield a triple-valued function in the region where $x/t \in \big[\lambda_i(u^+)\,,\ \lambda_i(u^-)\big]$.

2. Shocks. Assume again that the i-th family is genuinely nonlinear and that the state u^+ is connected to the right of u^- by an i-shock, i.e. $u^+ = S_i(\sigma)(u^-)$. Then, calling $\lambda \doteq \lambda_i(u^+,u^-)$ the Rankine–Hugoniot speed of the shock, the function

$$u(t,x) \;=\; \begin{cases} u^- & if \qquad x < \lambda t, \\ u^+ & if \qquad x > \lambda t, \end{cases} \tag{68}$$

(Fig. 26) provides a piecewise constant solution to the Riemann problem. Observe that, if $\sigma < 0$, than this solution is entropy admissible in the sense of Lax. Indeed, since the speed is monotonically increasing along the shock curve, recalling (65) we have

$$\lambda_i(u^+) \;<\; \lambda_i(u^-,u^+) \;<\; \lambda_i(u^-). \tag{69}$$

Hence the Lax admissibility conditions (50) hold. In the case $\sigma > 0$, however, one has $\lambda_i(u^-) < \lambda_i(u^+)$ and the conditions (50) are violated.

3. Contact discontinuities. Assume that the i-th field is linearly degenerate and that the state u^+ lies on the i-th rarefaction curve through u^-, i.e. $u^+ = R_i(\sigma)(u^-)$ for some σ. By assumption, the i-th characteristic speed λ_i is constant along this curve. Choosing $\lambda = \lambda(u^-)$, the piecewise constant function (68) then provides a

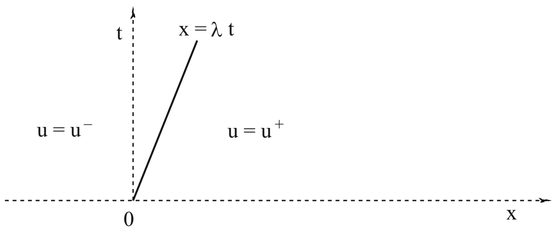

Fig. 26 A solution consisting of a single shock, or a contact discontinuity

solution to our Riemann problem. Indeed, the Rankine–Hugoniot conditions hold at the point of jump:

$$f(u^+) - f(u^-) = \int_0^\sigma Df\,(R_i(s)(u^-))\; r_i\,(R_i(s)(u^-))\; ds$$

$$= \int_0^\sigma \lambda(u^-)\, r_i\big(R_i(s)(u^-)\big)\, ds \;=\; \lambda_i(u^-)\cdot\Big(R_i(\sigma)(u^-) - u^-\Big). \tag{70}$$

In this case, the Lax entropy condition holds regardless of the sign of σ. Indeed,

$$\lambda_i(u^+) \;=\; \lambda_i(u^-, u^+) \;=\; \lambda_i(u^-). \tag{71}$$

Observe that, according to (70), for linearly degenerate fields the shock and rarefaction curves actually coincide: $S_i(\sigma)(u_0) = R_i(\sigma)(u_0)$ for all σ.

The above results can be summarized as follows. For a fixed left state u^- and $i \in \{1,\dots,n\}$ define the mixed curve

$$\Psi_i(\sigma)(u^-) \;=\; \begin{cases} R_i(\sigma)(u^-) & if \quad \sigma \geq 0, \\ S_i(\sigma)(u^-) & if \quad \sigma < 0. \end{cases} \tag{72}$$

In the special case where $u^+ = \Psi_i(\sigma)(u^-)$ for some σ, the Riemann problem can then be solved by an elementary wave: a rarefaction, a shock or a contact discontinuity.

3.4 General Solution of the Riemann Problem

Relying on the previous analysis, the solution of the general Riemann problem (51)–(52) can now be obtained by finding intermediate states $\omega_0 = u^-$, $\omega_1, \dots, \omega_n = u^+$ such that each pair of adjacent states ω_{i-1}, ω_i can be connected by an elementary wave, i. e.

$$\omega_i \;=\; \Psi_i(\sigma_i)(\omega_{i-1}) \qquad\qquad i = 1,\dots,n. \tag{73}$$

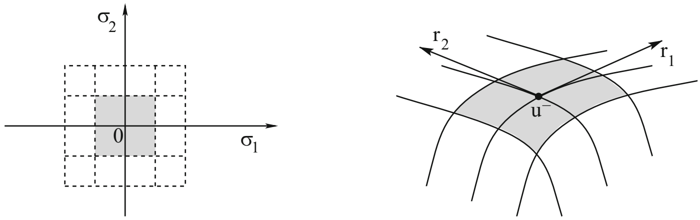

Fig. 27 The range of the map $(\sigma_1, \sigma_2) \mapsto \Psi_2(\sigma_2) \circ \Psi_1(\sigma_1)(u^-)$ covers a whole neighborhood of u^-

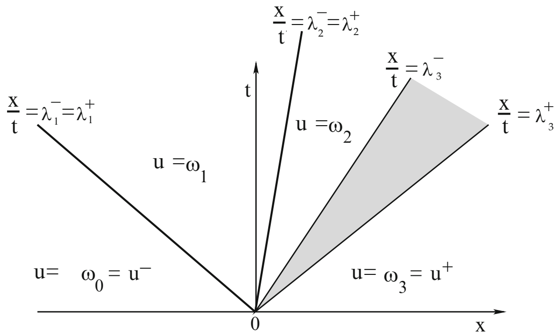

Fig. 28 A solution to the Riemann problem, consisting of a 1-shock, a 2-contact, and a 3-rarefaction

This can be done whenever u^+ is sufficiently close to u^-. Indeed, consider the map

$$\Lambda(\sigma_1, \ldots, \sigma_n) \;=\; \Psi_n(\sigma_n) \circ \cdots \circ \Psi_1(\sigma_1)(u^-).$$

Taking a first order Taylor expansion at the point $(\sigma_1, \ldots, \sigma_n) = (0, \ldots, 0)$ we obtain the affine map

$$(\sigma_1, \ldots, \sigma_n) \;\mapsto\; u^- + \sum_{i=1}^{n} \sigma_i r_i(u^-).$$

Since $\{r_1, \ldots, r_n\}$ is a basis of the space $I\!R^n$, the above map has full rank (it is one-to-one and surjective). We can thus apply the implicit function theorem and conclude that the nonlinear mapping Λ is a continuous bijection of a neighborhood of the origin in $I\!R^n$ onto a neighborhood of u^- (Fig. 27).

Therefore, for u^+ sufficiently close to u^-, there exist unique wave strengths $\sigma_1, \ldots \sigma_n$ such that

$$u^+ \;=\; \Psi_n(\sigma_n) \circ \cdots \circ \Psi_1(\sigma_1)(u^-). \tag{74}$$

In turn, these determine the intermediate states ω_i in (73). The complete solution is now obtained by piecing together the solutions of the n Riemann problems (Fig. 28)

$$u_t + f(u)_x = 0, \qquad u(0,x) = \begin{cases} \omega_{i-1} & if \quad x < 0, \\ \omega_i & if \quad x > 0, \end{cases} \tag{75}$$

on different sectors of the t-x plane. By construction, each of these problems has an entropy-admissible solution consisting of a simple wave of the i-th characteristic family. More precisely:

CASE 1: The i-th characteristic field is genuinely nonlinear and $\sigma_i > 0$. Then the solution of (75) consists of a centered rarefaction wave. The i-th characteristic speeds range over the interval $[\lambda_i^-, \ \lambda_i^+]$, defined as

$$\lambda_i^- \doteq \lambda_i(\omega_{i-1}), \qquad \lambda_i^+ \doteq \lambda_i(\omega_i).$$

CASE 2: Either the i-th characteristic field is genuinely nonlinear and $\sigma_i \le 0$, or else the i-th characteristic field is linearly degenerate (with σ_i arbitrary). Then the solution of (75) consists of an admissible shock or a contact discontinuity, traveling with Rankine–Hugoniot speed

$$\lambda_i^- \doteq \lambda_i^+ \doteq \lambda_i(\omega_{i-1}, \omega_i).$$

The solution to the original problem (51)–(52) can now be constructed by piecing together the solutions of the n Riemann problems (75), $i = 1, \dots, n$. Indeed, for $\sigma_1, \dots, \sigma_n$ sufficiently small, the speeds λ_i^-, λ_i^+ introduced above remain close to the corresponding eigenvalues $\lambda_i(u^-)$ of the matrix $A(u^-)$. By strict hyperbolicity and continuity, we can thus assume that the intervals $[\lambda_i^-, \lambda_i^+]$ are disjoint, i.e.

$$\lambda_1^- \le \lambda_1^+ < \lambda_2^- \le \lambda_2^+ < \cdots < \lambda_n^- \le \lambda_n^+.$$

Therefore, a piecewise smooth solution $u : [0, \infty) \times I\!R \mapsto I\!R^n$ is well defined by the assignment

$$u(t,x) = \begin{cases} u^- = \omega_0 & \text{if} \quad x/t \in \,]-\infty, \ \lambda_1^-[\,, \\ R_i(s)(\omega_{i-1}) & \text{if} \quad x/t = \lambda_i\big(R_i(s)(\omega_{i-1})\big) \in \big[\lambda_i^-, \ \lambda_i^+\big[\,, \\ \omega_i & \text{if} \quad x/t \in \big[\lambda_i^+, \ \lambda_{i+1}^-\big[\,, \\ u^+ = \omega_n & \text{if} \quad x/t \in \big[\lambda_n^+, \ \infty\big[\,. \end{cases} \tag{76}$$

Observe that this solution is self-similar, having the form $u(t,x) = \psi(x/t)$, with $\psi : I\!R \mapsto I\!R^n$ possibly discontinuous.

3.5 The Riemann Problem for the p-System

Example 12 (the p-system). Consider again the equations for isentropic gas dynamics (in Lagrangian coordinates)

$$\begin{cases} v_t - u_x = 0\,, \\ u_t + p(v)_x = 0. \end{cases} \tag{77}$$

Writing $U = (v, u)$, the Riemann problem takes the form

$$U(0,x) = \begin{cases} U^- = (v^-, u^-) & if \quad x < 0, \\ U^+ = (v^+, u^+) & if \quad x > 0. \end{cases} \tag{78}$$

Here u^-, u^+ are the velocities to the left and to the right of the initial jump, while $v^-, v^+ > 0$ are the specific volumes.

By (59), the 1-rarefaction curve through U^- is obtained by solving the Cauchy problem

$$\frac{du}{dv} = \sqrt{-p'(v)}, \qquad\qquad u(v^-) = u^-.$$

This yields the curve

$$R_1 = \left\{ (v,u); \quad u - u^- = \int_{v^-}^{v} \sqrt{-p'(y)}\, dy \right\}. \tag{79}$$

Similarly, the 2-rarefaction curve through the point U^- is

$$R_2 = \left\{ (v,u); \quad u - u^- = -\int_{v^-}^{v} \sqrt{-p'(y)}\, dy \right\}. \tag{80}$$

The shock curves S_1, S_2 through the left state U^- are obtained from the Rankine–Hugoniot conditions

$$\lambda(v - v^-) = -(u - u^-), \qquad\qquad \lambda(u - u^-) = p(v) - p(v^-). \tag{81}$$

One can use the first equation in (81) to obtain the shock speed λ. From the second equation, the shock curves are then computed as

$$S_1 = \left\{ (v,u); \qquad -(u-u^-)^2 = (v-v^-)\big(p(v) - p(v^-)\big), \quad \lambda \doteq -\frac{u-u^-}{v-v^-} < 0 \right\}, \tag{82}$$

$$S_2 = \left\{ (v,u); \qquad -(u-u^-)^2 = (v-v^-)\big(p(v) - p(v^-)\big), \quad \lambda \doteq -\frac{u-u^-}{v-v^-} > 0 \right\}. \tag{83}$$

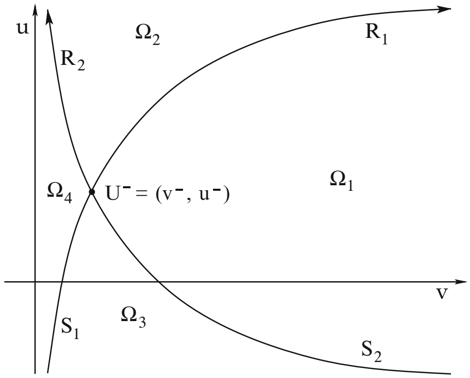

Fig. 29 Shocks and rarefaction curves through the point $U^- = (v^-, u^-)$

By (58)–(59) and the assumptions $p'(v) < 0$, $p''(v) > 0$, the directional derivatives of the eigenvalues λ_1, λ_2 in the direction of the corresponding eigenvectors r_1, r_2 are found to be

$$(D\lambda_1)r_1 \;=\; (D\lambda_2)r_2 \;=\; \frac{p''(v)}{2\sqrt{-p'(v)}} \;>\; 0. \tag{84}$$

Therefore, the Riemann problem (77)–(78) admits a solution in the form of a centered rarefaction wave provided that $U^+ \in R_1$, $v^+ > v^-$, or else $U^+ \in R_2$, $v^+ < v^-$. On the other hand, a shock connecting U^- with U^+ will be admissible if either $U^+ \in S_1$ and $v^+ < v^-$, or else $U^+ \in S_2$ and $v^+ > v^-$.

Taking the above admissibility conditions into account, we thus obtain four curves originating from the point $U^- = (v^-, u^-)$. Namely, the two rarefaction curves

$$\sigma \mapsto R_1(\sigma),\; R_2(\sigma) \qquad\qquad \sigma \geq 0,$$

and the two shock curves

$$\sigma \mapsto S_1(\sigma),\; S_2(\sigma) \qquad\qquad \sigma \leq 0.$$

In turn, these curves divide a neighborhood of U^- into four regions (Fig. 29):

$$\begin{array}{llll} \Omega_1: & \text{bounded by } R_1, S_2, & \quad \Omega_2: & \text{bounded by } R_1, R_2, \\ \Omega_3: & \text{bounded by } S_1, S_2, & \quad \Omega_4: & \text{bounded by } S_1, R_2. \end{array}$$

For $U^+ = (v^+, u^+)$ sufficiently close to $U^- = (v^-, u^-)$, the structure of the general solution to the Riemann problem is now determined by the location of the state U^+, with respect to the curves R_i, S_i (Fig. 30).

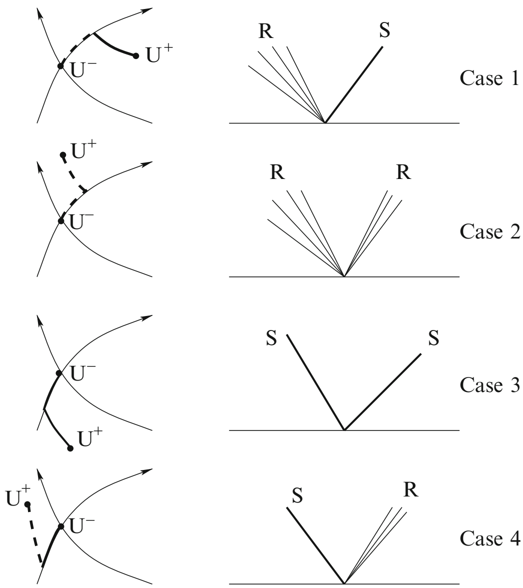

Fig. 30 Solution to the Riemann problem for the p-system. The four different cases

CASE 1: $U^+ \in \Omega_1$. The solution consists of a 1-rarefaction wave and a 2-shock.
CASE 2: $U^+ \in \Omega_2$. The solution consists of two centered rarefaction waves.
CASE 3: $U^+ \in \Omega_3$. The solution consists of two shocks.
CASE 4: $U^+ \in \Omega_4$. The solution consists of a 1-shock and a 2-rarefaction wave.

Remark 4. Consider a 2×2 strictly hyperbolic system of conservation laws. Assume that the i-th characteristic field is genuinely nonlinear. The relative position of the i-shock and the i-rarefaction curve through a point u_0 can be determined as follows (Fig. 24). Let $\sigma \mapsto R_i(\sigma)$ be the i-rarefaction curve, parameterized so that $\lambda_i\big(R_i(\sigma)\big) = \lambda_i(u_0) + \sigma$. Assume that, for some constant α, the point

$$S_i(\sigma) = R_i(\sigma) + \big(\alpha\sigma^3 + o(\sigma^3)\big)r_j(u_0) \tag{85}$$

lies on the i-shock curve through u_0, for all σ. Here the Landau symbol $o(\sigma^3)$ denotes a higher order infinitesimal, as $\sigma \to 0$. The wedge product of two vectors in $I\!R^2$ is defined as $\begin{pmatrix} a \\ b \end{pmatrix} \wedge \begin{pmatrix} c \\ d \end{pmatrix} \doteq ad - bc$. We then have

$$\begin{aligned} &\Psi(\sigma) \\ &\doteq \Big[R_i(\sigma) + \big(\alpha\sigma^3 + o(\sigma^3)\big)r_j(u_0) - u_0\Big] \wedge \Big[f\Big(R_i(\sigma) + \big(\alpha\sigma^3 + o(\sigma^3)\big)r_j(u_0)\Big) - f(u_0)\Big] \\ &\doteq A(\sigma) \wedge B(\sigma) \equiv 0. \end{aligned}$$

Indeed, the Rankine–Hugoniot equations imply that the vectors $A(\sigma)$ and $B(\sigma)$ are parallel. According to Leibnitz' rule, the fourth derivative is computed by

$$\begin{aligned}\frac{d^4}{d\sigma^4}\Psi = \ & \left(\frac{d^4}{d\sigma^4}A\right)\wedge B + 4\left(\frac{d^3}{d\sigma^3}A\right)\wedge\left(\frac{d}{d\sigma}B\right) + 6\left(\frac{d^2}{d\sigma^2}A\right)\wedge\left(\frac{d^2}{d\sigma^2}B\right)\\ & +4\left(\frac{d}{d\sigma}A\right)\wedge\left(\frac{d^3}{d\sigma^3}B\right) + A\wedge\left(\frac{d^4}{d\sigma^4}B\right)\end{aligned}$$

By the choice of the parametrization, $\frac{d}{d\sigma}\lambda_i\big(R_i(\sigma)\big)\equiv 1$. Hence

$$\begin{aligned}\frac{d}{d\sigma}f\big(R_i(\sigma)\big) &= \lambda_i\big(R_i(\sigma)\big)\frac{d}{d\sigma}R_i(\sigma)\,,\\ \frac{d^2}{d\sigma^2}f\big(R_i(\sigma)\big) &= \frac{d}{d\sigma}R_i(\sigma)+\lambda_i\big(R_i(\sigma)\big)\frac{d^2}{d\sigma^2}R_i(\sigma)\,,\\ \frac{d^3}{d\sigma^3}f\big(R_i(\sigma)\big) &= 2\frac{d^2}{d\sigma^2}R_i(\sigma)+\lambda_i\big(R_i(\sigma)\big)\frac{d^3}{d\sigma^3}R_i(\sigma).\end{aligned}$$

For convenience, we write $r_i\bullet r_j \doteq (Dr_j)r_i$ to denote the directional derivative of r_j in the direction of r_i. At $\sigma=0$ we have

$$A=B=0\,,\qquad \frac{d}{d\sigma}R_i = r_i(u_0)\,,\qquad \frac{d^2}{d\sigma^2}R_i = (r_i\bullet r_i)(u_0).$$

Using the above identities and the fact that the wedge product is anti-symmetric, we conclude

$$\begin{aligned}\frac{d^4}{d\sigma^4}\Psi\Big|_{\sigma=0} &= 4\left(\frac{d^3}{d\sigma^3}R_i+6\alpha r_j\right)\wedge\left(\lambda_i\frac{d}{d\sigma}R_i\right)+6\left(\frac{d^2}{d\sigma^2}R_i\right)\wedge\left(\frac{d}{d\sigma}R_i+\lambda_i\frac{d^2}{d\sigma^2}R_i\right)\\ &\quad +4\left(\frac{d}{d\sigma}R_i\right)\wedge\left(2\frac{d^2}{d\sigma^2}R_i+\lambda_i\frac{d^3}{d\sigma^3}R_i+6\alpha\lambda_j r_j\right)\\ &= 24\alpha(\lambda_i-\lambda_j)(r_j\wedge r_i)-2(r_i\bullet r_i)\wedge r_i = 0.\end{aligned}$$

The i-shock curve through u_0 is thus traced by points $S_i(\sigma)$ at (85), with

$$\alpha = \frac{(r_i\bullet r_i)\wedge r_i}{12(\lambda_i-\lambda_j)(r_j\wedge r_i)}. \tag{86}$$

The sign of α in (86) gives the position of the i-shock curve, relative to the i-rarefaction curve, near the point u_0. In particular, if $(r_i \bullet r_i) \wedge r_i \neq 0$, it is clear that these two curves do not coincide.

3.6 Error and Interaction Estimates

In this final section we provide two types of estimates, which will play a key role in the analysis of front tracking approximations.

Fix a left state u^-, a right state u^+, and a speed λ. If these satisfy the Rankine–Hugoniot equations, we have

$$\lambda(u^+ - u^-) - [f(u^+) - f(u^-)] \; = \; 0.$$

On the other hand, if these values are chosen arbitrarily, the only available estimate is

$$\lambda(u^+ - u^-) - [f(u^+) - f(u^-)] \; = \; \mathcal{O}(1) \cdot |u^+ - u^-|. \tag{87}$$

Here an throughout the sequel, the Landau symbol $\mathcal{O}(1)$ denotes a quantity which remains uniformly bounded as all variables $u^-, u^+, \lambda, \sigma \ldots$ range on bounded sets. The next lemma describes by how much the Rankine–Hugoniot equation fail to be satisfied, if the point u^+ lies on the i-rarefaction curve through u^- and we choose λ to be the i-th characteristic speed at the point u^-.

Lemma 3 (error estimate). *For $\sigma > 0$ small, one has the estimate*

$$\lambda_k(u^-)\Big[R_k(\sigma)(u^-) - u^-\Big] - \Big[f\big(R_k(\sigma)(u^-)\big) - f(u^-)\Big] \; = \; \mathcal{O}(1) \cdot \sigma^2. \tag{88}$$

Proof. Call $E(\sigma)$ the left hand side of (88). Clearly $E(0) = 0$. Differentiating w.r.t. σ at the point $\sigma = 0$ and recalling that $dR_k/d\sigma = r_k$, we find

$$\frac{dE}{d\sigma}\bigg|_{\sigma=0} = \lambda_k(u^-) r_k(u^-) - Df(u^-) r_k(u^-) = 0.$$

Since E varies smoothly with u^- and σ, the estimate (88) follows by Taylor's formula. □

Next, consider a left state u^l, a middle state u^m and a right state u^r (Fig. 31, left). Assume that the pair (u^l, u^m) is connected by a j-wave of strength σ', while the pair (u^m, u^r) is connected by an i-wave of strength σ'', with $i < j$. We are interested in the strength of the waves $(\sigma_1, \ldots, \sigma_n)$ in the solution of the Riemann problem where $u^- = u^l$ and $u^+ = u^r$. Roughly speaking, these are the waves determined by the

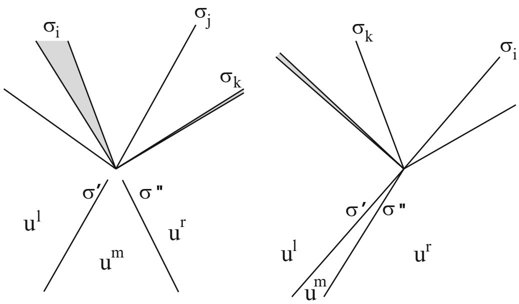

Fig. 31 Wave interactions. Strengths of the incoming and outgoing waves

interaction of the σ' and σ''. The next lemma shows that $\sigma_i \approx \sigma''$, $\sigma_j \approx \sigma'$ while $\sigma_k \approx 0$ for $k \neq i, j$.

A different type of interaction is considered in Fig. 31, right. Here the pair (u^l, u^m) is connected by an i-wave of strength σ', while the pair (u^m, u^r) is connected by a second i-wave, say of strength σ''. In this case, the strengths $(\sigma_1, \ldots, \sigma_n)$ of the outgoing waves satisfy $\sigma_i \approx \sigma' + \sigma''$ while $\sigma_k \approx 0$ for $k \neq i$. As usual, $\mathcal{O}(1)$ will denote a quantity which remains uniformly bounded as u^-, σ', σ'' range on bounded sets.

Lemma 4 (interaction estimates). *Consider the Riemann problem (51)–(52).*

(i) Recalling (72), assume that the right state is given by

$$u^+ = \Psi_i(\sigma'') \circ \Psi_j(\sigma')(u^-). \tag{89}$$

Let the solution consist of waves of size $(\sigma_1, \ldots, \sigma_n)$*, as in (74). Then*

$$|\sigma_i - \sigma''| + |\sigma_j - \sigma'| + \sum_{k \neq i,j} |\sigma_k| \;=\; \mathcal{O}(1) \cdot |\sigma' \sigma''|. \tag{90}$$

(ii) Next, assume that the right state is given by

$$u^+ = \Psi_i(\sigma'') \circ \Psi_i(\sigma')(u^-), \tag{91}$$

Then the waves $(\sigma_1, \ldots, \sigma_n)$ *in the solution of the Riemann problem are estimated by*

$$|\sigma_i - \sigma' - \sigma''| + \sum_{k \neq i} |\sigma_k| \;=\; \mathcal{O}(1) \cdot |\sigma' \sigma''| \big(|\sigma'| + |\sigma''|\big). \tag{92}$$

For a proof we refer to [11].

4 Global Solutions to the Cauchy Problem

In this chapter we study the global existence of weak solutions to the general Cauchy problem

$$u_t + f(u)_x = 0, \tag{93}$$

$$u(0,x) = \bar{u}(x). \tag{94}$$

Here the flux function $f : I\!R^n \mapsto I\!R^n$ is smooth, defined on a neighborhood of the origin. We always assume that the system is strictly hyperbolic, and that the assumption (H) introduced in the previous chapter holds.

A fundamental result proved by Glimm [34] provides the global existence of an entropy weak solution, for all initial data with suitably small total variation.

Theorem 2 (Global existence of weak solutions). *Assume that the system (93) is strictly hyperbolic, and that each characteristic field is either linearly degenerate or genuinely nonlinear.*

Then there exists a constant $\delta_0 > 0$ such that, for every initial condition $\bar{u} \in \boldsymbol{L}^1(I\!R;\ I\!R^n)$ with

$$Tot.Var.\{\bar{u}\} \le \delta_0\,, \tag{95}$$

the Cauchy problem (93)–(94) has a weak solution $u = u(t,x)$ defined for all $t \ge 0$.

In addition, one can prove the existence of a global solution satisfying all the admissibility conditions introduced in Sect. 2.3. A proof of Theorem 2 requires two main steps:

(a) Construct a sequence of approximate solutions u_ν.
(b) Show that a subsequence converges in L^1_{loc} to a weak solution u of the Cauchy problem.

Approximate solutions can be constructed by piecing together solutions to several Riemann problems. Two techniques have been developed in the literature:

- In the *Glimm scheme* (Fig. 40) one considers a fixed grid of points $(t_j, x_k) = (j\,\Delta t\,,\ k\,\Delta x)$ in the t-x plane, and solves a Riemann problem at each node of the grid.
- In a *front tracking approximation*, one constructs a piecewise constant approximate solution $u = u(t,x)$, whose jumps are located along a finite number of segments in the t-x plane (Fig. 33). A new Riemann problem is solved at each point where two fronts interact. These points depend on the particular solution being constructed.

Having constructed a sequence of approximate solutions $(u_\nu)_{\nu\ge1}$ (Fig. 32), one needs to extract a subsequence converging to some limit $u = u(t,x)$ in $\mathbf{L}^1_{loc}$. By Helly's compactness theorem, this can be achieved by establishing an a priori bound on the total variation Tot.Var.$\{u_\nu(t,\cdot)\}$, uniformly valid for $t > 0$ and $\nu \ge 1$.

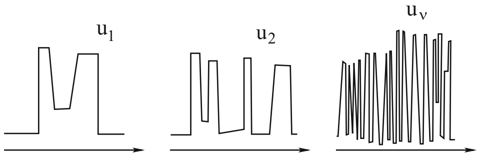

Fig. 32 Without a bound on the total variation, a sequence of approximate solutions may oscillate more and more, without admitting any convergent subsequence

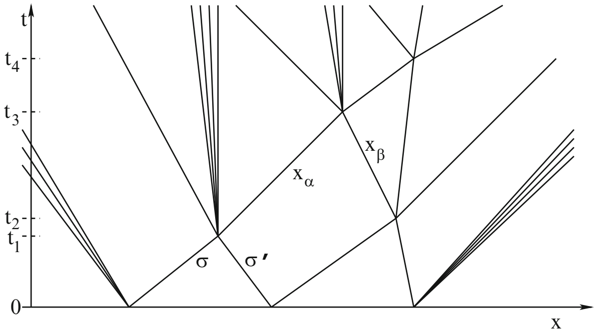

Fig. 33 An approximate solution obtained by front tracking

4.1 Front Tracking Approximations

In this section we describe the construction of front tracking approximations. This method was developed in [26, 28], and in [9] respectively for scalar conservation laws, for 2×2 systems, and for general $n \times n$ systems satisfying the assumptions (H). Further versions of this algorithm can also be found in [5,37,55]. An extension to fully general $n \times n$ systems, without the assumptions (H), is provided in [3].

Let the initial condition $\bar{u}$ be given and fix $\varepsilon > 0$. We now describe an algorithm which produces a piecewise constant approximate solution to the Cauchy problem (93)–(94). The construction (Fig. 33) starts at time $t = 0$ by taking a piecewise constant approximation $u(0, \cdot)$ of $\bar{u}$, such that

$$\text{Tot.Var.}\big\{u(0,\cdot)\big\} \le \text{Tot.Var.}\{\bar{u}\}, \qquad \int \big|u(0,x) - \bar{u}(x)\big|\, dx \le \varepsilon. \tag{96}$$

Let $x_1 < \cdots < x_N$ be the points where $u(0, \cdot)$ is discontinuous. For each $\alpha = 1, \ldots, N$, the Riemann problem generated by the jump $\big(u(0, x_\alpha-),\ u(0, x_\alpha+)\big)$ is approximately solved on a forward neighborhood of $(0, x_\alpha)$ in the t-x plane by a piecewise constant function, according to the following procedure.

Accurate Riemann Solver. Consider the general Riemann problem at a point $(\bar{t}, \bar{x})$,

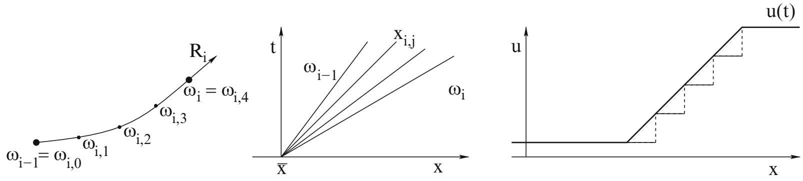

Fig. 34 Replacing a centered rarefaction wave by a rarefaction fan

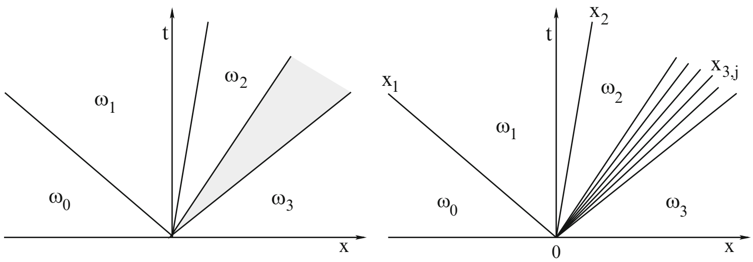

Fig. 35 *Left*: the exact solution to a Riemann problem. *Right*: a piecewise constant approximation. The centered rarefaction wave of the 3-d family has been replaced by a rarefaction fan

$$v_t + f(v)_x = 0, \qquad v(\bar{t}, x) = \begin{cases} u^- & if\ x < \bar{x}, \\ u^+ & if\ x > \bar{x}, \end{cases} \tag{97}$$

Recalling (72), let $\omega_0, \ldots, \omega_n$ be the intermediate states and $\sigma_1, \ldots, \sigma_n$ be the strengths of the waves in the solution, so that

$$\omega_0 = u^-, \quad \omega_n = u^+, \qquad \omega_i = \Psi_i(\sigma_i)(\omega_{i-1}) \qquad i = 1, \ldots, n. \tag{98}$$

If all jumps (ω_{i-1}, ω_i) were shocks or contact discontinuities, then this solution would be already piecewise constant. In general, the exact solution of (97) is not piecewise constant, because of the presence of centered rarefaction waves. These will be approximated by piecewise constant rarefaction fans, inserting additional states $\omega_{i,j}$ as follows.

If the i-th characteristic field is genuinely nonlinear and $\sigma_i > 0$, we divide the centered i-rarefaction into a number p_i of smaller i-waves, each with strength σ_i/p_i. Here we choose the integer p_i big enough so that $\sigma/p_i < \varepsilon$. For $j = 1, \ldots, p_i$, we now define the intermediate states and wave-fronts (Fig. 34)

$$\omega_{i,j} = R_i(j\sigma_i/p_i)(\omega_{i-1}), \qquad x_{i,j}(t) = \bar{x} + (t - \bar{t})\lambda_i(\omega_{i,j-1}). \tag{99}$$

Replacing each centered rarefaction wave with a rarefaction fan, we thus obtain a piecewise constant approximate solution to the Riemann problem (Fig. 35).

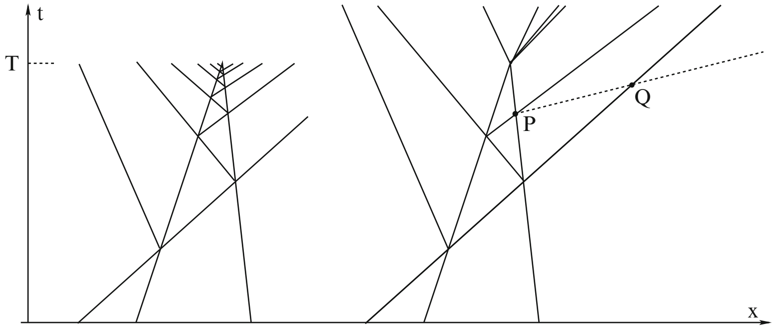

Fig. 36 *Left*: the number of wave fronts can become infinite in finite time. *Right*: by using the simplified Riemann solver at two interaction points P and Q, the total number of fronts remains bounded

We now resume the construction of a front tracking solution to the original Cauchy problem (93)–(94). Having solved all the Riemann problems at time $t = 0$, the approximate solution u can be prolonged until a first time t_1 is reached, when two wave-fronts interact (Fig. 33). Since $u(t_1, \cdot)$ is still a piecewise constant function, the corresponding Riemann problems can again be approximately solved within the class of piecewise constant functions. The solution u is then continued up to a time t_2 where a second interaction takes place, etc... We remark that, by an arbitrary small change in the speed of one of the wave fronts, it is not restrictive to assume that at most two incoming fronts collide, at each given time $t > 0$. This will considerably simplify all subsequent analysis, since we don't need to consider the case where three or more incoming fronts meet together.

The above construction can be continued for all times $t > 0$, as long as

(a) The total variation Tot.Var.$\{u(t, \cdot)\}$ remains small enough. This guarantees that all jumps $u(t, x-), u(t, x+)$ are small, hence the corresponding Riemann problems admit a solution.
(b) The total number of fronts remains finite.

Bounds on the total variations will be discussed in the next section. Here we observe that a naive implementation of the front tracking algorithm can produce an infinite number of fronts within finite time (Fig. 36).

As shown in [9], this can be avoided by occasionally implementing a *Simplified Riemann Solver*, which introduces one single additional front (Fig. 37). In this case, the solution is continued by means of two outgoing fronts of exactly the same strength as the incoming one. All other waves resulting from the interaction are lumped together in a single front, traveling with a constant speed $\hat{\lambda}$, strictly larger than all characteristic speeds.

In the end, for a given $\varepsilon > 0$, this modified front tracking algorithm generates a piecewise constant ε-approximate solution $u = u(t, x)$, defined as follows.

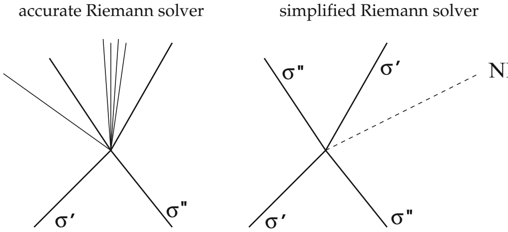

Fig. 37 *Left*: the solution to a Riemann problem obtained by the Accurate Riemann Solver introduces several new wave fronts. *Right*: the Simplified Riemann solver produces two outgoing fronts of the same strength as the incoming ones, plus a small *Non-Physical* front

Definition 6 (front tracking approximate solution). A piecewise constant function $u = u(t,x)$, defined for $t \geq 0$, $x \in R$, is called an *ε-approximate front tracking solution* to the Cauchy problem (93)–(94) provided that

(i) The initial condition is approximately attained, namely $\|u(0,\cdot) - \bar{u}\|_{\mathbf{L}^1} \leq \varepsilon$.
(ii) All shock fronts and all contact discontinuities satisfy the Rankine–Hugoniot equations, as well as the admissibility conditions.
(iii) Each rarefaction front has strength $\leq \varepsilon$.
(iv) At each time $t > 0$, the total strength of all non-physical fronts in $u(t,\cdot)$ is $\leq \varepsilon$.
(v) The total variation of $u(t,\cdot)$ satisfies a uniform bound, depending only on Tot.Var.$\{\bar{u}\}$.

– By a *shock front* we mean a jump whose right and left states satisfy $u^+ = S_i(\sigma)(u^-)$ for some $\sigma \in I\!R$ and $i \in \{1,\ldots,n\}$. This travels with Rankine–Hugoniot speed $\lambda = \lambda_i(u^-,u^+) = \frac{f(u^+)-f(u^-)}{u^+-u^-}$.
– By a *rarefaction front* we mean a jump whose right and left states satisfy $u^+ = R_i(\sigma)(u^-)$ for some σ, i. This travels with speed $\lambda = \lambda_i(u^+)$, i.e. with the characteristic speed of its right state.
– By a *non-physical front* we mean a jump whose right and left states u^+, u^- are arbitrary. This travels with a fixed speed $\hat{\lambda}$, strictly greater than all characteristic speeds.

4.2 *Bounds on the Total Variation*

In this section we derive bounds on the total variation of a front tracking approximation $u(t,\cdot)$, uniformly valid for all $t \geq 0$. These estimates will be obtained from Lemma 4, using an interaction functional.

We begin by introducing some notation. At a fixed time t, let x_α, $\alpha = 1,\ldots,N$, be the locations of the fronts in $u(t,\cdot)$. Moreover, let $|\sigma_\alpha|$ be the strength of the wave-front at x_α, say of the family $k_\alpha \in \{1,\ldots,n\}$. Following [34], consider the two functionals

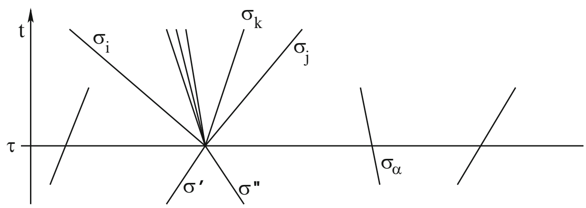

Fig. 38 Estimating the change in the total variation at a time where two fronts interact

$$V(t) \doteq V\big(u(t)\big) \doteq \sum_{\alpha} |\sigma_\alpha|\,, \tag{100}$$

measuring the *total strength of waves* in $u(t,\cdot)$, and

$$Q(t) \doteq Q\big(u(t)\big) \doteq \sum_{(\alpha,\beta)\in\mathscr{A}} |\sigma_\alpha \sigma_\beta|\,, \tag{101}$$

measuring the *wave interaction potential*. In (101), the summation ranges over the set $\mathscr{A}$ of all couples of approaching wave-fronts:

Definition 7 (approaching fronts). Two fronts, located at points $x_\alpha < x_\beta$ and belonging to the characteristic families $k_\alpha, k_\beta \in \{1,\ldots,n\}$ respectively, are *approaching* if $k_\alpha > k_\beta$ or else if $k_\alpha = k_\beta$ and at least one of the wave-fronts is a shock of a genuinely nonlinear family.

Roughly speaking, two fronts are approaching if the one behind has the larger speed (and hence it can collide with the other, at some future time).

Now consider the approximate solution $u = u(t,x)$ constructed by the front tracking algorithm. It is clear that the quantities $V\big(u(t)\big)$, $Q\big(u(t)\big)$ remain constant except at times where an interaction occurs. At a time τ where two fronts of strength $|\sigma'|, |\sigma''|$ collide, the interaction estimates (90) or (92) yield

$$\Delta V(\tau) \doteq V(\tau+) - V(\tau-) = \mathscr{O}(1)\cdot|\sigma'\sigma''|, \tag{102}$$

$$\Delta Q(\tau) \doteq Q(\tau+) - Q(\tau-) = -|\sigma'\sigma''| + \mathscr{O}(1)\cdot|\sigma'\sigma''|\cdot V(\tau-). \tag{103}$$

Indeed (Fig. 38), after time τ the two colliding fronts σ', σ'' are no longer approaching. Hence the product $|\sigma'\sigma''|$ is no longer counted within the summation (101). On the other hand, the new waves emerging from the interaction (having strength $\mathscr{O}(1)\cdot|\sigma'\sigma''|$) can approach all the other fronts not involved in the interaction (which have total strength $\leq V(\tau-)$).

If V remains sufficiently small, so that $\mathscr{O}(1)\cdot V(\tau-) \leq 1/2$, from (103) it follows

$$Q(\tau+) - Q(\tau-) \leq -\frac{|\sigma'\sigma''|}{2}. \tag{104}$$

By (102) and (104) we can thus choose a constant C_0 large enough so that the quantity

$$\Upsilon(t) \doteq V(t) + C_0 Q(t)$$

decreases at every interaction time, provided that V remains sufficiently small.

We now observe that the total strength of waves is an equivalent way of measuring the total variation. Indeed, for some constant C one has

$$\text{Tot.Var.}\big\{u(t)\big\} \;\leq\; V\big(u(t)\big) \;\leq\; C \cdot \text{Tot.Var.}\big\{u(t)\big\}. \tag{105}$$

Moreover, the definitions (100)–(101) trivially imply $Q \leq V^2$. If the total variation of the initial data $u(0,\cdot)$ is sufficiently small, the previous estimates show that the quantity $V + C_0 Q$ is nonincreasing in time. Therefore

$$\text{Tot.Var.}\big\{u(t)\big\} \;\leq\; V\big(u(t)\big) \;\leq\; V\big(u(0)\big) + C_0 Q\big(u(0)\big). \tag{106}$$

This provides a uniform bound on the total variation of $u(t,\cdot)$ valid for all times $t \geq 0$.

An important consequence of the bound (106) is that, at every time τ where two fronts interact, the corresponding Riemann problem can always be solved. Indeed, the left and right states differ by the quantity

$$|u^+ - u^-| \;\leq\; \text{Tot.Var.}\big\{u(\tau)\big\}\,,$$

which remains small.

Another consequence of the bound on the total variation is the continuity of $t \mapsto u(t,\cdot)$ as a function with values in $\mathbf{L}^1_{\text{loc}}$. More precisely, there exists a Lipschitz constant L' such that

$$\int_{-\infty}^{\infty} \big|u(t,x) - u(t',x)\big|\,dx \;\leq\; L'|t-t'| \qquad \text{for all} \quad t,t' \geq 0. \tag{107}$$

Indeed, if no interaction occurs inside the interval $[t,t']$, the left hand side of (107) can be estimated simply as

$$\begin{aligned} \big\|u(t) - u(t')\big\|_{\mathbf{L}^1} &\leq\; |t-t'| \textstyle\sum_\alpha |\sigma_\alpha|\,|\dot{x}_\alpha| \\ &\leq\; |t-t'| \cdot [\text{total strength of all wave fronts}] \cdot [\text{maximum speed}] \\ &\leq\; L' \cdot |t-t'|, \end{aligned} \tag{108}$$

for some uniform constant L'. The case where one or more interactions take place within $[t,t']$ is handled in the same way, observing that the map $t \mapsto u(t,\cdot)$ is continuous across interaction times.

4.3 Convergence to a Limit Solution

Given any sequence $\varepsilon_\nu \to 0+$, by the front tracking algorithm we obtain a sequence of piecewise constant functions u_ν, where each $u_n u$ is an ε_ν-approximate solution to the Cauchy problem (93)–(94).

By (107) the maps $t \mapsto u_\nu(t, \cdot)$ are uniformly Lipschitz continuous w.r.t. the $\mathbf{L}^1$ distance. We can thus apply Helly's compactness theorem (see Theorem A.1 in the Appendix) and extract a subsequence which converges to some limit function u in $\mathbf{L}^1_{loc}$, also satisfying (107).

By the second relation in (96), as $\varepsilon_\nu \to 0$ we have $u_\nu(0) \to \bar{u}$ in $\mathbf{L}^1_{\text{loc}}$. Hence the initial condition (94) is clearly attained. To prove that u is a weak solution of the Cauchy problem, it remains to show that, for every $\phi \in \mathscr{C}^1_c$ with compact support contained in the open half plane where $t > 0$, one has

$$\int_0^\infty \int_{-\infty}^\infty \phi_t(t,x)u(t,x) + \phi_x(t,x) f(u(t,x))\, dx dt = 0. \tag{109}$$

Since the u_ν are uniformly bounded and f is uniformly continuous on bounded sets, it suffices to prove that

$$\lim_{\nu \to 0} \int_0^\infty \int_{-\infty}^\infty \Big\{\phi_t(t,x)u_\nu(t,x) + \phi_x(t,x) f\big(u_\nu(t,x)\big)\Big\}\, dx dt \;=\; 0. \tag{110}$$

Choose $T > 0$ such that $\phi(t,x) = 0$ whenever $t \notin [0,T]$. For a fixed ν, at any time t call $x_1(t) < \cdots < x_N(t)$ the points where $u_\nu(t,\cdot)$ has a jump, and set

$$\Delta u_\nu(t, x_\alpha) \doteq u_\nu(t, x_\alpha+) - u_\nu(t, x_\alpha-),$$

$$\Delta f\big(u_\nu(t,x_\alpha)\big) \doteq f\big(u_\nu(t,x_\alpha+)\big) - f\big(u_\nu(t,x_\alpha-)\big).$$

Observe that the polygonal lines $x = x_\alpha(t)$ subdivide the strip $[0,T] \times I\!R$ into finitely many regions Γ_j where u_ν is constant (Fig. 39). Introducing the vector

$$\Phi \doteq \big(\phi \cdot u_\nu\ ,\ \ \phi \cdot f(u_\nu)\big),$$

by the divergence theorem the double integral in (110) can be written as

$$\sum_j \iint_{\Gamma_j} \text{div}\, \Phi(t,x)\, dt dx = \sum_j \int_{\partial \Gamma_j} \Phi \cdot \mathbf{n}\, d\sigma. \tag{111}$$

Here $\partial \Gamma_j$ is the oriented boundary of Γ_j, while $\mathbf{n}$ denotes an outer normal. Observe that $\mathbf{n} d\sigma = \pm(\dot{x}_\alpha, -1) dt$ along each polygonal line $x = x_\alpha(t)$, while $\phi(t,x) = 0$ along the lines $t = 0, t = T$. By (111) the expression within square brackets in (110) is computed by

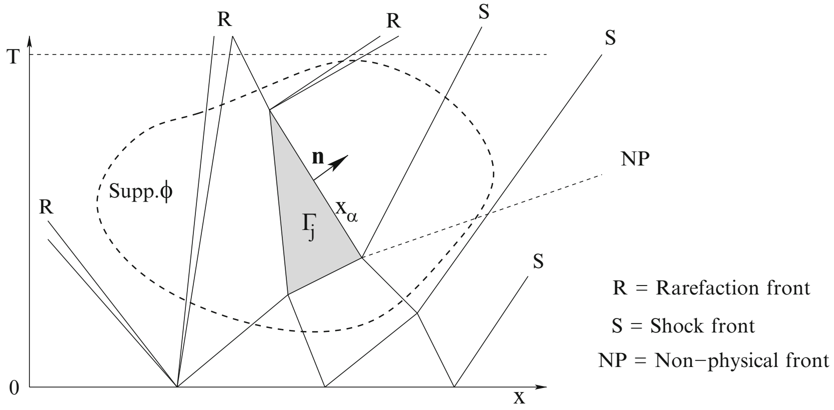

Fig. 39 Estimating the error in an approximate solution obtained by front tracking

$$\int_0^T \sum_\alpha \Big[\dot{x}_\alpha(t) \cdot \Delta u_\nu(t, x_\alpha) - \Delta f\big(u_\nu(t, x_\alpha)\big)\Big]\phi\big(t, x_\alpha(t)\big)\, dt. \qquad (112)$$

Here, for each $t \in [0, T]$, the sum ranges over all fronts of $u_\nu(t, \cdot)$. To estimate the above integral, let σ_α be the signed strength of the wave-front at x_α. If this wave is a shock or or contact discontinuity, by construction the Rankine–Hugoniot equations are satisfied exactly, i.e.

$$\dot{x}_\alpha(t) \cdot \Delta u_\nu(t, x_\alpha) - \Delta f\big(u_\nu(t, x_\alpha)\big) = 0. \qquad (113)$$

On the other hand, if the wave at x_α is a rarefaction front, its strength will satisfy $\sigma_\alpha \in]0, \varepsilon_\nu[$. Therefore, the error estimate (88) yields

$$\Big|\dot{x}_\alpha(t) \cdot \Delta u_\nu(t, x_\alpha) - \Delta f\big(u_\nu(t, x_\alpha)\big)\Big| \;=\; \mathcal{O}(1) \cdot |\sigma_\alpha|^2 \;=\; \mathcal{O}(1) \cdot \varepsilon_\nu |\sigma_\alpha|. \qquad (114)$$

Finally, if the jump at x_α is a non-physical front of strength $|\sigma_\alpha| \doteq |u_\nu(x_\alpha+) - u_\nu(x_\alpha-)|$, by (87) we have the estimate

$$\Big|\dot{x}_\alpha(t) \cdot \Delta u_\nu(t, x_\alpha) - \Delta f\big(u_\nu(t, x_\alpha)\big)\Big| \;=\; \mathcal{O}(1) \cdot |\sigma_\alpha|. \qquad (115)$$

Summing over all wave-fronts and recalling that the total strength of waves in $u_\nu(t, \cdot)$ satisfies a uniform bound independent of t, ν, we obtain

$$
\begin{aligned}
&\limsup_{\nu\to\infty}\left|\sum_{\alpha}\Big[\dot{x}_\alpha(t)\cdot\Delta u_\nu(t,x_\alpha)-\Delta f\big(u_\nu(t,x_\alpha)\big)\Big]\phi\big(t,x_\alpha(t)\big)\right| \\
&\quad\le\ \Big(\max_{t,x}\big|\phi(t,x)\big|\Big)\cdot\limsup_{\nu\to\infty}\left\{\mathcal{O}(1)\cdot\sum_{\alpha\in\mathcal{R}}\varepsilon_\nu|\sigma_\alpha|+\mathcal{O}(1)\cdot\sum_{\alpha\in\mathcal{N}\mathcal{P}}|\sigma_\alpha|\right\} \\
&\quad=\ 0.
\end{aligned}
\tag{116}
$$

The limit (110) is now a consequence of (116). This shows that u is a weak solution to the Cauchy problem. For all details we refer to [11].

5 The Glimm Scheme

The fundamental paper of Glimm [34] contained the first rigorous proof of existence of global weak solutions to hyperbolic systems of conservation laws. For several years, the Glimm approximation scheme has provided the foundation for most of the theoretical results on the subject. We shall now describe this algorithm in a somewhat simplified setting, for systems where all characteristic speeds remain inside the interval $[0, 1]$. This is not a restrictive assumption. Indeed, consider any hyperbolic system of the form

$$u_t + A(u)u_x = 0,$$

and assume that all eigenvalues of A remain inside the interval $[-M, M]$. Performing the linear change of independent variables

$$y = x + Mt, \qquad\qquad \tau = 2Mt,$$

we obtain a new system

$$u_\tau + A^*(u)u_y = 0, \qquad\qquad A^*(u) \doteq \frac{1}{2M}\,A(u) + \frac{1}{2}\,I$$

where all eigenvalues of the matrix A^* now lie inside the interval $[0, 1]$.

To construct an approximate solution to the Cauchy problem

$$u_t + f(u)_x = 0, \qquad\qquad u(0,x) = \bar{u}(x), \tag{117}$$

we start with a grid in the t-x plane having step size $\Delta t = \Delta x$, with nodes at the points

$$P_{jk} = (t_j, x_k) \doteq (j\Delta t,\ k\Delta x) \qquad\qquad j,k \in \mathbb{Z}.$$

Moreover, we shall need a sequence of real numbers $\theta_1, \theta_2, \theta_3, \ldots$ *uniformly distributed* over the interval $[0, 1]$. This means that, for every $\lambda \in [0, 1]$, the percentage of points θ_i, $1 \le i \le N$ which fall inside $[0, \lambda]$ should approach λ as $N \to \infty$, i.e.:

$$\lim_{N\to\infty} \frac{\#\{j\ ;\ 1 \le j \le N,\ \ \theta_j \in [0, \lambda]\,\}}{N} = \lambda \qquad \text{for each } \lambda \in [0, 1]. \tag{118}$$

By $\#I$ we denote here the cardinality of a set I.

At time $t = 0$, the Glimm algorithm starts by taking an approximation of the initial data $\bar{u}$, which is constant on each interval of the form $\big]x_{k-1},\ x_k\big[$, and has jumps only at the nodal points $x_k \doteq k\,\Delta x$. To fix the ideas, we shall take

$$u(0, x) = \bar{u}(x_k) \qquad \text{for all } \ x \in [x_k,\ x_{k+1}[. \tag{119}$$

For times $t > 0$ sufficiently small, the solution is then obtained by solving the Riemann problems corresponding to the jumps of the initial approximation $u(0, \cdot)$ at the nodes x_k. Since by assumption all waves speeds are contained in $[0, 1]$, waves generated from different nodes remain separated at least until the time $t_1 = \Delta t$. The solution can thus be prolonged on the whole time interval $[0,\ \Delta t[$. For bigger times, waves emerging from different nodes may cross each other, and the solution would become extremely complicated. To prevent this, a restarting procedure is adopted. Namely, at time $t_1 = \Delta t$ the function $u(t_1-, \cdot)$ is approximated by a new function $u(t_1+, \cdot)$ which is piecewise constant, having jumps exactly at the nodes $x_k \doteq k\,\Delta x$. Our approximate solution u can now be constructed on the further time interval $[\Delta t,\ 2\Delta t[$, again by piecing together the solutions of the various Riemann problems determined by the jumps at the nodal points x_k. At time $t_2 = 2\Delta t$, this solution is again approximated by a piecewise constant function, etc...

A key aspect of the construction is the restarting procedure. At each time $t_j \doteq j\,\Delta t$, we need to approximate $u(t_j-, \cdot)$ with a a piecewise constant function $u(t_j+, \cdot)$, having jumps precisely at the nodal points x_k. This is achieved by a random sampling technique. More precisely, we look at the number θ_j in our uniformly distributed sequence. On each interval $[x_{k-1},\ x_k[$, the old value of our solution at the intermediate point $x_k^* = \theta_j x_k + (1-\theta_j)x_{k-1}$ becomes the new value over the whole interval:

$$u(t_j+,\ x) = u\big(t_j-,\ \ \theta_j x_k + (1-\theta_j)x_{k-1}\big) \qquad \text{for all } \ x \in [x_{k-1},\ x_k[. \tag{120}$$

An approximate solution constructed in this way is shown in Fig. 40. The asterisks mark the points where the function is sampled. For sake of illustration, we choose $\theta_1 = 1/2$, $\theta_2 = 1/3$.

For a strictly hyperbolic system of conservation laws, satisfying the hypotheses (H) in Sect. 3, the fundamental results of J. Glimm [34] and T.P. Liu [46] have established that

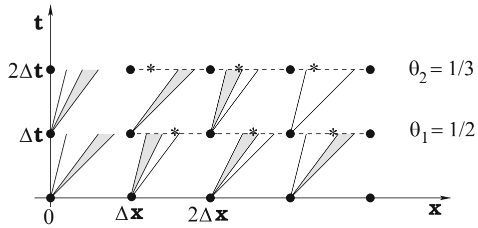

Fig. 40 An approximate solution constructed by the Glimm scheme

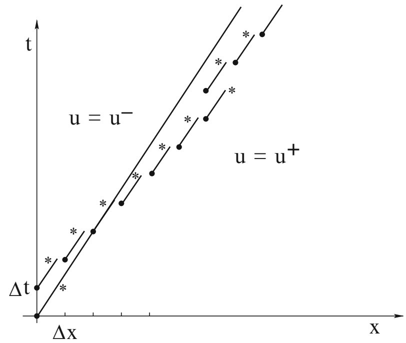

Fig. 41 Applying the Glimm scheme to a solution consisting of a single shock

1. If the initial data $\bar{u}$ has small total variation, then an approximate solution can be constructed by the above algorithm for all times $t \geq 0$. The total variation of $u(t, \cdot)$ remains small.
2. Letting the grid size $\Delta t = \Delta x$ tend to zero and using always the same sequence of numbers $\theta_j \in [0, 1]$, one obtains a sequence of approximate solutions u_ν. By Helly's compactness theorem, one can extract a subsequence that converges to some limit function $u = u(t, x)$ in $\mathbf{L}^1_{\text{loc}}$.
3. If the numbers θ_j are uniformly distributed over the interval $[0, 1]$, i.e. if (118) holds, then the limit function u provides a weak solution to the Cauchy problem (117).

The importance of the sequence θ_j being uniformly distributed can be best appreciated in the following example.

Example 10. Consider a Cauchy problem of the form (117). Assume that the exact solution consists of exactly one single shock, traveling with speed $\lambda \in [0, 1]$, say

$$U(t, x) = \begin{cases} u^+ & if \qquad x > \lambda t, \\ u^- & if \qquad x < \lambda t. \end{cases}$$

Consider an approximation of this solution obtained by implementing the Glimm algorithm (Fig. 41). By construction, at each time $t_j \doteq j\Delta t$, the position of the shock in this approximate solution must coincide with one of the nodes of the grid.

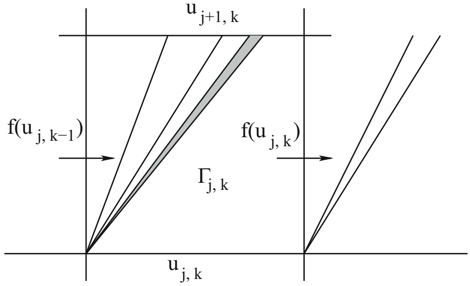

Fig. 42 Approximations leading to the Godunov scheme

Observe that, passing from t_{j-1} to t_j, the position $x(t)$ of the shock remains the same if the j-th sampling point lies on the left, while it moves forward by Δx if the j-th sampling point lies on the right. In other words,

$$x(t_j) \;=\; \begin{cases} x(t_{j-1}) & if \qquad \theta_j \in]\lambda, 1], \\ x(t_{j-1}) + \Delta x & if \qquad \theta_j \in [0, \lambda]. \end{cases} \tag{121}$$

Let us fix a time $T > 0$, and take $\Delta t \doteq T/N$. From (121) it now follows

$$x(T) \;=\; \#\big\{j\ ;\ \ 1 \leq j \leq N,\ \ \theta_j \in [0, \lambda]\,\big\} \cdot \Delta t$$

$$=\; \frac{\#\big\{j\ ;\ \ 1 \leq j \leq N,\ \ \theta_j \in [0, \lambda]\,\big\}}{N} \cdot T.$$

It is now clear that the assumption (118) on the uniform distribution of the sequence $\{\theta_j\}_{j\geq 1}$ is precisely what is needed to guarantee that, as $N \to \infty$ (equivalently, as $\Delta t \to 0$), the location $x(T)$ of the shock in the approximate solution converges to the exact value λT.

Remark 7. At each restarting time t_j we need to approximate the BV function $u(t_j-, \cdot)$ with a new function which is piecewise constant on each interval $[x_{k-1},\ x_k[$. Instead of the sampling procedure (120), an alternative method consists of taking average values:

$$u(t_j+,\ x) \;\doteq\; \frac{1}{\Delta x}\int_{x_{k-1}}^{x_k} u(t_j-,\ y)\, dy \qquad\qquad \text{for all } \ x \in [x_{k-1},\ x_k[. \tag{122}$$

Calling u_{jk} the constant value of $u(t_j+)$ on the interval $[x_{k-1},\ x_k[$, an application of the divergence theorem on the square Γ_{jk} (Fig. 42) yields

$$u_{j+1,k} \;=\; u_{j,k} + \big[f(u_{j,k-1}) - f(u_{j,k})\big] \tag{123}$$

Indeed, all wave speeds are in [0, 1], hence

$$u(t, x_{k-1}) = u_{j,k-1}, \qquad u(t, x_k) = u_{j,k} \qquad \text{for all } t \in [t_j, t_{j+1}[.$$

The finite difference scheme (122) is the simplest version of the Godunov (upwind) scheme. It is very easy to implement numerically, since it does not require the solution of any Riemann problem. Unfortunately, as shown in [22], in general it is not possible to obtain a priori bounds on the total variation of solutions constructed by the Godunov method. Proving the convergence of these approximations remains an outstanding open problem.

The remaining part of this chapter will be concerned with error bounds, for solutions generated by the Glimm scheme.

Observe that, at each restarting time $t_j = j\,\Delta t$, the replacement of $u(t_j-)$ with the piecewise constant function $u(t_j+)$ produces an error measured by

$$\big\| u(t_j+) - u(t_j-) \big\|_{\mathbf{L}^1}$$

As the time step $\Delta t = T/N$ approaches zero, the total sum of all these errors does not converge to zero, in general. This can be easily seen in Example 10, where we have

$$\begin{aligned}\sum_{j=1}^{N} \big\| u(t_j+) - u(t_j-) \big\|_{\mathbf{L}^1} &\geq \sum_{j=1}^{N} |u^+ - u^-| \cdot \Delta t \cdot \min\big\{(1-\lambda),\ \lambda\big\} \\ &= |u^+ - u^-| \cdot T \cdot \min\big\{(1-\lambda),\ \lambda\big\}.\end{aligned}$$

This fact makes it difficult to obtain sharp error estimates for solutions generated by the Glimm scheme. Roughly speaking, the approximate solutions converge to the correct one not because the total errors become small, but because, by the randomness of the sampling choice, small errors eventually cancel each other in the limit.

Clearly, the speed of convergence of the Glimm approximate solutions as $\Delta t, \Delta x \to 0$ strongly depends on how well the sequence $\{\theta_i\}$ approximates a uniform distribution on the interval [0, 1]. In this connection, let us introduce

Definition 8. Let a sequence of numbers $\theta_j \in [0,1]$ be given. For fixed integers $0 \leq m < n$, the *discrepancy* of the set $\{\theta_m, \ldots, \theta_{n-1}\}$ is defined as

$$D_{m,n} \doteq \sup_{\lambda \in [0,1]} \left| \lambda - \frac{\#\big\{ j\ ;\ m \leq j < n,\ \ \theta_j \in [0,\lambda] \big\}}{n-m} \right|. \tag{124}$$

We now describe a simple method for defining the numbers θ_j, so that the corresponding discrepancies $D_{m,n}$ approach zero as $n - m \to \infty$, at a nearly optimal rate. Write the integer k in decimal digits, then invert the order of the digits and put a zero in front:

$$\theta_1 = 0.1\,, \quad \ldots \quad , \quad \theta_{759} = 0.957\,, \quad \ldots \quad , \quad \theta_{39022} = 0.22093\,, \quad \ldots \tag{125}$$

For the sequence (125) one can prove that the discrepancies satisfy

$$D_{m,n} \;\le\; C \cdot \frac{1 + \ln(n-m)}{n-m} \qquad\qquad \text{for all } \; n > m \ge 0, \tag{126}$$

for some constant C. For approximate solutions constructed in terms of the above sequences (θ_j), using the restarting procedures (119)–(120), the following estimates were proved in [18].

Theorem 3 (Error estimates for the Glimm scheme). *Given any initial data $\bar{u} \in \mathbf{L}^1$ with small total variation, call $u^{\mathrm{exact}}(t,\cdot) = S_t\bar{u}$ the exact solution of the Cauchy problem (117). Moreover, let $u^{\mathrm{Glimm}}(t,\cdot)$ be the approximate solution generated by the Glimm scheme, in connection with a grid of size $\Delta t = \Delta x$ and a fixed sequence $(\theta_j)_{j\ge 0}$ satisfying (126). For every fixed time $T \ge 0$, letting the grid size tend to zero, one has the error estimate*

$$\lim_{\Delta x \to 0} \frac{\big\| u^{\mathrm{Glimm}}(T,\cdot) - u^{\mathrm{exact}}(T,\cdot)\big\|_{\mathbf{L}^1}}{\sqrt{\Delta x}\cdot |\ln \Delta x|} \;=\; 0. \tag{127}$$

In other words, the $\mathbf{L}^1$ error tends to zero faster then $\sqrt{\Delta x}\cdot|\ln \Delta x|$, i.e. just slightly slower than the square root of the grid size.

To prove Theorem 6, using a fundamental lemma of T.P. Liu [46], one first constructs a front tracking approximate solution $u = u(t,x)$ that coincides with u^{Glimm} at the initial time $t = 0$ and at the terminal time $t = T$. The $\mathbf{L}^1$ distance between $u(T,\cdot)$ and the exact solution $S_T\bar{u}$ can then be estimated using the error formula (7). For all details we refer to [18]. See also the recent paper [4] for a more general result.

6 Continuous Dependence on the Initial Data

Consider again the Cauchy problem (93)–(94), for a strictly hyperbolic system of conservation laws, satisfying the assumptions (H). Given two solutions u, v, in order to estimate the difference $\|u(t) - v(t)\|_{\mathbf{L}^1}$ one could try to follow a standard approach. Namely, set $w = u - v$, derive an evolution equation for w, and show that

$$\frac{d}{dt}\,\|w(t)\| \;\le\; C\,\|w(t)\|. \tag{128}$$

By Gronwall's lemma, this implies

$$\|u(t) - v(t)\| \;\le\; e^{Ct}\,\|u(0) - v(0)\|.$$

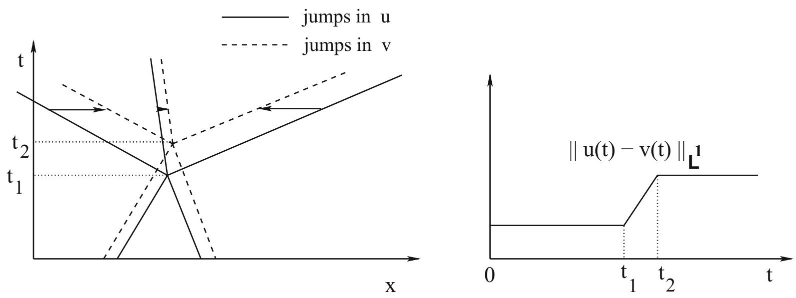

Fig. 43 *Left*: the solutions u and v differ only in the location of the shocks, and for the time of interaction. *Right*: even if u and v are very close, during the short time interval between interaction times, the distance $\|u - v\|_{\mathbf{L}^1}$ can increase rapidly

In particular, if $u(0) = v(0)$, then $u(t) = v(t)$ for all $t > 0$, proving the uniqueness of the solution to the Cauchy problem.

The above approach works well for smooth solutions of the hyperbolic system (93), but fails in the presence of shocks. Indeed, for two solutions u, v of a hyperbolic system containing shocks, the $\mathbf{L}^1$ distance can increase rapidly during short time intervals (Fig. 43).

6.1 Unique Solutions to the Scalar Conservation Law

In the case of a scalar conservation law, the fundamental works of A.I. Volpert [59] and S. Kruzhkov [39] have established:

Theorem 4 (Well posedness for the scalar Cauchy problem). *Let $f : I\!R \mapsto I\!R$ be any smooth flux. Then, for any initial data $\bar{u} \in \boldsymbol{L}^\infty$, the Cauchy problem (93)–(94) has a unique entropy-admissible weak solution, defined for all times $t \geq 0$. The corresponding flow is contractive in the $\boldsymbol{L}^1$ distance. Namely, for any two admissible solutions, one has*

$$\|u(t) - v(t)\|_{\boldsymbol{L}^1} \leq \|u(0) - v(0)\|_{\boldsymbol{L}^1} \qquad \textit{for all } t \geq 0. \tag{129}$$

For a proof in the one-dimensional case, see [11]. We observe that the $\mathbf{L}^1$ distance between two solutions u, v remains constant in time, as long as shocks do not appear. An intuitive way to understand this fact, shown in Fig. 44, is as follows. Think of the x-u plane as filled by an incompressible fluid, moving horizontally with speed $(\dot{x}, \dot{u}) = (f'(u), 0)$. Consider the fluid particles that at time $t = 0$ lie in the region enclosed between the graphs of $u(0, \cdot)$ and $v(0, \cdot)$ (the shaded areas in Fig. 44). As long as these solutions remain continuous, the method of characteristics shows that at any positive time t these same particles of fluid will have moved to the region enclosed between the graphs of $u(t, \cdot)$ and $v(t, \cdot)$. Hence the area of these region remains constant in time.

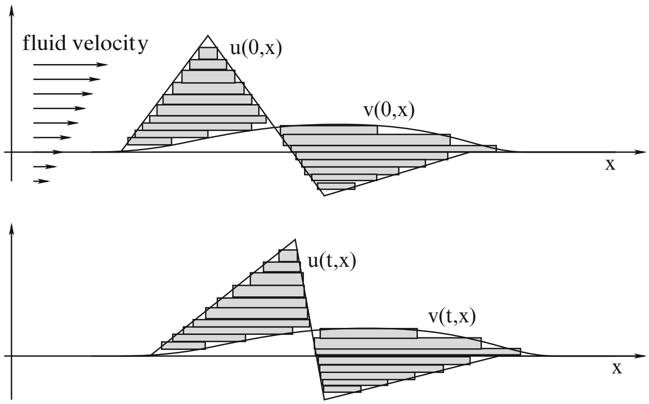

Fig. 44 The $\mathbf{L}^1$ distance between two continuous solutions remains constant in time

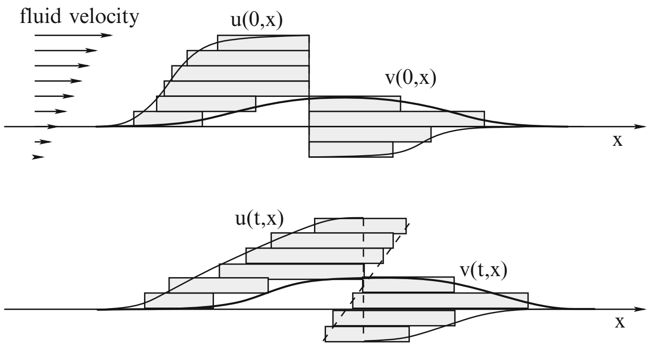

Fig. 45 The $\mathbf{L}^1$ distance decreases when a shock in one solution crosses the graph of the other solution

On the other hand, if a shock in one of the solutions crosses the graph of the other solution, then the $\mathbf{L}^1$ distance $\|u - v\|_{\mathbf{L}^1}$ decreases in time (Fig. 45).

6.2 Linear Hyperbolic Systems

We consider here another special case, where the system is linear with constant coefficients.

$$u_t + Au_x = 0 \qquad\qquad u \in I\!R^n. \tag{130}$$

Let $\{l_1, \ldots, l_n\}$ and $\{r_1, \ldots, r_n\}$ be dual bases of left and right eigenvectors of the matrix A, as in (8). Instead of the norm

$$\|u\|_{\mathbf{L}^1} \doteq \int |u(x)|\,dx$$

where $|u|$ is the Euclidean norm of a vector $u = (u_1, \ldots, u_n) \in I\!R^n$, one can use the equivalent norm

$$\|u\|_A \doteq \sum_{i=1}^{n} \int |l_i \cdot u(x)|\,dx. \tag{131}$$

By linearity, for any two solutions u, v, the difference $w = u - v$ satisfies still the same equation:

$$w_t + Aw_x = 0.$$

From the explicit representation (14), it now follows that

$$\|w(t)\|_A = \|w(0)\|_A \qquad \text{for all } t \in I\!R.$$

In other words, the flow generated by the linear homogeneous equation (130) is a group of isometries w.r.t. the distance $\|u - v\|_A$, namely

$$\|u(t) - v(t)\|_A = \|u(0) - v(0)\|_A \qquad \text{for all } t \in I\!R.$$

6.3 Nonlinear Systems

We always assume that the system (93) is strictly hyperbolic, and satisfies the hypotheses (H), so that each characteristic field is either linearly degenerate or genuinely nonlinear. The analysis in the previous chapter has shown the existence of a global entropy weak solution of the Cauchy problem for every initial data with sufficiently small total variation. More precisely, recalling the definitions (100)–(101), consider a domain of the form

$$\mathscr{D} \doteq cl\Big\{u \in \mathbf{L}^1(I\!R; I\!R^n);\ \ u \text{ is piecewise constant},\ \ \Upsilon(u) \doteq V(u) + C_0 \cdot Q(u) < \delta_0\Big\}, \tag{132}$$

where cl denotes closure in $\mathbf{L}^1$. With a suitable choice of the constants C_0 and $\delta_0 > 0$, for every $\bar{u} \in \mathscr{D}$, one can construct a sequence of ε-approximate front tracking solutions converging to a weak solution u taking values inside $\mathscr{D}$. Observe that, since the proof of convergence relied on a compactness argument, no information was obtained on the uniqueness of the limit. The main goal of the section is to show that this limit is unique and depends continuously on the initial data.

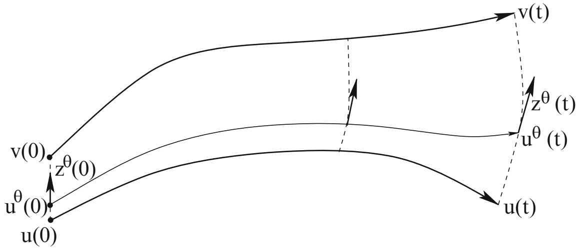

Fig. 46 Estimating the distance between two solutions by a homotopy method

Theorem 5. *For every $\bar{u} \in \mathscr{D}$, as $\varepsilon \to 0$ every sequence of ε-approximate solutions $u_\varepsilon : [0, \infty[\mapsto \mathscr{D}$ of the Cauchy problem (93)–(94), obtained by the front tracking method, converges to a unique limit solution $u : [0, \infty[\mapsto \mathscr{D}$. The map $(\bar{u}, t) \mapsto u(t, \cdot) \doteq S_t \bar{u}$ is a uniformly Lipschitz semigroup, i.e.:*

$$S_0 \bar{u} = \bar{u}, \qquad S_s(S_t \bar{u}) = S_{s+t} \bar{u}, \tag{133}$$

$$\big\| S_t \bar{u} - S_s \bar{v} \big\|_{\mathbf{L}^1} \le L \cdot \big(\| \bar{u} - \bar{v} \|_{\mathbf{L}^1} + |t - s| \big) \qquad \textit{for all } \bar{u}, \bar{v} \in \mathscr{D}, \ \ s, t \ge 0. \tag{134}$$

This result was first proved in [14] for 2×2 systems, then in [21] for general $n \times n$ systems, using a (lengthy and technical) homotopy method. Here the idea is to consider a path of initial data $\gamma_0 : \theta \mapsto u^\theta(0)$ connecting $u(0)$ with $v(0)$. Then one constructs the path $\gamma_t : \theta \mapsto u^\theta(t)$, parameterized by $\theta \in [0, 1]$, connecting the corresponding solutions at time t. By careful estimates on the tangent vector $z^\theta(t) \doteq d u^\theta(t)/d\theta$, one shows that the length of γ_t can be uniformly bounded in terms of the length of the initial path γ_0 (Fig. 46).

Relying on ideas introduced by T.P. Liu and T. Yang in [48, 49], the paper [20] provided a much simpler proof of the continuous dependence result, which will be described here. An extension of the above result to initial-boundary value problems for hyperbolic conservation laws has recently appeared in [30]. All of the above results deal with solutions having small total variation. The existence of solutions, and the well posedness of the Cauchy problem for large BV data was studied respectively in [54] and in [41].

To prove the uniqueness of the limit of front tracking approximations, we need to estimate the distance between any two ε-approximate solutions u, v of (93). For this purpose we introduce a functional $\Phi = \Phi(u, v)$, uniformly equivalent to the $\mathbf{L}^1$ distance, which is "almost decreasing" along pairs of solutions. Recalling the construction of shock curves at (62), given two piecewise constant functions $u, v : I\!R \mapsto R^n$, we consider the scalar functions q_i defined implicitly by

$$v(x) = S_n\big(q_n(x)\big) \circ \cdots \circ S_1\big(q_1(x)\big)\big(u(x)\big). \tag{135}$$

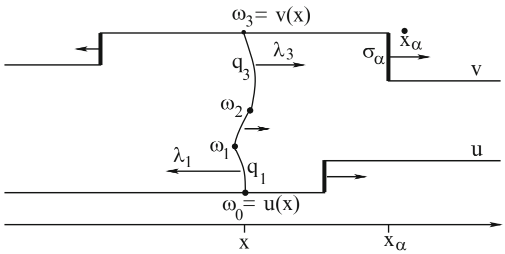

Fig. 47 Decomposing a jump $(u(x),\ v(x))$ in terms of n (possibly non-admissible) shocks

Remark 5. If we wanted to solve the Riemann problem with data $u^- = u(x)$ and $u^+ = v(x)$ only in terms of shock waves (possibly not entropy-admissible), then the corresponding intermediate states would be

$$\omega_0(x) = u(x), \qquad \omega_i(x) = S_i\big(q_i(x)\big) \circ \cdots \circ S_1\big(q_1(x)\big)\big(u(x)\big) \qquad i = 1, \ldots, n. \tag{136}$$

Moreover, $q_1(x), \ldots, q_n(x)$ would be the sizes of these shocks (Fig. 47). Since the pair of states (ω_{i-1}, ω_i) is connected by a shock, the corresponding speed $\lambda_i(u^-, u^+)$ is well defined. In particular, one can determine whether the i-shock q_i located at x is approaching a j-wave located at some other point x'. It is useful to think of $q_i(x)$ as the strength of the i-th component in the jump $\big(u(x),\ v(x)\big)$. In the linear case (130) we would simply have $q_i = l_i \cdot (v - u)$, and our functional would eventually reduce to (131).

If the shock curves are parameterized by arc-length, on a compact neighborhood of the origin one has

$$\big|v(x) - u(x)\big| \ \le\ \sum_{i=1}^{n} \big|q_i(x)\big| \ \le\ C\,\big|v(x) - u(x)\big| \tag{137}$$

for some constant C. We now consider the functional

$$\Phi(u, v) \ \doteq\ \sum_{i=1}^{n} \int_{-\infty}^{\infty} \big|q_i(x)\big| W_i(x)\, dx, \tag{138}$$

where the weights W_i are defined by setting:

$$\begin{aligned} W_i(x) & \\ &\doteq 1 + \kappa_1 \cdot \big[\text{total strength of waves in } u \text{ and in } v \text{ which approach the } i-\text{wave } q_i(x)\big] \\ &\qquad + \kappa_2 \cdot \big[\text{wave interaction potentials of } u \text{ and of } v\big] \\ &\doteq 1 + \kappa_1 A_i(x) + \kappa_2\big[Q(u) + Q(v)\big]. \end{aligned} \tag{139}$$

Since these weights remain uniformly bounded as u ranges in the domain $\mathcal{D}$, from (137)–(139) it follows

$$\|u-v\|_{\mathbf{L}^1} \leq \Phi(u,v) \leq C_1 \cdot \|v-u\|_{\mathbf{L}^1} \tag{140}$$

for some constant C_1 and all $u, v \in \mathcal{D}$. A key estimate proved in [20] shows that, for any two ε-approximate front tracking solutions $u, v : [0,T] \mapsto \mathcal{D}$, there holds

$$\frac{d}{dt}\Phi(u(t),v(t)) \leq C_2\varepsilon, \tag{141}$$

for some constant C_2.

Relying on this estimate, we now prove Theorem 5. Let $\bar{u} \in \mathcal{D}$ be given. Consider any sequence $(u_\nu)_{\nu\geq 1}$, such that each u_ν is an ε_ν-approximate front tracking solution of the Cauchy problem (93)–(94). For every $\mu, \nu \geq 1$ and $t \geq 0$, by (140) and (141) it now follows

$$\begin{aligned} \big\|u_\mu(t)-u_\nu(t)\big\|_{\mathbf{L}^1} &\leq \Phi\big(u_\mu(t),\ u_\nu(t)\big) \\ &\leq \Phi\big(u_\mu(0),\ u_\nu(0)\big) + C_2 t\cdot\max\{\varepsilon_\mu,\ \varepsilon_\nu\} \\ &\leq C_1\big\|u_\mu(0)-u_\nu(0)\big\|_{\mathbf{L}^1} + C_2 t\cdot\max\{\varepsilon_\mu,\ \varepsilon_\nu\}. \end{aligned} \tag{142}$$

Since the right hand side of (142) approaches zero as $\mu, \nu \to \infty$, the sequence is Cauchy and converges to a unique limit. The semigroup property (133) is an immediate consequence of uniqueness. Finally, let $\bar{u}, \bar{v} \in \mathcal{D}$ be given. For each $\nu \geq 1$, let u_ν, v_ν be ε_ν-approximate front tracking solutions of the Cauchy problem, with initial data $\bar{u}$ and $\bar{v}$, respectively. Using again (140) and (141) we deduce

$$\begin{aligned} \big\|u_\nu(t)-v_\nu(t)\big\|_{\mathbf{L}^1} &\leq \Phi\big(u_\nu(t),\ v_\nu(t)\big) \\ &\leq \Phi\big(u_\nu(0),\ v_\nu(0)\big) + C_2 t\varepsilon_\nu \\ &\leq C_1\Big(\|u_\nu(0)-\bar{u}\|_{\mathbf{L}^1} + \|\bar{u}-\bar{v}\|_{\mathbf{L}^1} + \big\|\bar{v}-v_\nu(0)\big\|_{\mathbf{L}^1}\Big) + C_2 t\varepsilon_\nu. \end{aligned}$$

Letting $\nu \to \infty$ we obtain $\big\|u(t)-v(t)\big\|_{\mathbf{L}^1} \leq C_1 \cdot \|\bar{u}-\bar{v}\|_{\mathbf{L}^1}$, proving the Lipschitz continuous dependence w.r.t. the initial data.

7 Uniqueness of Solutions

According to the analysis in the previous chapters, the solution of the Cauchy problem (93)–(94) obtained as limit of front tracking approximations is unique and depends Lipschitz continuously on the initial data, in the $\mathbf{L}^1$ norm. This basic result, however, leaves open the question whether other weak solutions may exist, possibly constructed by different approximation algorithms. We will show that this is not the case: indeed, every entropy admissible solution, satisfying some minimal regularity

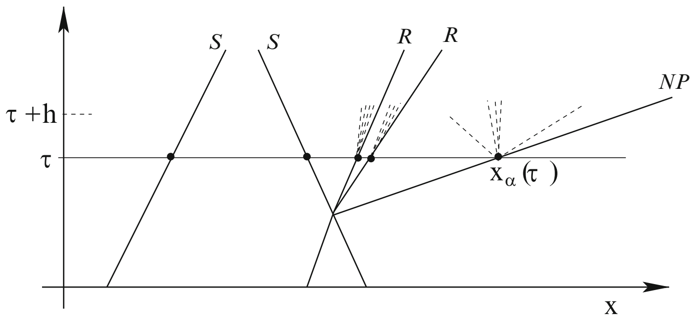

Fig. 48 The exact solution (*dotted lines*) which, at time τ, coincides with the value of a piecewise constant front tracking approximation

assumptions, necessarily coincides with the one obtained as limit of front tracking approximations.

7.1 An Error Estimate for Front Tracking Approximations

As a first step, we estimate the distance between an approximate solution, obtained by the front tracking method, and the exact solution of the Cauchy problem (93)–(94), given by the semigroup trajectory $t \mapsto u(t,\cdot) = S_t\bar{u}$. Let $u^\varepsilon : [0,T] \mapsto \mathscr{D}$ be an ε-approximate front tracking solution, according to Definition 6. We claim that the corresponding error can then be estimated as

$$\left\|u^\varepsilon(T,\cdot) - S_T\bar{u}\right\|_{\mathbf{L}^1} \;=\; \mathscr{O}(1)\cdot\varepsilon(1+T). \tag{143}$$

To see this, we first estimate the limit

$$\lim_{h\to 0+} \frac{\left\|u^\varepsilon(\tau+h) - S_h u^\varepsilon(\tau)\right\|_{\mathbf{L}^1}}{h}$$

at any time $\tau \in [0,T]$ where no wave-front interaction takes place. Let $u^\varepsilon(\tau,\cdot)$ have jumps at points $x_1 < \cdots < x_N$.

For each α, call ω_α the self-similar solution of the Riemann problem with data $u^\pm = u(\tau,\ x_\alpha\pm)$. We observe that, for $h > 0$ small enough, the semigroup trajectory $h \mapsto S_h u(\tau)$ is obtained by piecing together the solutions of these Riemann problems (Fig. 48). Splitting the set of all wave-fronts into shocks, rarefactions, and non-physical fronts, we estimate

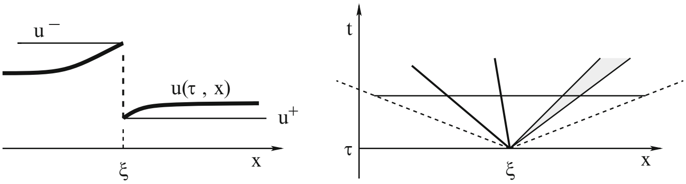

Fig. 49 In a forward neighborhood of a point (τ, ξ) where u has a jump, the admissible solution u should be asymptotically equivalent to the solution of a Riemann problem

$$
\begin{aligned}
&\lim_{h\to 0+} \frac{\left\| u^\varepsilon(\tau+h) - \widetilde{S}_h u^\varepsilon(\tau)\right\|_{\mathbf{L}^1}}{h} \\
&\quad = \sum_{\alpha\in\mathscr{R}\cup\mathscr{S}\cup\mathscr{N}\mathscr{P}} \left(\lim_{h\to 0+} \frac{1}{h} \int_{x_\alpha-\rho}^{x_\alpha+\rho} \left| u^\varepsilon(\tau+h, x) - \omega_\alpha(h,\ x - x_\alpha)\right| dx \right) \\
&\quad = \sum_{\alpha\in\mathscr{R}} \mathscr{O}(1)\cdot\varepsilon\,|\sigma_\alpha| + \sum_{\alpha\in\mathscr{N}\mathscr{P}} \mathscr{O}(1)\cdot|\sigma_\alpha| \ = \ \mathscr{O}(1)\cdot\varepsilon.
\end{aligned}
\tag{144}
$$

Here ρ can be any suitably small positive number. From the bound (144) and the error formula (7) in the Appendix, we finally obtain

$$
\begin{aligned}
\left\| u^\varepsilon(T,\cdot) - S_T\bar{u}\right\|_{\mathbf{L}^1} &\le \left\| S_T u^\varepsilon(0,\cdot) - S_T\bar{u}\right\|_{\mathbf{L}^1} + \left\| u^\varepsilon(T,\cdot) - S_T u^\varepsilon(0,\cdot)\right\|_{\mathbf{L}^1} \\
&\le L\cdot\left\| u^\varepsilon(0,\cdot) - \bar{u}\right\|_{\mathbf{L}^1} + L\cdot\int_0^T \left\{ \liminf_{h\to 0+} \frac{\left\| u^\varepsilon(\tau+h) - S_h u^\varepsilon(\tau)\right\|_{\mathbf{L}^1}}{h} \right\} d\tau \\
&= \mathscr{O}(1)\cdot\varepsilon + \mathscr{O}(1)\cdot\varepsilon T.
\end{aligned}
$$

7.2 Characterization of Semigroup Trajectories

In this section, we describe a set of conditions which, among all weak solutions of the system (93) characterizes precisely the ones obtained as limits of front tracking approximations. These conditions, introduced in [10], are obtained by locally comparing a given solution with two types of approximations.

1. Comparison with solutions to a Riemann problem.

Let $u = u(t, x)$ be a weak solution. Fix a point (τ, ξ). Define $U^\sharp = U^\sharp_{(\tau,\xi)}$ as the solution of the Riemann problem corresponding to the jump at (τ, ξ) (Fig. 49):

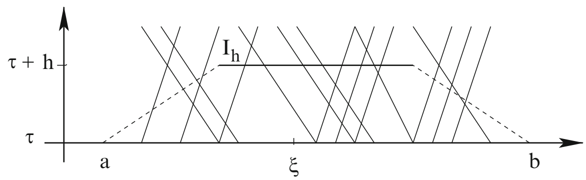

Fig. 50 The solution to a linearized hyperbolic system

$$w_t + f(w)_x = 0, \qquad w(\tau, x) = \begin{cases} u^+ \doteq u(\tau, \xi+) & if \quad x > \xi \\ u^- \doteq u(\tau, \xi-) & if \quad x < \xi \end{cases}$$

We expect that, if u satisfies the admissibility conditions, then u will be asymptotically equal to $U^\sharp$ in a forward neighborhood of the point (τ, ξ). More precisely, for every $\hat{\lambda} > 0$, one should have

$$\lim_{h\to 0+} \frac{1}{h} \int_{\xi - h\hat{\lambda}}^{\xi + h\hat{\lambda}} \left| u(\tau + h,\ x) - U^\sharp_{(\tau,\xi)}(\tau + h,\ x) \right| dx \ = \ 0. \tag{E1}$$

2. Comparison with solutions to a linear hyperbolic problem.

Fix again a point (τ, ξ), and choose $\hat{\lambda} > 0$ larger than all wave speeds. Define $U^\flat = U^\flat_{(\tau,\xi)}$ as the solution of the linear Cauchy problem (Fig. 50)

$$w_t + \widetilde{A} w_x = 0 \qquad w(\tau, x) = u(\tau, x)$$

with "frozen" coefficients: $\widetilde{A} \doteq A\big(u(\tau, \xi)\big)$. Then, for $a < \xi < b$ and $h > 0$, we expect that the difference between these two solutions should be estimated by

$$\frac{1}{h} \int_{a+\hat{\lambda}h}^{b-\hat{\lambda}h} \left| u(\tau + h,\ x) - U^\flat(\tau + h,\ x) \right| dx \ = \ \mathcal{O}(1) \cdot \Big(\text{Tot.Var.}\{u(\tau, \cdot);\ ]a, b[\} \Big)^2 \tag{E2}$$

A heuristic motivation for the above estimate is as follows. The functions u, w satisfy

$$u_t = -A(u) u_x\,, \qquad w_t = -\widetilde{A} w_x\,, \qquad u(\tau) = w(\tau).$$

Hence

$$\int_{a+\hat{\lambda}h}^{b-\hat{\lambda}h} \left| u(\tau + h, x) - U^\flat(\tau + h, x) \right| dx \approx \int_\tau^{\tau+h} \int_{J(t)} \left| A(u(t,x)) u_x - A(u(\tau, \xi)) w_x \right| dx dt, \tag{145}$$

where $J(t) \doteq \,]a + (t-\tau)\hat\lambda\,,\ \ b - (t-\tau)\hat\lambda\,[$. We now have

$$\int_{J(t)} \Big(|u_x(t,x)| + |w_x(t,x)| \Big)\, dx = \mathcal{O}(1) \cdot \text{Tot.Var.}\Big\{ u(\tau,\cdot);\ \ ]a,\, b[\Big\}\,,$$

$$\sup_{\tau<t<\tau+h,\ \ x\in J(t)} \Big| A(u(t,x)) - A(u(\tau,\xi)) \Big| = \mathcal{O}(1) \cdot \text{Tot.Var.}\big\{ u(\tau,\cdot);\ \ ]a,\, b[\big\}.$$

Therefore, for each time $t \in [\tau,\ \tau+h]$, the integrand on the right hand side of (145) is of the same order of magnitude as the square of the total variation. This yields (E2).

It can be proved that all solutions obtained as limits of front tracking approximations satisfy the estimates (E1)–(E2), for every τ, ξ, a, b. The following theorem, proved in [10], shows that the estimates (E1)–(E2) completely characterize semigroup trajectories, among all Lipschitz continuous functions $u : [0,T] \mapsto \mathbf{L}^1$ with values in the domain $\mathcal{D}$ defined at (132) .

Theorem 6 (Characterization of semigroup trajectories). *Let $u : [0,T] \mapsto \mathcal{D}$ be Lipschitz continuous w.r.t. the $\mathbf{L}^1$ distance. Then u is a weak solution to the system of conservation laws*

$$u_t + f(u)_x = 0$$

obtained as limit of front tracking approximations if and only if the estimates (E1)–(E2) are satisfied for a.e. $\tau \in [0,T]$, at every $\xi \in I\!R$.

The proof is based on the fact that the two estimates (E1) and (E2) together imply that

$$\lim_{h\to 0+} \frac{\|u(\tau+h) - S_h u(\tau)\|_{\mathbf{L}^1}}{h} = 0 \qquad \text{for a.e. } \tau. \tag{146}$$

Hence, by the error formula (7) in the Appendix,

$$\|u(t) - S_t u(0)\|_{\mathbf{L}^1} \le L \cdot \int_0^T \left\{ \liminf_{h\to 0+} \frac{\big\|u(\tau+h) - S_h u(\tau)\big\|_{\mathbf{L}^1}}{h} \right\} d\tau = 0$$

for all $t \ge 0$.

In order to prove (146), choose points x_i such that $\text{Tot.Var.}\Big\{ u(\tau)\,;\ \ ]x_{i-1}\,,\ x_i[\Big\} < \varepsilon$ for every i. For $h > 0$ small, we split an integral over the entire real line into a sum of integrals over different intervals, as shown in Fig. 51:

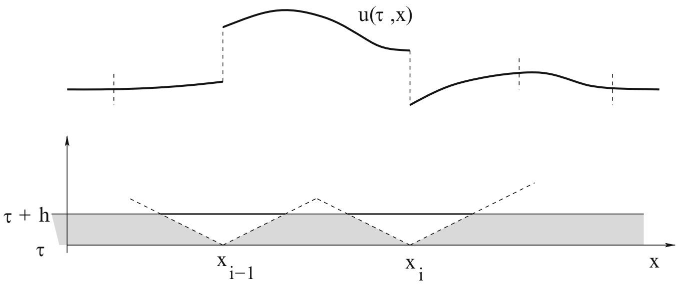

Fig. 51 Proving the asymptotic error estimate (146)

$$
\begin{aligned}
&\frac{1}{h}\int_{-\infty}^{\infty}\Big|u(\tau+h,x)-S_h u(\tau)(x)\Big|\,dx\\
&= \sum_i \frac{1}{h}\int_{x_i-\hat\lambda h}^{x_i+\hat\lambda h}\Big\{\Big|u(\tau+h,x)-U_i^\sharp(\tau+h,x)\Big|+\Big|S_h u(\tau)(x)-U_i^\sharp(\tau+h,x)\Big|\Big\}\,dx\\
&\quad+\sum_i \frac{1}{h}\int_{x_{i-1}+\hat\lambda h}^{x_i-\hat\lambda h}\Big\{\Big|u(\tau+h,x)-U_i^\flat(\tau+h,x)\Big|+\Big|S_h u(\tau)(x)-U_i^\flat(\tau+h,x)\Big|\Big\}\,dx\\
&= \sum_i A_i+\sum_i B_i\,.
\end{aligned}
$$

The estimate (E1) implies $A_i \to 0$ as $h \to 0$, while the estimate (E2) implies $B_i \le \varepsilon\cdot\text{Tot.Var.}\Big\{u(\tau)\,;\;\,]x_{i-1}\,,\;x_i[\Big\}$, and hence

$$\sum_i B_i \;\le\; \varepsilon\cdot\text{Tot.Var.}\Big\{u(\tau)\,;\;I\!R\Big\} \;=\; \mathcal{O}(\varepsilon).$$

Since $\varepsilon > 0$ is arbitrary, this proves (146).

7.3 Uniqueness Theorems

Relying on Theorem 6, there is a natural strategy in order to prove uniqueness of solutions to the Cauchy problem:

1. Introduce a suitable set of admissibility + regularity assumptions.
2. Show that these assumptions imply the estimates (E1) and (E2).

For sake of clarity, a complete set of assumptions is listed below.

(A1) **(Conservation Equations)** The function $u = u(t,x)$ is a weak solution of the Cauchy problem (93)–(94), taking values within the domain $\mathcal{D}$ of a semigroup S. More precisely, $u : [0,T] \mapsto \mathscr{D}$ is continuous w.r.t. the $\mathbf{L}^1$ distance. The identity $u(0,\cdot) = \bar{u}$ holds in $\mathbf{L}^1$, and moreover

$$\iint \big(u\varphi_t + f(u)\varphi_x\big)\,dxdt = 0 \tag{147}$$

for every $\mathscr{C}^1$ function φ with compact support contained inside the open strip $]0,T[\times I\!R$.

(A2) **(Lax Admissibility Conditions)** Let u have an approximate jump discontinuity at some point $(\tau,\xi) \in]0,T[\times I\!R$. More precisely, assume that there exists states $u^-, u^+ \in I\!R^n$ and a speed $\lambda \in I\!R$ such that, calling

$$U(t,x) \doteq \begin{cases} u^- & if \quad x < \lambda t, \\ u^+ & if \quad x > \lambda t, \end{cases} \tag{148}$$

there holds

$$\lim_{r\to 0+} \frac{1}{r^2}\int_{-r}^{r}\int_{-r}^{r} \Big|u(\tau+t,\ \xi+x) - U(t,x)\Big|\,dxdt = 0. \tag{149}$$

By Theorem 1, the piecewise constant function U must be a weak solution to the system of conservation laws, satisfying the Rankine–Hugoniot equations (29). In particular, the jump $u^+ - u^-$ should be an eigenvector of the averaged matrix $A(u^-,u^+)$, say of the i-th family, for some $i \in \{1,\dots,n\}$. In this case, we assume that the following shock admissibility conditions hold:

$$\lambda_i(u^-) \ \geq\ \lambda\ \geq\ \lambda_i(u^+). \tag{150}$$

(A3) **(Tame Oscillation Condition)** For some constants $C, \hat{\lambda}$ the following holds. For every point $x \in I\!R$ and every $t, h > 0$ one has

$$\big|u(t+h,x) - u(t,x)\big| \ \leq\ C\cdot \text{Tot.Var.}\Big\{u(t,\cdot);\ \ [x-\hat{\lambda}h,\ x+\hat{\lambda}h]\Big\}. \tag{151}$$

(A4) **(Bounded Variation Condition)** There exists $\delta > 0$ such that, for every space-like curve $\big\{t = \tau(x)\big\}$ with $|d\tau/dx| \leq \delta$ a.e., the function $x \mapsto u\big(\tau(x),x\big)$ has locally bounded variation.

Remark 6. The condition (A3) restricts the oscillation of the solution. An equivalent, more intuitive formulation is the following (see Fig. 52). For some constant $\hat{\lambda}$ larger than all characteristic speeds, given any interval $[a,b]$ and $t \geq 0$, the oscillation of u on the triangle $\Delta \doteq \big\{(s,y):\ \ s\geq t,\ a+\hat{\lambda}(s-t) < y < b-\hat{\lambda}(s-t)\big\}$, defined as

$$\text{Osc}\big\{u;\ \Delta\big\} \doteq \sup_{(s,y),(s',y')\in\Delta} \big|u(s,y) - u(s',y')\big|,$$

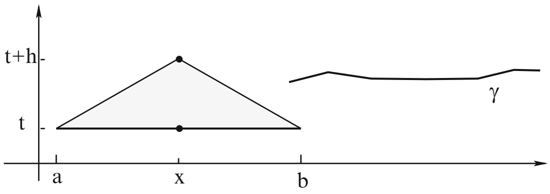

Fig. 52 Illustrating the tame oscillation and the bounded variation condition

is bounded by a constant multiple of the total variation of $u(t,\cdot)$ on $[a,b]$.

The assumption (A4) simply requires that, for some fixed $\delta > 0$, the function u has bounded variation along every space-like curve γ which is "almost horizontal" (Fig. 52). Indeed, the condition is imposed only along curves of the form $\{t = \tau(x);\ x \in [a,b]\}$ with

$$\big|\tau(x) - \tau(x')\big| \leq \delta|x - x'| \qquad \text{for all } x, x' \in [a,b].$$

One can prove that all of the above assumptions are satisfied by weak solutions obtained as limits of Glimm or wave-front tracking approximations [11]. The following result shows that the entropy weak solution of the Cauchy problem (93)–(94) is unique within the class of functions that satisfy either the additional regularity condition (A3), or (A4).

Theorem 7. *Assume that the function $u : [0,T] \mapsto \mathscr{D}$ is continuous (w.r.t. the $\mathbf{L}^1$ distance), taking values in the domain of the semigroup S generated by the system (93). If* (A1), (A2) *and* (A3) *hold, then*

$$u(t,\cdot) = S_t \bar{u} \qquad \textit{for all } t \in [0,T]. \tag{152}$$

In particular, the weak solution that satisfies these conditions is unique. The same conclusion holds if the assumption (A3) *is replaced by* (A4).

The first part of this theorem was proved in [15], the second part in [17]. Both of these papers extend the result in [16], where this approach to uniqueness was first developed.

8 The Vanishing Viscosity Approach

In view of the previous uniqueness and stability results, one expects that the entropy-admissible weak solutions of the hyperbolic system

$$u_t + f(u)_x = 0 \tag{153}$$

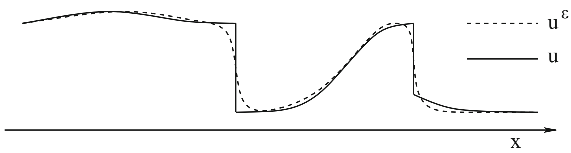

Fig. 53 A discontinuous solution to the hyperbolic system and a viscous approximation

should coincide with the unique limits of solutions to the parabolic system

$$u_t^\varepsilon + f(u^\varepsilon)_x = \varepsilon\, u_{xx}^\varepsilon \tag{154}$$

letting the viscosity coefficient $\varepsilon \to 0$. For smooth solutions, this convergence is easy to show. However, one should keep in mind that a weak solution of the hyperbolic system (153) in general is only a function with bounded variation, possibly with a countable number of discontinuities. In this case, as the smooth functions u^ε approach the discontinuous solution u, near points of jump their gradients u_x^ε tend to infinity (Fig. 53), while their second derivatives u_{xx}^ε become even more singular. Therefore, establishing the convergence $u^\varepsilon \to u$ is a highly nontrivial matter. In earlier literature, results in this direction relied on three different approaches:

1. Comparison principles for parabolic equations. For a scalar conservation law, the existence, uniqueness and global stability of vanishing viscosity solutions was first established by Oleinik [51] in one space dimension. The famous paper by Kruzhkov [39] covers the more general class of $\mathbf{L}^\infty$ solutions and is also valid in several space dimensions.

2. Singular perturbations. This technique was developed by Goodman and Xin [36], and covers the case where the limit solution u is piecewise smooth, with a finite number of non-interacting, entropy admissible shocks. See also [58] and [53], for further results in this direction.

3. Compensated compactness. With this approach, introduced by Tartar and DiPerna [29], one first considers a weakly convergent subsequence $u^\varepsilon \rightharpoonup u$. For a class of 2×2 systems, one can show that this weak limit u actually provides a distributional solution to the nonlinear system (153). The proof relies on a compensated compactness argument, based on the representation of the weak limit in terms of Young measures, which must reduce to a Dirac mass due to the presence of a large family of entropies.

Since the hyperbolic Cauchy problem is known to be well posed within a space of functions with small total variation, it is natural to develop a theory of vanishing viscosity approximations within the same space BV. This was indeed accomplished in [7], in the more general framework of nonlinear hyperbolic systems not necessarily in conservation form. The only assumptions needed here are the strict hyperbolicity of the system and the small total variation of the initial data.

Theorem 8 (BV estimates and convergence of vanishing viscosity approximations). *Consider the Cauchy problem for the hyperbolic system with viscosity*

$$u_t^\varepsilon + A(u^\varepsilon)u_x^\varepsilon \;=\; \varepsilon\, u_{xx}^\varepsilon \qquad\qquad u^\varepsilon(0,x) = \bar{u}(x). \tag{155}$$

Assume that the matrices $A(u)$ are strictly hyperbolic (i.e., they have real, distinct eigenvalues), and depend smoothly on u in a neighborhood of the origin. Then there exist constants C, L, L' and $\delta > 0$ such that the following holds. If

$$Tot.Var.\{\bar{u}\} \ < \ \delta\,, \qquad \qquad \|\bar{u}\|_{\mathbf{L}^\infty} \ < \ \delta, \tag{156}$$

then for each $\varepsilon > 0$ the Cauchy problem (155)$_\varepsilon$ has a unique solution u^ε, defined for all $t \geq 0$. Adopting a semigroup notation, this will be written as $t \mapsto u^\varepsilon(t,\cdot) \doteq S_t^\varepsilon \bar{u}$.

In addition, one has:

$$\textbf{\textit{BV bounds :}} \qquad \qquad Tot.Var.\left\{S_t^\varepsilon \bar{u}\right\} \ \leq \ C \ Tot.Var.\{\bar{u}\}. \tag{157}$$

$$\mathbf{L}^1 \textbf{\textit{ stability :}} \qquad \qquad \left\|S_t^\varepsilon \bar{u} - S_t^\varepsilon \bar{v}\right\|_{\mathbf{L}^1} \ \leq \ L \left\|\bar{u} - \bar{v}\right\|_{\mathbf{L}^1}, \tag{158}$$

$$\left\|S_t^\varepsilon \bar{u} - S_s^\varepsilon \bar{u}\right\|_{\mathbf{L}^1} \ \leq \ L' \left(|t-s| + \left|\sqrt{\varepsilon t} - \sqrt{\varepsilon s}\,\right|\right). \tag{159}$$

Convergence: *As $\varepsilon \to 0+$, the solutions u^ε converge to the trajectories of a semigroup S such that*

$$\left\|S_t \bar{u} - S_s \bar{v}\right\|_{\mathbf{L}^1} \ \leq \ L \ \|\bar{u} - \bar{v}\|_{\mathbf{L}^1} + L' \, |t-s|. \tag{160}$$

These vanishing viscosity limits can be regarded as the unique vanishing viscosity solutions *of the hyperbolic Cauchy problem*

$$u_t + A(u) u_x \ = \ 0, \qquad \qquad u(0,x) = \bar{u}(x). \tag{161}$$

In the conservative case $A(u) = Df(u)$, every vanishing viscosity solution is a weak solution of

$$u_t + f(u)_x \ = \ 0, \qquad \qquad u(0,x) = \bar{u}(x)\,, \tag{162}$$

satisfying the Liu admissibility conditions.

Assuming, in addition, that each characteristic field is genuinely nonlinear or linearly degenerate, the vanishing viscosity solutions coincide with the unique limits of Glimm and front tracking approximations.

In the genuinely nonlinear case, an estimate on the rate of convergence of these viscous approximations was provided in [19]:

Theorem 9 (Convergence rate). *For the strictly hyperbolic system of conservation laws (162), assume that every characteristic field is genuinely nonlinear. At any time $t > 0$, the difference between the corresponding solutions of (155) and (162) can be estimated as*

$$\left\|u^\varepsilon(t,\cdot) - u(t,\cdot)\right\|_{\mathbf{L}^1} \ = \ \mathcal{O}(1) \cdot (1+t)\sqrt{\varepsilon}\,|\ln \varepsilon| \ Tot.Var.\{\bar{u}\}.$$

In the following sections we outline the main ideas of the proof of Theorem 8. For details, see [7] or the lecture notes [12].

8.1 Local Decomposition by Traveling Waves

As a preliminary, observe that u^ε is a solution of (155) if and only if the rescaled function $u(t,x) \doteq u^\varepsilon(\varepsilon t, \varepsilon x)$ is a solution of the parabolic system with unit viscosity

$$u_t + A(u)u_x = u_{xx}\,, \tag{163}$$

with initial data $u(0,x) = \bar{u}(\varepsilon x)$. Clearly, the stretching of the space variable has no effect on the total variation. Notice however that the values of u^ε on a fixed time interval $[0,T]$ correspond to the values of u on the much longer time interval $[0,\ T/\varepsilon]$. To obtain the desired BV bounds for the viscous solutions u^ε, it suffices to study solutions of (163). However, we need estimates uniformly valid for all times $t \geq 0$, depending only on the total variation of the initial data $\bar{u}$.

To provide a uniform estimate on Tot.Var.$\{u(t,\cdot)\} = \|u_x(t,\cdot)\|_{\mathbf{L}^1}$, we decompose the gradient u_x along a basis of unit vectors $\tilde{r}_1,\dots,\tilde{r}_n$, say

$$u_x = \sum_i v_i \tilde{r}_i\,. \tag{164}$$

We then derive an evolution equation for these gradient components, of the form

$$v_{i,t} + (\tilde{\lambda}_i v_i)_x - v_{i,xx} = \phi_i \qquad\qquad i = 1,\dots,n\,, \tag{165}$$

Since the left hand side of (165) is in conservation form, we have

$$\|u_x(t)\| \leq \sum_{i=1}^n \|v_i(t,\cdot)\|_{\mathbf{L}^1} \leq \sum_i \left(\|v_i(0,\cdot)\|_{\mathbf{L}^1} + \int_0^t \|\phi_i(s,\cdot)\|_{\mathbf{L}^1}\, ds \right). \tag{166}$$

A crucial point in the entire analysis is the choice of the unit vectors $\tilde{r}_i$. A natural guess would be to take $\tilde{r}_i = r_i(u)$, the i-th eigenvector of the hyperbolic matrix $A(u)$. This was indeed the decomposition used in Sect. 1.6. As in (22), we thus write

$$u_x = \sum_i u_x^i r_i \qquad\qquad u_x^i \doteq l_i \cdot u_x\,, \tag{167}$$

so that (163) takes the form

$$u_t = -\sum_i \lambda_i u_x^i r_i + \sum_i (u_x^i r_i)_x. \tag{168}$$

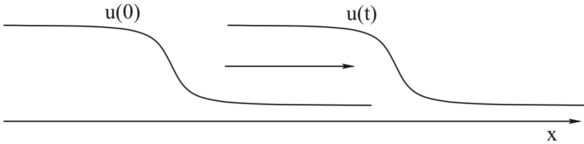

Fig. 54 For a viscous traveling wave, the source terms ϕ_i are usually not integrable

Differentiating the first equation in (167) w.r.t. t and the equation in (168) w.r.t. x, and equating the results, we obtain an evolution equation for the gradient components u_x^i, namely

$$(u_x^i)_t + (\lambda_i u_x^i)_x - (u_x^i)_{xx} = \phi_i(u, u_x^1, \ldots, u_x^n) \doteq l_i \cdot \sum_{j<k} \lambda_k [r_k, r_j] u_x^j u_x^k$$

$$+ l^i \cdot \left\{ 2 \sum_{j,k} (r_k \bullet r_j)(u_x^j)_x u_x^k + \sum_{j,k,\ell} \Big(r_\ell \bullet (r_k \bullet r_j) - (r_\ell \bullet r_k) \bullet r_j \Big) u_x^j u_x^k u_x^\ell \right\}. \tag{169}$$

Here $r_k \bullet r_j \doteq (Dr_j)r_k$ denotes the directional derivative of r_j along r_k, while $[r_k, r_j] \doteq (Dr_j)r_k - (Dr_k)r_j$ is the Lie bracket of the two vector fields. Relying on the above formula, in order to achieve BV bounds uniformly valid for $t \in [0, \infty[$, we would need $\int_0^\infty \int |\phi_i| \, dxdt < \infty$. Unfortunately this does not hold, in general. Indeed, for a typical solution having the form of a traveling wave $u(t,x) = \bar{u}(x - \lambda t)$, as in Fig. 54, the source terms do not vanish identically: $\phi_i \not\equiv 0$. Therefore

$$\int_0^t \int |\phi_i(\tau, x)| \, dxd\tau = t \cdot \int |\phi_i(0,x)| \, dx \to \infty \qquad \text{as } t \to \infty$$

To readdress this situation, a key idea is to decompose u_x not along the eigenvectors $r_1, \ldots, r_n$ of $A(u)$, but along a basis $\{\tilde{r}_1, \ldots \tilde{r}_n\}$ of **gradients of viscous traveling waves**.

We recall that a traveling wave solution of the viscous hyperbolic system (163) is a solution of the form

$$u(t,x) = U(x - \sigma t). \tag{170}$$

Here the constant $\sigma = -U_t/U_x$ is the speed of the wave. Inserting (170) in (163), we see that the function U should satisfy the second order O.D.E.

$$U'' = \big(A(U) - \sigma\big)U'. \tag{171}$$

As shown in Fig. 55, we wish to decompose $u_x = \sum_i U_i'$ locally as sum of gradients of traveling waves. More precisely, given (u, u_x, u_{xx}) at a point x, we seek traveling wave profiles $U_1, \ldots, U_n$ such that

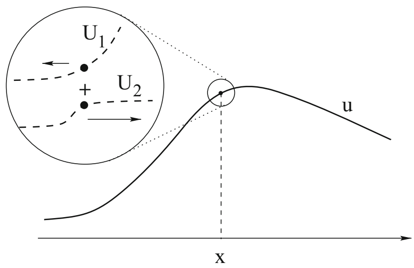

Fig. 55 Decomposing the function u as the superposition of two viscous traveling profiles, in a neighborhood of a point x

$$U_i'' = \big(A(U_i) - \sigma_i\big)U_i', \qquad U_i(x) = u(x) \qquad i = 1, \ldots, n, \tag{172}$$

$$\sum_i U_i'(x) = u_x(x), \qquad \sum_i U_i''(x) = u_{xx}(x). \tag{173}$$

Observe that, having fixed $u(x)$, the system (172)–(173) yields

- $n + n$ scalar equations.
- $n^2 + n$ free parameters: the vectors $U_1'(x), \ldots, U_n'(x) \in I\!R^n$, describing the first derivatives of the traveling waves, and the scalars $\sigma_1, \ldots, \sigma_n$, describing the speeds.

For $n > 1$, the system is under-determined. To achieve a unique decomposition, further restrictions must thus be imposed on the choice of the traveling wave profiles. Indeed, for each given state $u \in I\!R^n$ and $i = 1, \ldots, n$, we should select a two-parameter family of traveling waves through u. This is done using the center manifold theorem [13].

To begin with, we replace the second order O.D.E. (171) describing traveling waves with an equivalent first order system:

$$\begin{cases} \dot u = v, \\ \dot v = \big(A(u) - \sigma\big)v, \\ \dot\sigma = 0. \end{cases} \tag{174}$$

This consists of $n + n + 1$ O.D.E's. Notice that the last equation simply says that the speed σ is a constant. Fix a state $u^* \in I\!R^n$. Linearizing (171) at the equilibrium point $P^* = (u^*, 0, \lambda_i(u^*))$, one obtains the system

$$\begin{pmatrix} \dot u \\ \\ \dot v \\ \\ \dot\sigma \end{pmatrix} = \begin{pmatrix} 0 & I & 0 \\ \\ 0 & A(u^*) - \lambda_i(u^*)I & 0 \\ \\ 0 & 0 & 0 \end{pmatrix} \begin{pmatrix} u \\ \\ v \\ \\ \sigma \end{pmatrix} \in I\!R^{n+n+}. \tag{175}$$

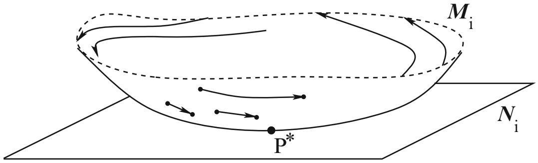

Fig. 56 The linear subspace $\mathcal{N}_i$ and the center manifold $\mathcal{M}_i$ tangent to $\mathcal{N}_i$ at the equilibrium point P^*

Recalling that $A(u^*)$ is a $n \times n$ matrix with real and distinct eigenvalues, one checks that the center subspace $\mathcal{N}_i$ for the $(2n+1) \times (2n+1)$ matrix in (175) (i.e., the invariant subspace corresponding to all generalized eigenvalues with zero real part) has dimension $n + 2$.

By the center manifold theorem, for each $i = 1, \ldots, n$, the nonlinear system (174) has a center manifold $\mathcal{M}_i$ of dimension $n + 2$, tangent to the center subspace $\mathcal{N}_i$ at P^* (Fig. 56).

A more detailed analysis shows that on $\mathcal{M}_i$ we can choose coordinates $(u, v^i, \sigma_i) \in I\!R^{n+1+1}$. Here v^i is the signed strength of the traveling wave profile through u, and σ_i is its speed. In other words, at any given point $\bar{x}$, for every (u, v^i, σ_i) in a neighborhood of $(u^*, 0, \lambda_i(u^*))$, there exists a unique solution to (171) such that

$$U_i(\bar{x}) = u, \qquad U_i'' = (A(U_i) - \sigma_i)U_i', \qquad U_i'(\bar{x}) = v^i \tilde{r}_i$$

for some unit vector $\tilde{r}_i = \tilde{r}_i(u, v^i, \sigma_i)$.

The previous construction in terms of center manifold trajectories provides a decomposition of u_x along a basis of *generalized eigenvectors*: $\tilde{r}_i(u, v^i, \sigma_i)$. These are unit vectors, close to the usual eigenvectors $r_i(u)$ of the matrix $A(u)$, which depend on two additional parameters.

Defining the corresponding *generalized eigenvalues* in terms of a scalar product:

$$\tilde{\lambda}_i(u, v^i, \sigma_i) \doteq \langle \tilde{r}_i \,,\ A(u)\tilde{r}_i \rangle,$$

one can prove the key identity

$$(A(u) - \tilde{\lambda}_i)\tilde{r}_i = v^i \big(\tilde{r}_{i,u}\tilde{r}_i + \tilde{r}_{i,v}(\tilde{\lambda}_i - \sigma_i)\big). \tag{176}$$

This replaces the standard identity

$$\big(A(u) - \lambda_i\big) r_i = 0 \tag{177}$$

satisfied by the eigenvectors and eigenvalues of $A(u)$. The additional terms on the right hand side of (176) play a crucial role, achieving a cancellation in the source terms ϕ_i in (165). Eventually, this allows us to prove that these source terms are globally integrable, in t and x.

8.2 Evolution of Gradient Components

Let $(u, u_x, u_{xx}) \in I\!R^{3n}$ be given, in a neighborhood of the origin. For convenience, instead of the decomposition (172)–(173), it is convenient to set $u_t = u_{xx} - A(u)u_x$ and seek a decomposition of the form

$$\begin{cases} u_x = \sum v^i \tilde{r}_i(u, v^i, \sigma_i) \\ \\ u_t = \sum w^i \tilde{r}_i(u, v^i, \sigma_i) \end{cases} \qquad \text{with} \quad \sigma_i \approx -\frac{w^i}{v^i}.$$

After a lengthy computation, one finds that these components satisfy a system of evolution equations of the form

$$\begin{cases} v^i_t + (\tilde{\lambda}_i v^i)_x - v^i_{xx} = \phi_i \\ w^i_t + (\tilde{\lambda}_i w^i)_x - w^i_{xx} = \psi_i \end{cases} \tag{178}$$

A detailed analysis of the right hand sides of (178) shows that these source terms can be estimated as

$$\phi_i,\ \psi_i = \mathcal{O}(1) \cdot \textstyle\sum_j |w^j + \sigma_j v^j| \cdot \Big(|v^j w^j| + |v^j_x| + |w^j_x|\Big) \qquad \textbf{(wrong speed)}$$

$$+\mathcal{O}(1) \cdot \textstyle\sum_j |w^j_x v^j - v^j_x w^j| \qquad \textbf{(change in speed, linear)}$$

$$+\mathcal{O}(1) \cdot \textstyle\sum_j \left| v^j \left(\frac{w^j}{v^j}\right)_x \right|^2 \qquad \textbf{(change in speed, quadratic)}$$

$$+\mathcal{O}(1) \cdot \textstyle\sum_{j \neq k} \Big(|v^j v^k| + |v^j_x v^k| + |v^j w^k| + |v^j_x w^k| + |w^j w^k|\Big)$$

(interaction of waves of different families)

See [7] for detailed computations. Here we can only give an intuitive motivation for how these source terms arise. If u is precisely a j-traveling wave profile on the center manifold $\mathcal{M}_j$, say $u(t,x) = U_j(x - \sigma_j t)$, then by the key identity (176) it follows that all source terms vanish identically (Fig. 57). In essence, the size of these source terms is determined by how much the second order jet (u, u_x, u_{xx}) in our solution u differs from the jet of a traveling wave profile (Fig. 58).

Wrong speed. In a traveling wave profile $u(t,x) = U(t - \sigma t)$, the speed is the constant value $\sigma = -U_t/U_x$. However, near a point x_0 where $u_x = 0$, the speed of a traveling wave would be $\sigma = -u_t/u_x \to \infty$. Since we want $\sigma_i \approx \lambda_i(u^*)$, i.e., close to the i-th characteristic speed, a cut-off function must be used. These source terms describe by how much the identity $\sigma_i = -w^i/v^i$ is violated.

Change in wave speed. These terms account for local interactions of waves of the same family. Think of the viscous traveling j-wave that best approximates u at a point x, and at a nearby point x'. In general, these two profiles will not be the same, hence some local interaction between them will occur. A measure of how much the

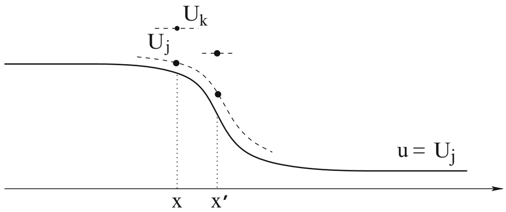

Fig. 57 If u coincides with a traveling wave profile, say of the j-th family, then all source terms vanish identically

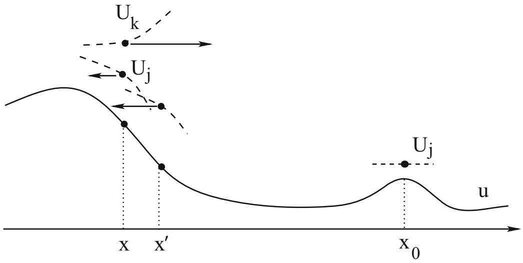

Fig. 58 Source terms arise because of (1) Interactions of j-waves with k-waves, (2) Interactions between waves of the same j-th family, if their speed varies with x, (3) Points x_0 where the decomposition in traveling profiles cannot be performed exactly

j-traveling profile changes, as the point x varies, is provided by the change in speed: $(\sigma_j)_x$

Assuming that the speed satisfies $\sigma_j = -w^j/v^j$, one has

$$\left|(\sigma_j)_x\right| = \frac{|w_x^j v^j - v_x^j w^j|}{|v^j|^2}.$$

The terms related to change in wave speeds can thus be written as products:

$$[\text{strength of the wave}]^2 \times [\text{rate of change of the speed}]^\alpha$$

with $\alpha = 1, 2$. More precisely,

$$\mathcal{O}(1) \cdot \sum_{j=1}^{n} |v^j|^2 \left|(\sigma_j)_x\right| + \mathcal{O}(1) \cdot \sum_{j=1}^{n} |v^j|^2 \left|(\sigma_j)_x\right|^2.$$

Transversal wave interactions. In general, at a given point x, waves of distinct families $j \neq k$ are present. These terms model interactions between these different waves.

8.3 Lyapunov Functionals

We seek uniform bounds on the norms $\|v^i(t)\|_{\mathbf{L}^1}$, $\|w^i(t)\|_{\mathbf{L}^1}$, independent of time. Since the left hand sides of (178) are in conservation form, it suffices to show that all source terms are uniformly integrable in both variables t, x. To prove that

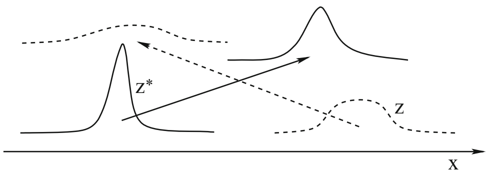

Fig. 59 Interaction of two viscous waves of different families

$$\int_0^\infty \|\phi_i(\tau)\|_{\mathbf{L}^1}\, d\tau \;<\; \infty, \qquad\qquad \int_0^\infty \|\psi_i(\tau)\|_{\mathbf{L}^1}\, d\tau \;<\; \infty,$$

we construct suitable Lyapunov functionals $\Psi(u) \geq 0$ such that

$$\|\phi_i(t)\|_{\mathbf{L}^1}, \|\psi_i(t)\|_{\mathbf{L}^1} \;\leq\; -\frac{d}{dt}\Psi(u(t))$$

In other words, at each time t, the $\mathbf{L}^1$ norm of source terms should be controlled by the rate of decrease of the functional. A summary of the basic estimates is as follows:

Wrong speed	$\Longrightarrow$	**Parabolic energy estimates**
Change in wave speed, linear	$\Longrightarrow$	**Area functional**
Change in wave speed, quadratic	$\Longrightarrow$	**Curve length functional**
Interaction of waves of different families	$\Longrightarrow$	**Wave interaction potential**

In the remainder of this section we describe the main ideas involved in the construction of these functionals.

1. Lyapunov functionals for a pair of linear parabolic equations.

Consider the system of two linear, scalar parabolic equations

$$\begin{cases} z_t + \big[\lambda(t,x)\, z\big]_x - z_{xx} \;=\; 0, \\ z_t^* + \big[\lambda^*(t,x)\, z^*\big]_x - z_{xx}^* \;=\; 0. \end{cases}$$

Assume that the propagation speeds λ and λ^* are strictly different:

$$\inf_{t,x} \lambda^*(t,x) - \sup_{t,x} \lambda(t,x) \;\geq\; c \;>\; 0.$$

It is useful to think of $z(\cdot)$ as the density of waves with slow speed λ, while $z^*(\cdot)$ is the density of waves with fast speed λ^*. The *instantaneous amount of interaction* between z and z^* is defined as (Fig. 59)

$$I(t) \;\doteq\; \int \big|z(t,x)\big| \cdot \big|z^*(t,x)\big|\, dx.$$

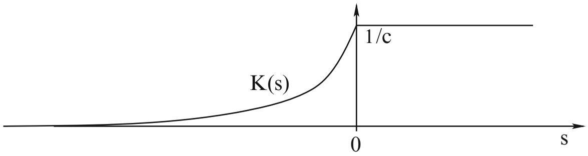

Fig. 60 The interaction kernel K defined at (180)

In order to bound the total amount of interaction, we introduce a *potential for transversal wave interactions* with :

$$Q(z, z^\sharp) \doteq \iint K(x-y)\,|z(x)|\,|z\sharp(y)|\,dxdy\,, \tag{179}$$

with (Fig. 60)

$$K(s) \doteq \begin{cases} 1/c & if \quad s \geq 0, \\ e^{cs/2}/c & if \quad s < 0. \end{cases} \tag{180}$$

Computing the distributional derivatives of the kernel K, one checks that $cK' - 2K''$ is precisely the Dirac distribution, i.e. a unit mass at the origin. We now compute

$$\begin{aligned} \frac{d}{dt} Q\big(z(t), z^\sharp(t)\big) &= \frac{d}{dt} \iint K(x-y)|z(x)|\,|z^\sharp(y)|\,dxdy \\ &= \iint K(x-y)\Big\{\big(z_{xx} - (\lambda z)_x\big)\mathrm{sgn}z(x)|z^\sharp(y)| + |z(x)|\Big(z^\sharp_{yy} - (\lambda^\sharp z^\sharp)_y\Big)\mathrm{sgn}z^\sharp(y)\Big\}\,dxdy \\ &\leq \iint K'(x-y)\Big\{\lambda|z(x)|\,|z^\sharp(y)| - \lambda^\sharp|z(x)|\,|z^\sharp(y)|\Big\}\,dxdy \\ &\quad + \iint K''(x-y)\Big\{|z(x)|\,|z^\sharp(y)| + |z(x)|\,|z^\sharp(y)|\Big\}\,dxdy \\ &\leq -\iint \big(cK' - 2K''\big)|z(x)|\,|z^\sharp(y)|\,dxdy = -\int |z(x)|\,|z^\sharp(x)|\,dx \end{aligned}$$

Therefore, since $Q \geq 0$, for every $T \geq 0$ we have

$$\begin{aligned} \int_0^T\!\!\int |z(t,x)|\,|z^\sharp(t,x)|\,dxdt &\leq Q\big(z(0), z^\sharp(0)\big) - Q\big(z(T), z^\sharp(T)\big) \\ &\leq \tfrac{1}{c}\,\big\|z(0)\big\|_{\mathbf{L}^1}\big\|z^\sharp(0)\big\|_{\mathbf{L}^1}. \end{aligned}$$

Using functionals of the form (179), one can control the source terms

$$\mathscr{O}(1)\cdot\sum_{j\neq k}\Big[|v^j v^k| + |v^j_x v^k| + |v^j w^k| + |v^j_x w^k| + |w^j w^k|\Big]$$

accounting for interaction of waves of different families.

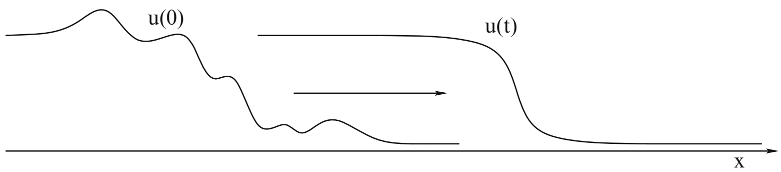

Fig. 61 As $t \to +\infty$, the solution to a scalar viscous conservation law is expected to approach a traveling wave profile

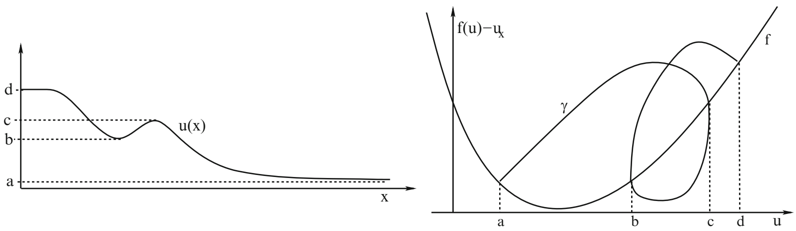

Fig. 62 *Left*: the graph of a function $u = u(x)$. *Right*: the corresponding curve $x \mapsto \gamma(x) = \Big(u(x),\ f(u(x)) - u_x(x)\Big)$

2. Lyapunov functionals for a scalar viscous conservation law
Consider a scalar conservation law with viscosity:

$$u_t + f(u)_x \;=\; u_{xx}. \tag{181}$$

We seek functionals that decrease in time, along every solution of (181). As $t \to +\infty$, we expect that the solution will approach a viscous traveling wave profile. One could thus look for a Lyapunov functional describing how far u is from a viscous traveling wave profile (Fig. 61).

For this purpose, it is convenient to adopt a variable transformation. Given a scalar function $u = u(x)$, consider the curve (Fig. 62)

$$\gamma \;\doteq\; \begin{pmatrix} u \\ f(u) - u_x \end{pmatrix} \;=\; \begin{pmatrix} \text{conserved quantity} \\ \text{flux} \end{pmatrix} \tag{182}$$

Observe that $u(\cdot)$ is a traveling wave profile if and only if the corresponding curve γ is a segment. Indeed

$$-\frac{u_t}{u_x} \;=\; \frac{f(u)_x - u_{xx}}{u_x} \;=\; \text{constant} \;=\; [\text{wave speed}]$$

if and only if

$$\frac{d}{du}\Big[f(u) - u_x\Big] \;=\; \Big[f(u) - u_x\Big]_x \cdot \frac{1}{u_x} \;=\; \text{constant.}$$

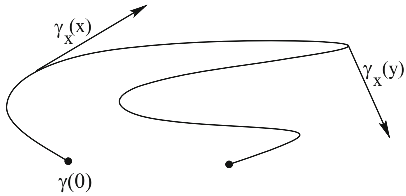

Fig. 63 Defining the area functional

If now $u = u(t,x)$ provides a solution to the viscous conservation law (181), the corresponding curve γ in (182) evolves according to the vector equation

$$\gamma_t + f'(u)\gamma_x = \gamma_{xx}. \tag{183}$$

Recalling that

$$\gamma \doteq \begin{pmatrix} u \\ f(u) - u_x \end{pmatrix}, \qquad \gamma_x = \begin{pmatrix} v \\ w \end{pmatrix} \doteq \begin{pmatrix} u_x \\ -u_t \end{pmatrix}. \tag{184}$$

we find two functionals associated with (183). One is

$$\textbf{Curve Length:} \qquad L(\gamma) \doteq \int |\gamma_x|\,dx = \int \sqrt{v^2+w^2}\,dx. \tag{185}$$

Indeed, a direct computation yields

$$\frac{d}{dt}L\big(\gamma(t)\big) = -\int \frac{|v|\Big[(w/v)_x\Big]^2}{\big(1+(w/v)^2\big)^{3/2}}\,dx.$$

Using functionals of this type, one controls the source terms

$$\mathcal{O}(1)\cdot\left|v^j\left(\frac{w^j}{v^j}\right)_x\right|^2 \qquad \text{(change in wave speed, quadratic).}$$

The second functional is (see Fig. 63)

$$\textbf{Area functional:} \qquad Q(\gamma) \doteq \frac{1}{2}\iint_{x<y}\Big|\gamma_x(x)\wedge\gamma_x(y)\Big|\,dx\,dy \tag{186}$$

If γ evolves in the direction of curvature, then Q controls the area swept by the curve: $|dA| \le -dQ$. This can best be understood thinking of polygonal approximations (Fig. 64). If γ is a polygonal with sides $\mathbf{v}_j$, the double integral in (186) is computed by a finite sum:

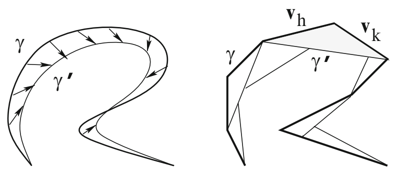

Fig. 64 The decrease in the area functional bounds the area swept by the curve in its motion

$$Q(\gamma) \;=\; \frac{1}{2}\sum_{i<j}\big|\mathbf{v}_i \wedge \mathbf{v}_j\big|. \tag{187}$$

If we now replace two consecutive edges $\mathbf{v}_h, \mathbf{v}_k$ by a single segment, the area of the corresponding triangle is

$$|dA| \;=\; \frac{1}{2}\big|\mathbf{v}_h \wedge \mathbf{v}_k\big| \leq -dQ$$

Indeed, the term $\frac{1}{2}\big|\mathbf{v}_h \wedge \mathbf{v}_k\big|$ is now missing from the sum in (187), while the sum of all other terms remains the same, or decreases.

Recalling (183)–(184), we now compute

$$-\frac{dQ}{dt} \;\geq\; \left|\frac{dA}{dt}\right| \;=\; \int |\gamma_t \wedge \gamma_x|\,dx \;=\; \int |\gamma_{xx} \wedge \gamma_x|\,dx \;=\; \int |v_x w - v w_x|\,dx.$$

As a consequence, the integral over time of the right hand side can be estimated by

$$\int_0^\infty \int |v_x w - v w_x|\,dx\,dt \;\leq\; \int_0^\infty \left|\frac{d}{dt}Q\big(\gamma(t)\big)\right|\,dt \;\leq\; Q\big(\gamma(0)\big)$$

Using functionals of this type, one can control the source terms

$$\mathcal{O}(1)\cdot|v_x^j w^j - v^j w_x^j| \qquad\qquad \text{(change in wave speed, linear).}$$

8.4 Continuous Dependence on the Initial Data

The techniques described in the previous section provide uniform estimates on the total variation of a solution u to the system (163). Similar techniques can also be used to estimate the size of first order perturbations.

Indeed, let u be solution of (163) and assume that, for each $\varepsilon > 0$, the function

$$u^\varepsilon(t,x) \;=\; u(t,x) + \varepsilon\, z(t,x) + o(\varepsilon)$$

is also a solution, with $o(\varepsilon)$ denoting an infinitesimal of higher order w.r.t. ε. Inserting the above expansion in (163) and collecting terms of order ε, one finds that the function z must satisfy the the linearized variational equation

$$z_t + \big[DA(u)\cdot z\big]u_x + A(u)z_x \;=\; z_{xx}. \tag{188}$$

Assuming that the total variation of u remains small, one can prove the estimate

$$\big\|z(t,\cdot)\big\|_{\mathbf{L}^1} \;\leq\; L\,\big\|z(0,\cdot)\big\|_{\mathbf{L}^1} \qquad \text{for all } \; t \geq 0\,, \tag{189}$$

for a uniform constant L. The above estimate is valid for every solution u of (163) having small total variation and every $\mathbf{L}^1$ solution of the corresponding system (188).

Relying on (189), a standard homotopy argument yields the Lipschitz continuity of the flow of (163) w.r.t. the initial data, uniformly in time. Indeed, let any two solutions u, v of (163) be given (Fig. 46). We can connect them by a smooth path of solutions u^θ, whose initial data satisfy

$$u^\theta(0,x) \;\doteq\; \theta u(0,x) + (1-\theta)v(0,x) \qquad\qquad \theta\in[0,1].$$

The distance $\big\|u(t,\cdot)-v(t,\cdot)\big\|_{\mathbf{L}^1}$ at any later time $t > 0$ is clearly bounded by the length of the path $\theta \mapsto u^\theta(t)$. In turn, this can be computed by integrating the norm of a tangent vector. Calling $z^\theta \doteq du^\theta/d\theta$, each vector z^θ is a solution of the corresponding (188), with u replaced by u^θ. Using (190) we thus obtain

$$\begin{aligned}\big\|u(t,\cdot)-v(t,\cdot)\big\|_{\mathbf{L}^1} \;&\leq\; \int_0^1 \left\|\frac{d}{d\theta}u^\theta(t)\right\|_{\mathbf{L}^1} d\theta \;=\; \int_0^1 \big\|z^\theta(t)\big\|_{\mathbf{L}^1}\,d\theta\\ &\leq\; L\int_0^1 \big\|z^\theta(0)\big\|_{\mathbf{L}^1}\,d\theta \;=\; L\,\big\|u(0,\cdot)-v(0,\cdot)\big\|_{\mathbf{L}^1}.\end{aligned} \tag{190}$$

8.5 The Semigroup of Vanishing Viscosity Limit Solutions

The estimates on the total variation and on the continuous dependence on the initial data, obtained in the previous sections were valid for solutions of the system (163) with unit viscosity matrix. By the simple rescaling of coordinates $t \mapsto \varepsilon t$, $x \mapsto \varepsilon x$, all of the above estimates remain valid for solutions u^ε of the system $(155)_\varepsilon$. In this way one obtains the a priori bounds (157) and (158).

As soon as the global BV bounds are established, by a compactness argument one obtains the existence of a strong limit $u^{\varepsilon_m} \to u$ in $\mathbf{L}^1_{loc}$, for some sequence $\varepsilon_m \to 0$. In the conservative case where $A = Df$, by Lemma 1 in Sect. 2 this limit $u = u(t, x)$ provides a weak solution to the Cauchy problem (162).

At this stage, it only remains to prove that the limit is unique, i.e. it does not depend on the choice of the sequence $\varepsilon_m \to 0$. For a system in conservative form, and with the standard assumption (H) that each field is either genuinely nonlinear or linearly degenerate, we can apply Theorem 7 in Sect. 7, and conclude that the limit of vanishing viscosity approximations is unique and coincides with the limit of Glimm and of front tracking approximations.

To handle the general non-conservative case, some additional work is required. Relying on the analysis in [6], one first considers Riemann initial data and shows that in this special case the vanishing viscosity solution is unique and can be accurately described. In a second step, one proves that any weak solution obtained as limit vanishing viscosity approximations is also a "viscosity solution", i.e. it satisfies the local integral estimates (E1)–(E2) in Sect. 7.2, where $U^\sharp$ is now the unique solution of a Riemann problem obtained as limit of viscous approximations [6]. By an argument introduced in [10], a Lipschitz semigroup is completely determined as soon as one specifies its local behavior for piecewise constant initial data. Characterizing its trajectories as "viscosity solutions" one thus establishes the uniqueness of the semigroup of vanishing viscosity limits.

9 Extensions and Open Problems

With the papers [7,20,34], the well-posedness of the Cauchy problem for hyperbolic conservation laws in one space dimension has been essentially settled, within the class of solutions with small total variation. Extensions of these well-posedness results to the initial-boundary value problem and to balance laws with source terms can be found in [30] and in [1], respectively.

A major remaining open problem concerns the solutions with large total variation. Results in this direction can be found in [23] and [35]. As proved by M. Lewicka [41], for a large class of hyperbolic systems the solutions are unique and depend continuously on the initial data, as long as their total variation remains bounded. The key question is whether the total variation can blow up in finite time, if the initial data is sufficiently large. An example constructed by K. Jenssen [38] shows that this can indeed happen, for some strictly hyperbolic system. One should remark, however, that the 3×3 system considered in [38] does not come from any realistic physical model. In particular, it does not admit any strictly convex entropy. One may thus conjecture that the presence of a strictly convex entropy restricts the possibility of a finite time blow up. More specifically, it is an important open problem to understand whether finite blow up in the total variation norm can occur for solutions to the Euler equations of gas dynamics.

We remark that, since hyperbolic conservation laws are a class of nonlinear evolution equations, one might expect to observe some rich dynamics: periodic orbits, bifurcation, chaotic behavior, etc... However, the present theory does not include any of this. The reason is that, as long as one considers only solutions with small total variation, the dynamics is mostly trivial. As proved by T.P. Liu [47], letting time $t \to +\infty$, every solution with small total variation converges asymptotically to the solution of a Riemann problem. It is only for large BV solutions that some interesting dynamics will likely be observed—provided that some global existence theorem can be established.

In connection with vanishing viscosity approximations, uniform BV bounds for systems of balance laws with dissipative sources were established in [24]. Viscous approximations to the initial-boundary value problem, with suitable boundary conditions, have been studied by Ancona and Bianchini [2].

Up to now, all results on a priori BV bounds, stability and convergence of viscous approximations have dealt with "artificial viscosity", assuming that the diffusion coefficient is independent of the state u. A more realistic model would be

$$u_t + f(u)_x = (B(u)u_x)_x \,, \tag{191}$$

where B is a positive definite viscosity matrix, possibly depending on the state u. It remains an outstanding open problem to establish similar results in connection with the more general system (191).

Appendix

We collect here some results of mathematical analysis, which were used in previous sections.

9.1 Compactness Theorems

Let Ω be an open subset of $I\!R^m$. We denote by $\mathbf{L}^1_{loc}(\Omega;\, I\!R^n)$ the space of locally integrable functions on Ω. This is the space of all functions $u : \Omega \mapsto I\!R^n$ whose restriction to every compact subset $K \subset \Omega$ is integrable. The space $\mathbf{L}^1_{loc}$ is not a normed space. However, it is a Fréchet space: for every compact $K \subset \Omega$, the mapping

$$u \mapsto \int_K |u(x)|\, dx$$

is a seminorm on $\mathbf{L}^1_{loc}$.

Next, consider a (possibly unbounded) interval $J \subseteq I\!R$ and a map $u : J \mapsto I\!R^n$. The *total variation* of u is defined as

$$\text{Tot.Var.}\{u\} \doteq \sup \left\{ \sum_{j=1}^{N} \left| u(x_j) - u(x_{j-1}) \right| \right\} , \tag{1}$$

where the supremum is taken over all $N \geq 1$ and all $(N+1)$-tuples of points $x_j \in J$ such that $x_0 < x_1 < \cdots < x_N$. If the right hand side of (1) is bounded, we say that u has bounded variation, and write $u \in BV$.

Lemma A.1 (properties of functions with bounded variation). *Let $u :]a, b[\mapsto I\!R^n$ have bounded variation. Then, for every $x \in]a, b[$, the left and right limits*

$$u(x-) \doteq \lim_{y \to x-} u(y), \qquad\qquad u(x+) \doteq \lim_{y \to x+} u(y)$$

are well defined. Moreover, u has at most countably many points of discontinuity.

By the above lemma, if u has bounded variation, we can redefine the value of u at each point of jump by setting $u(x) \doteq u(x+)$. In particular, if we are only interested in the $\mathbf{L}^1$-equivalence class of a BV function u, by possibly changing the values of u at countably many points we can assume that u is right continuous.

We state below a version of Helly's compactness theorem, which provides the basic tool in the proof of existence of weak solutions. For a proof, see [11].

Theorem A.1 (Compactness for a family of BV functions). *Consider a sequence of functions $u_\nu : [0, \infty[\times I\!R \mapsto I\!R^n$ with the following properties.*

$$\text{Tot.Var.}\big\{u_\nu(t, \cdot)\big\} \leq C, \qquad \big|u_\nu(t, x)\big| \leq M \qquad \text{for all } t, x, \tag{2}$$

$$\int_{-\infty}^{\infty} \big|u_\nu(t, x) - u_\nu(s, x)\big|\, dx \leq L|t - s| \qquad \text{for all } t, s \geq 0, \tag{3}$$

for some constants C, M, L. Then there exists a subsequence u_μ which converges to some function u in $\mathbf{L}^1_{\text{loc}}\big([0, \infty) \times I\!R;\ I\!R^n\big)$. This limit function satisfies

$$\int_{-\infty}^{\infty} \big|u(t, x) - u(s, x)\big|\, dx \leq L|t - s| \qquad \text{for all } t, s \geq 0. \tag{4}$$

The point values of the limit function u can be uniquely determined by requiring that

$$u(t, x) = u(t, x+) \doteq \lim_{y \to x+} u(t, y) \qquad \text{for all } t, x. \tag{5}$$

In this case, one has

$$\text{Tot.Var.}\big\{u(t, \cdot)\big\} \leq C, \qquad \big|u(t, x)\big| \leq M \qquad \text{for all } t, x. \tag{6}$$

9.2 An Elementary Error Estimate

Let $\mathscr{D}$ be a closed subset of a Banach space E and consider a Lipschitz continuous semigroup $S : \mathscr{D} \times [0, \infty[\mapsto \mathscr{D}$. More precisely, assume that

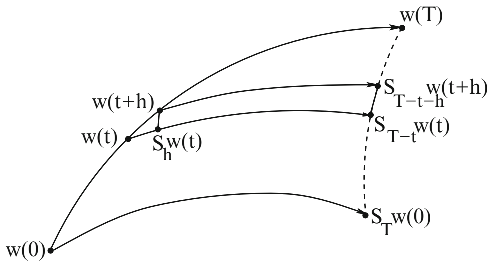

Fig. 65 Comparing the approximate solution w with the trajectory of the semigroup having the same initial data

(i) $S_0 u = u, \qquad S_s S_t u = S_{s+t} u.$
(ii) $\|S_t u - S_s v\| \;\leq\; L \cdot \|u - v\| + L' \cdot |t - s|.$

Given a Lipschitz continuous map $w : [0, T] \mapsto \mathscr{D}$, the following theorem estimates the difference between w and the trajectory of the semigroup S starting at $w(0)$. For the proof we again refer to [11].

Theorem A.2 (Error estimate for a Lipschitz flow). *Let $S : \mathscr{D} \times [0, \infty[\mapsto \mathscr{D}$ be a continuous flow satisfying the properties (i)–(ii). For every Lipschitz continuous map $w : [0, T] \mapsto \mathscr{D}$ one then has the estimate*

$$\big\|w(T) - S_T w(0)\big\| \;\leq L \int_0^T \left\{ \liminf_{h \to 0+} \frac{\big\|w(t+h) - S_h w(t)\big\|}{h} \right\} dt. \tag{7}$$

Remark 9. The integrand in (7) can be regarded as the instantaneous error rate for w at time t. Since the flow is uniformly Lipschitz continuous, during the time interval $[t, T]$ this error is amplified at most by a factor L (see Fig. 65).

9.3 The Center Manifold Theorem

Let A be an $n \times n$ matrix and consider the Cauchy problem for a linear system of O.D.E's with constant coefficients

$$\dot{x} = Ax\,, \qquad\qquad x(0) = \bar{x}. \tag{8}$$

The explicit solution can be written as

$$x(t) = e^{tA}\bar{x}\,, \qquad\qquad e^{tA} \doteq \sum_{k=0}^{\infty} \frac{t^k A^k}{k!}.$$

We say that a subspace $V \subset I\!R^n$ is **invariant** for the flow of (8) if $x \in V$ implies $e^{At}x \in V$ for all $t \in I\!R$. A natural way to decompose the space $I\!R^n$ as the sum of three invariant subspaces is now described. Consider the eigenvalues of A, i.e. the

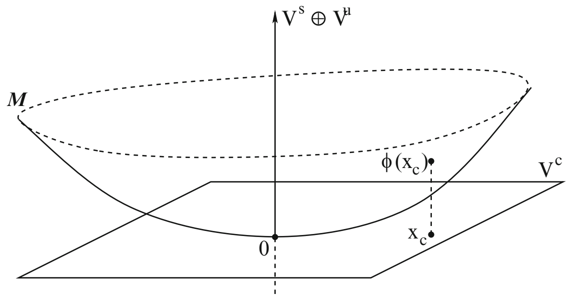

Fig. 66 The center subspace V^c and the center manifold $\mathscr{M}$, tangent to V^c at the origin

zeroes of the polynomial $p(\zeta) \doteq \det(\zeta I - A)$. These are finitely many points in the complex plane.

The space $I\!R^n$ can then be decomposed as the sum of a stable, an unstable and a center subspace, respectively spanned by the (generalized) eigenvectors corresponding to eigenvalues with negative, positive and zero real part. We thus have

$$I\!R^n = V^s \oplus V^u \oplus V^c$$

with continuous projections

$$\pi_s : I\!R^n \mapsto V^s, \qquad \pi_u : I\!R^n \mapsto V^u, \qquad \pi_c : I\!R^n \mapsto V^c,$$

$$x = \pi_s x + \pi_c x + \pi_u x.$$

These projections commute with A and hence with the exponential e^{At} as well:

$$\pi_s e^{At} = e^{At}\pi_s, \qquad \pi_u e^{At} = e^{At}\pi_u, \qquad \pi_c e^{At} = e^{At}\pi_c.$$

In particular, these subspaces are invariant for the flow of (8).

Next, consider the nonlinear system

$$\dot{x} = f(x). \tag{9}$$

Assume that $f(0) = 0$ and $Df(0) = A$, so that (8) provides a first order Taylor approximation to (9). According to the center manifold theorem, the nonlinear system (9) admits an invariant manifold $\mathscr{M}$, which at the origin is tangent to the center subspace V^c, as shown in Fig. 66. In the following theorem, the solution of (9) with initial data $x(0) = x_0$ will be denoted by $t \mapsto x(t, x_0)$. For a proof we refer to [13].

Theorem A.3 (Existence and properties of center manifold). *Let $f : I\!R^n \mapsto I\!R^n$ be a vector field in $\mathscr{C}^{k+1}$ (here $k \geq 1$), with $f(0) = 0$. Consider the matrix $A = Df(0)$, and let V^s, V^u, V^c be the corresponding stable, unstable, and center subspaces. Then there exists $\delta > 0$ and a local center manifold $\mathscr{M}$ with the following properties.*

(i) There exists a $\mathscr{C}^k$ *function* $\phi : V^c \mapsto I\!R^n$ *with* $\pi_c\,\phi(x_c) = x_c$ *such that*

$$\mathscr{M} \;=\; \Big\{\phi(x_c)\,; \quad x_c \in V^c\,, \quad |x_c| < \delta\Big\}.$$

(ii) The manifold $\mathscr{M}$ *is locally invariant for the flow of (9), i.e.* $x_0 \in \mathscr{M}$ *implies* $x(t, x_0) \in \mathscr{M}$*, for all* t *sufficiently close to zero.*

(iii) $\mathscr{M}$ *is tangent to* V^c *at the origin.*

(iv) Every globally bounded orbit remaining in a suitably small neighborhood of the origin is entirely contained inside $\mathscr{M}$*.*

(v) Given any trajectory such that $x(t) \to 0$ *as* $t \to +\infty$*, there exists* $\eta > 0$ *and a trajectory* $t \mapsto y(t) \in \mathscr{M}$ *on the center manifold such that*

$$e^{\eta t}\,\big|x(t) - y(t)\big| \to 0 \qquad\qquad as \quad t \to +\infty.$$

References

1. D. Amadori, L. Gosse, G. Guerra, Global BV entropy solutions and uniqueness for hyperbolic systems of balance laws. Arch. Ration. Mech. Anal. **162**, 327–366 (2002)
2. F. Ancona, S. Bianchini, Vanishing viscosity solutions of hyperbolic systems of conservation laws with boundary, in *"WASCOM 2005"–13th Conference on Waves and Stability in Continuous Media* (World Scientific, Hackensack, 2006), pp. 13–21
3. F. Ancona, A. Marson, Existence theory by front tracking for general nonlinear hyperbolic systems. Arch. Ration. Mech. Anal. **185**, 287–340 (2007)
4. F. Ancona, A. Marson, A locally quadratic Glimm functional and sharp convergence rate of the Glimm scheme for nonlinear hyperbolic systems. Arch. Ration. Mech. Anal. **196**, 455–487 (2010)
5. P. Baiti, H.K. Jenssen, On the front tracking algorithm. J. Math. Anal. Appl. **217**, 395–404 (1998)
6. S. Bianchini, On the Riemann problem for non-conservative hyperbolic systems. Arch. Ration. Mech. Anal. **166**, 1–26 (2003)
7. S. Bianchini, A. Bressan, Vanishing viscosity solutions to nonlinear hyperbolic systems. Ann. Math. **161**, 223–342 (2005)
8. A. Bressan, Contractive metrics for nonlinear hyperbolic systems. Indiana Univ. J. Math. **37**, 409–421 (1988)
9. A. Bressan, Global solutions of systems of conservation laws by wave-front tracking. J. Math. Anal. Appl. **170**, 414–432 (1992)
10. A. Bressan, The unique limit of the Glimm scheme. Arch. Ration. Mech. Anal. **130**, 205–230 (1995)
11. A. Bressan, *Hyperbolic Systems of Conservation Laws. The One Dimensional Cauchy Problem* (Oxford University Press, Oxford, 2000)
12. A. Bressan, BV solutions to systems of conservation laws by vanishing viscosity, C.I.M.E. course in Cetraro, 2003, in *Springer Lecture Notes in Mathematics*, vol. 1911, ed. by P. Marcati (Springer-Verlag, Berlin, 2007), pp. 1–78
13. A. Bressan, A tutorial on the Center Manifold Theorem, C.I.M.E. course in Cetraro, 2003, in *Springer Lecture Notes in Mathematics*, vol. 1911, ed. by P. Marcati (Springer-Verlag, Berlin, 2007), pp. 327–344

14. A. Bressan, R.M. Colombo, The semigroup generated by 2×2 conservation laws. Arch. Ration. Mech. Anal. **133**, 1–75 (1995)
15. A. Bressan, P. Goatin, Oleinik type estimates and uniqueness for $n \times n$ conservation laws. J. Differ. Equat. **156**, 26–49 (1999)
16. A. Bressan, P. LeFloch, Uniqueness of weak solutions to hyperbolic systems of conservation laws. Arch. Ration. Mech. Anal. **140**, 301–317 (1997)
17. A. Bressan, M. Lewicka, A uniqueness condition for hyperbolic systems of conservation laws. Discrete. Cont. Dyn. Syst. **6**, 673–682 (2000)
18. A. Bressan, A. Marson, Error bounds for a deterministic version of the Glimm scheme. Arch. Ration. Mech. Anal. **142**, 155–176 (1998)
19. A. Bressan, T. Yang, On the convergence rate of vanishing viscosity approximations. Comm. Pure Appl. Math. **57**, 1075–1109 (2004)
20. A. Bressan, T.P. Liu, T. Yang, L^1 stability estimates for $n \times n$ conservation laws. Arch. Ration. Mech. Anal. **149**, 1–22 (1999)
21. A. Bressan, G. Crasta, B. Piccoli, Well posedness of the Cauchy problem for $n \times n$ systems of conservation laws. Am. Math. Soc. Mem. **694** (2000)
22. A. Bressan, K. Jenssen, P. Baiti, An instability of the Godunov scheme. Comm. Pure Appl. Math. **59**, 1604–1638 (2006)
23. C. Cheverry, Systèmes de lois de conservation et stabilité BV [Systems of conservation laws and BV stability]. Mém. Soc. Math. Fr. **75** (1998) (in French)
24. C. Christoforou, Hyperbolic systems of balance laws via vanishing viscosity. J. Differ. Equat. **221**, 470–541 (2006)
25. M.G. Crandall, The semigroup approach to first order quasilinear equations in several space variables. Isr. J. Math. **12** 108–132, (1972)
26. C. Dafermos, Polygonal approximations of solutions of the initial value problem for a conservation law. J. Math. Anal. Appl. **38**, 33–41 (1972)
27. C. Dafermos, *Hyperbolic Conservation Laws in Continuum Physics* (Springer, Berlin, 1999)
28. R.J. DiPerna, Global existence of solutions to nonlinear hyperbolic systems of conservation laws. J. Differ. Equat. **20**, 187–212 (1976)
29. R. DiPerna, Convergence of approximate solutions to conservation laws. Arch. Ration. Mech. Anal. **82**, 27–70 (1983)
30. C. Donadello, A. Marson, Stability of front tracking solutions to the initial and boundary value problem for systems of conservation laws. Nonlinear Differ. Equat. Appl. **14**, 569-592 (2007)
31. L.C. Evans, *Partial Differential Equations* (American Mathematical Society, Providence, 1998)
32. L.C. Evans, R.F. Gariepy, *Measure Theory and Fine Properties of Functions* (CRC Press, Boca Raton, Fl, 1992)
33. M. Garavello, B. Piccoli, in *Traffic Flow on Networks. Conservation Laws Models* (AIMS Series on Applied Mathematics, Springfield, 2006)
34. J. Glimm, Solutions in the large for nonlinear hyperbolic systems of equations. Comm. Pure Appl. Math. **18**, 697–715 (1965)
35. J. Glimm, P. Lax, Decay of solutions of systems of nonlinear hyperbolic conservation laws. Am. Math. Soc. Mem. **101** (1970)
36. J. Goodman, Z. Xin, Viscous limits for piecewise smooth solutions to systems of conservation laws. Arch. Ration. Mech. Anal. **121**, 235–265 (1992)
37. H. Holden, N.H. Risebro, *Front Tracking for Hyperbolic Systems of Conservation Laws* (Springer, New York, 2002)
38. H.K. Jenssen, Blowup for systems of conservation laws. SIAM J. Math. Anal. **31**, 894–908 (2000)
39. S. Kruzhkov, First-order quasilinear equations with several space variables. Mat. Sb. **123**, 228–255 (1970). English translation in Math. USSR Sb. **10**, 217–273 (1970)
40. P.D. Lax, Hyperbolic systems of conservation laws II. Comm. Pure Appl. Math. **10**, 537–566 (1957)
41. M. Lewicka, Well-posedness for hyperbolic systems of conservation laws with large BV data. Arch. Ration. Mech. Anal. **173**, 415–445 (2004)

42. T.-T. Li, *Global Classical Solutions for Quasilinear Hyperbolic Systems* (Wiley, Chichester, 1994)
43. M. Lighthill, G. Whitham, On kinematic waves, II. A theory of traffic flow on long crowded roads. Proc. R. Soc. Lond. A **229**, 317–345 (1955)
44. T.P. Liu, The Riemann problem for general systems of conservation laws. J. Differ. Equat. **18**, 218–234 (1975)
45. T.P. Liu, The entropy condition and the admissibility of shocks. J. Math. Anal. Appl. **53**, 78–88 (1976)
46. T.P. Liu, The deterministic version of the Glimm scheme. Comm. Math. Phys. **57**, 135–148 (1977)
47. T.P. Liu, Linear and nonlinear large-time behavior of solutions of general systems of hyperbolic conservation laws. Comm. Pure Appl. Math. **30**, 767–796 (1977)
48. T.-P. Liu, T. Yang, L^1 stability of conservation laws with coinciding Hugoniot and characteristic curves. Indiana Univ. Math. J. **48**, 237–247 (1999)
49. T.-P. Liu, T. Yang, L^1 stability of weak solutions for 2×2 systems of hyperbolic conservation laws. J. Am. Math. Soc. **12**, 729–774 (1999)
50. Y. Lu, *Hyperbolic Conservation Laws and the Compensated Compactness Method* (Chapman & Hall/CRC, Boca Raton, 2003)
51. O. Oleinik, Discontinuous solutions of nonlinear differential equations. Am. Math. Soc. Transl. **26**, 95–172 (1963)
52. B. Riemann, Über die Fortpflanzung ebener Luftwellen von endlicher Schwingungsweite. Göttingen Abh. Math. Cl. **8**, 43–65 (1860)
53. F. Rousset, Viscous approximation of strong shocks of systems of conservation laws. SIAM J. Math. Anal. **35**, 492–519 (2003)
54. S. Schochet, Sufficient conditions for local existence via Glimm's scheme for large BV data. J. Differ. Equat. **89**, 317–354 (1991)
55. S. Schochet, The essence of Glimm's scheme, in *Nonlinear Evolutionary Partial Differential Equations*, ed. by X. Ding, T.P. Liu (American Mathematical Society/International Press, Providence, RI, 1997), pp. 355–362
56. D. Serre, *Systems of Conservation Laws*, vols. 1–2 (Cambridge University Press, Cambridge, 1999)
57. J. Smoller, *Shock Waves and Reaction-Diffusion Equations* (Springer, New York, 1983)
58. S.H. Yu, Zero-dissipation limit of solutions with shocks for systems of hyperbolic conservation laws. Arch. Ration. Mech. Anal. **146**, 275–370 (1999)
59. A.I. Volpert, The spaces BV and quasilinear equations. Math. USSR Sbornik **2**, 225–267 (1967)

http://www.springer.com/978-3-642-32159-7

Modelling and Optimisation of Flows on Networks
Cetraro, Italy 2009, Editors: Benedetto Piccoli, Michel
Rascle
Ambrosio, L.; Bressan, A.; Helbing, D.; Klar, A.; Zuazua,
E. - Piccoli, B.; Rascle, M. (Eds.)
2013, XIV, 497 p. 141 illus., 32 illus. in color., Softcover
ISBN: 978-3-642-32159-7